FINNISH METEOROLOGICAL INSTITUTE CONTRIBUTIONS

NO. 107

STUDY ON SOOT AND OTHER REFRACTORY COMPONENTS FROM VARIOUS COMBUSTION PROCESSES

Anna Frey

Department of Physics

Faculty of Science

University of Helsinki

Helsinki, Finland

ACADEMIC DISSERTATION in Atmospheric Sciences

To be presented, with the permission of the Faculty of Science of the University of Helsinki, for public criticism in Auditorium E204 of the Department of Physics on April 25th, 2014, at 12 o'clock noon.

Finnish Meteorological Institute

Helsinki 2014

Author's Address: Finnish Meteorological Institute
P.O. Box 503, FI-00101 Helsinki, Finland
anna.frey@fmi.fi

Supervisors: Research Professor Risto Hillamo
Finnish Meteorological Institute
Atmospheric Aerosols
Helsinki, Finland

Professor Markku Kulmala
University of Helsinki
Department of Physics
Helsinki, Finland

Docent Aki Virkkula
Finnish Meteorological Institute
Air Quality
Helsinki, Finland

Pre-examiners: Professor Jyrki Mäkelä
Tampere University of Technology
Department of Physics
Tampere, Finland

Dr. Radovan Krejci
Department of Applied Environmental Science
Stockholm University
Stockholm, Sweden

Opponent: Docent Jorma Joutsensaari
University of Eastern Finland
Department of Applied Physics
Kuopio, Finland

Custos: Professor Tuukka Petäjä
University of Helsinki
Department of Physics
Helsinki, Finland

ISBN 978-951-697-825-6 (paperback)
ISSN 0782-6117
Unigrafia Oy
Helsinki 2014

ISBN 978-951-697-826-3 (pdf)
http://ethesis.helsinki.fi
Helsingin yliopiston verkkojulkaisut
Helsinki 2014

FINNISH METEOROLOGICAL INSTITUTE

Series title, number and report code of publication
Finnish Meteorological Institute Contributions
No. 107
FMI-CONT-107

Published by Finnish Meteorological Institute
(Erik Palménin aukio 1), P.O. Box 503
FIN-00101 Helsinki, Finland

Date: April 2014

Author(s)
Anna Frey

Title
Study on soot and other refractory components from various combustion processes

Abstract

Combustion processes emit remarkable amount of particles into the atmosphere. These particles are released e.g. from the spark ignition and diesel engines of road-traffic and from the combustion processes of small and large-scale energy production. Burning technologies and conditions as well as fuels combusted influence strongly on physical and chemical characteristics of particle emissions. It is important to know the properties of these emissions and causes behind them to analyze their impact on global radiative balance as well as on local and regional air quality and human health.

The objective of this thesis was to improve knowledge of chemical and physical properties of particles emitted from different combustion processes using modern measurement and data handling techniques. The thesis mostly concentrated on refractory part of the particles that is, the part that is highly heat resistant (i.e. black carbon (BC), low-volatile organics, inorganic minerals).

One part of the thesis tested a method that enabled the determination of non-volatile (or refractory) fraction of particles from the ambient air that was supposed to be soot emitted from traffic. The results were compared with other measurement and modelling results leading to possibility to estimate the mixing state and refractive indices of particles. The results showed that the method reliable gave information about soot fraction, mixing state and refractive indices of ambient air particles. It was possible to estimate when air masses were influenced by particles freshly emitted from traffic.

In addition to method testing, the thesis concentrated on studies of primary particle emissions from residential wood and wood pellet combustion as well as from large-scale combustion of heavy fuel oil (HFO) and coal. The emissions were characterized based on versatile instrumentation and data handling techniques leading to the information about chemical composition, size distribution, optical, radiative forcing and hygroscopic properties of particles emitted from investigated combustion cases. Overall, particle emissions of large-scale combustion of oil and coal were clearly lower than those of small-scale wood fuel combustion. However, differences inside large- and small-scale combustion were also significant depending on combustion and cleaning technique, fuel and combustion conditions. Especially particles emitted from masonry heater included remarkable fractions of particulate organic matter and BC whereas large-scale hardly emitted any. High BC fraction led to low single scattering albedo and thus, to positive radiative forcing effect over a dark surface. Surprisingly, also some cases of HFO combustion led to particle emissions with positive radiative forcing effect. Particle emissions of HFO combustion were also hygroscopic indicating that these particles could have significant effect on cloud formation in the atmosphere. In coal combustion, effective cleaning technique diminished the uncleaned emissions, which also were rather low, to a fraction from the original emissions.

To conclude, versatile measurement and analyze techniques used in the investigations of this thesis enabled accurate characterization of particles emitted from different combustion sources. The results clearly showed that the knowledge of the cause and effects relationship between combustion process and particle properties is crucial in assessment of climatic and health effects of particles and on the other hand, in finding the combustion techniques that minimize emissions.

Publishing unit
Finnish Meteorological Institute, Atmospheric Composition Research

Classification (UDC)
504.05 504.064 541.182.2/.3
551.510

Keywords
small-scale combustion, large-scale combustion, soot, optical properties, chemical composition, particle size distribution

ISSN and series title
0782-6117 Finnish Meteorological Institute Contributions

ISBN
978-951-697-825-6 (paperback)
978-951-697-826-3 (pdf)

Language
English

Pages
170

ILMATIETEEN LAITOS

Julkaisun sarja, numero ja raporttikoodi
Finnish Meteorological Institute Contributions
No. 107
FMI-CONT-107

Julkaisija Ilmatieteen laitos,
(Erik Palménin aukio 1), PL 503
00101 Helsinki

Julkaisuaika: Huhtikuu 2014

Tekijä(t)
Anna Frey

Nimeke
Polttoprosessien noki ja muut vaikeasti haihtuvat komponentit

Tiivistelmä

Erilaiset polttoprosessit, kuten moottoriajoneuvot tieliikenteessä sekä energian pien- ja suurtuotanto, ovat merkittäviä hiukkaspäästöjen lähteitä. Polttoteknologia ja -olosuhteet sekä polttoaine vaikuttavat selvästi hiukkaspäästöjen kemiallisiin ja fysikaalisiin ominaisuuksiin. Onkin tärkeä tuntea päästöhiukkasten ominaisuudet ja niihin vaikuttavat tekijät, jotta niiden vaikutuksia globaaliin ilmastoon, paikalliseen ja alueelliseen ilmanlaatuun sekä ihmisten terveyteen voidaan arvioida.

Tämän väitöskirjan tavoitteena oli parantaa ja monipuolistaa tietämystä polttoprosessien hiukkaspäästöjen fysikaalisista ja kemiallisista ominaisuuksista käyttäen nykyaikaisia mittaus- ja datan analysointitekniikoita. Väitöskirjassa keskityttiin pääosin päästöjen siihen osaan, joka voidaan määritellä vaikeasti haihtuvaksi tai tulenkestäväksi (refractory, musta hiili, haihtumattomat orgaaniset yhdisteet, epäorgaaniset mineraalit).

Yksi osa väitöskirjatutkimuksesta testasi mittausjärjestelmää, joka mahdollisti haihtumattomien komponenttien osuuden määrittämisen kaupungin taustailmasta mitatuissa hiukkasissa. Tämä osuus koostui todennäköisimmin liikennepäästöjen nokihiukkasista. Työssä verrattiin ja yhdisteltiin useiden mittalaitteiden ja mallinnusten tuottamia tuloksia. Tutkimus osoitti, että käytetyillä menetelmillä pystytään luotettavasti saamaan tietoa nokihiukkasten osuudesta, hiukkasten seosominaisuuksista sekä taitekertoimista. Menetelmällä pystyttiin arvioimaan milloin primäärisillä liikennepäästöillä oli vaikutusta ilmamassoihin.

Tämän väitöskirjatyön yhteydessä tutkittiin myös puun ja puupellettien pienpolton sekä suurissa tuotantolaitoksissa poltettavan raskaan polttoöljyn ja kivihiilen primäärisiä hiukkaspäästöjä. Monipuolisten mittaus- ja data-analyysitekniikoiden avulla saatiin tietoa eri polttotilanteiden hiukkaspäästöjen kemiallisesta koostumuksesta, hiukkaskokojakaumista, optisista ja säteilypakote ominaisuuksista sekä hygroskooppisuudesta. Tulokset osoittivat, että kivihiiltä ja raskasta polttoöljyä polttavien suurtuotantolaitosten hiukkaspäästöt olivat selvästi pienemmät kuin puun ja puupellettien poltosta aiheutuvat hiukkaspäästöt. Erot hiukkaspäästöissä pienpolton ja suurtuotantolaitosten eri polttotilanteiden välillä olivat myös selviä. Päästöihin vaikuttivat poltto- ja puhdistustekniikka, polttoaine ja palamisolosuhteet. Etenkin varaavan takan hiukkaspäästöt sisälsivät huomattavan määrän mustaa hiiltä ja orgaanisia aineita, kun taas suurtuotantolaitosten päästöissä näiden komponenttien osuudet olivat olemattomat. Suuri mustan hiilen osuus johti matalaan yksittäissironta-albedoon mikä johtaisi positiiviseen säteilypakotteeseen tummien pintojen yllä. Yllättäen myös osa raskaan polttoöljyn polttokokeista johti päästöihin, joilla olisi lämmittävä vaikutus tummilla pinnoilla. Raskaan polttoöljyn poltosta syntyvät hiukkaset olivat myös selvästi hygroskooppisia, joten niillä voisi olla merkittävä vaikutus myös pilvien muodostumiseen. Kivihiilen polton puhdistamattomat hiukkaspäästöt olivat varsin matalat ja tehokas savukaasujen puhdistustekniikka vähensi lopulliset päästöt vain murto-osaan alkuperäisistä.

Tässä väitöskirjatutkimuksessa käytettiin monipuolisia mittaus- ja analyysitekniikoita, jotka mahdollistivat polttoprosesseista aiheutuvien hiukkaspäästöjen tarkan ja monipuolisen analysoinnin. Tulokset näyttivät, että syy-seuraussuhteiden tuntemus polttoprosessien ja hiukkasten ominaisuuksien välillä on erittäin tärkeää, kun halutaan arvioida hiukkasten ilmasto- ja terveysvaikutuksia. Toisaalta polttoprosessien aiheuttamien päästöjen tuntemus mahdollistaa parhaiden mahdollisten polttotekniikoiden kehittämisen ja käyttöönoton.

Julkaisijayksikkö
Ilmatieteen laitos, Ilmakehän koostumuksen tutkimus

Luokitus (UDK)
504.05 504.064 541.182.2/.3
551.510

Asiasanat
pienpoltto, energian suurtuotanto, noki, optiset ominaisuudet, kemiallinen koostumus, hiukkaskokojakauma

ISSN ja avainnimike
0782-6117 Finnish Meteorological Institute Contributions

ISBN
978-951-697-825-6 (nidottu)
978-951-697-826-3 (pdf)

Kieli
englanti

Sivumäärä
170

Acknowledgements

The research of this thesis was carried out at the Air Quality Department of the Finnish Meteorological Institute and at the Physics Department of the Leibniz Institute for Tropospheric Research. The work was financially supported by the Finnish Meteorological Institute, the Marie Curie fellowship program, the Cluster for Energy and Environment (Cleen Ltd) Measurement, Monitoring and Environmental Assessment (MMEA) Work package 4.5.2., the Academy of Finland and the Finnish Funding Agency of Technology and Innovation.

I am grateful for the Director of the Research and Development Division, Professor Yrjö Viisanen, for the former Head of Unit of the Air Quality, Professor Jaakko Kukkonen and for the Head of Unit of the Atmospheric Composition Research, Docent Heikki Lihavainen for the opportunity to work and finish my PhD in the Departments they have been leading. I want to thank one of my supervisors Professor Risto Hillamo for his efforts for the funding for the interesting projects in which I had possibility to work and further my studies. Professor Alfred Wiedensohler and his working group are acknowledged for giving me the opportunity to carry out part of the research of this thesis at the Leibniz Institute for Tropospheric Research. I am most grateful to Docent Aki Virkkula who patiently supervised me and gave me the best scientific support one can have. Professors Markku Kulmala and Tuukka Petäjä from the Department of Physics, University of Helsinki are acknowledged for support to my post-graduate studies.

I wish to thank the official pre-examiners of the thesis, Professor Jyrki Mäkelä from the Tampere University of Technology and Dr. Radovan Krejci from the Stockholm University for their careful review of the thesis and excellent comments. I highly appreciate that Docent Jorma Joutsensaari from the University of Eastern Finland promised to be my official opponent in the public examination of this thesis.

I am thankful for all my co-authors and the other colleagues who took part in the research of this thesis. I especially wish to acknowledge my former colleagues at the Air Quality Department for inspiring, encouraging and pleasant working environment. I want to direct especial thanks for my nearest colleagues in the Air Quality group: Hilkka, Karri, Sanna, Minna, Samara and Kimmo. Timo Mäkelä is acknowledged for the support and co-operation in the technical field of my studies. I am grateful also to Eija, who has been sharing many wonderful moments with me both in working and spare time.

While finishing my thesis, the Head of Observation Services Unit, Keijo Leminen, gave me an interesting and challenging possibility to extend my expertise offering me a new position. I am

really grateful to him for his confidence. This possibility also gave me enthusiasm to finish this thesis. Also my colleagues in my present position at the Observation Services Unit are thanked for cheerful and encouraging working atmosphere.

I am most thankful to my family, my mother, father and my sister, for giving me all their support and love. They have always believed in me, even during the times I didn't. I have been happy to have three lovely godchildren, Daniel, Aino and Antti who have shown me enormous small wonders and joys of the world. I want to thank these important children in my life for extending my world view. I also wish to thank all my wonderful friends from the various periods of my life who have shared many memorable moments with me. I want to thank them for the fruitful experiences and all the fun we have had and will have together.

My deepest and warmest thanks are directed to my beloved Antti who has been by my side during all these years. Thanks for giving me your endless love and support and for making my life happy and fun.

Espoo, March 2014

Anna Frey

Abbreviations

APS	Aerodynamic particle sizer
BC	Black carbon
CPC	Condensation particle counter
C-PP	Coal-fired power plant
D_a	Particle aerodynamic diameter (µm, nm)
D_p	Particle geometric diameter (µm, nm)
DMA	Differential mobility analyzer
DMPS	Differential mobility particle sizer
DR	Dilution ratio
DSP	Desulfurization plant
E_F	Emission factor (mg MJ^{-1})
EC	Elemental carbon
ELPI	Electrical low pressure impactor
ESP	Electrostatic precipitator
FMPS	Fast mobility particle sizer
FPS	Fine particle sampler, dilution system
GF	Growth factor
GMD	Geometric mean diameter
GSD	Geometric standard deviation
HFO	Heavy fuel oil
HFO-HS	Heavy fuel oil-fired heating station
HPAEC-MS	High-performance anion-exchange chromatograph mass spectrometer

HTDMA	Hygroscopic tandem differential mobility analyzer
IC	Ion chromatography
ICP-MS	Inductively coupled plasma mass spectrometer
ICP-OES	Inductively coupled plasma optical emission spectrometer
LC-MS	Liquid chromatograph mass spectrometer
LFO	Light fuel oil
LV	Less volatile
M_{BC}	Mass concentration of black carbon particles (µg m^{-3})
M_{LV}	Mass concentration of less volatile particles (µg m^{-3})
MA	Monosaccharide anhydrides
MAAP	Multi-angle absorption photometer
MAE	Mass absorption efficiency (m^2 g^{-1})
MEE	Mass extinction efficiency (m^2 g^{-1})
MH	Masonry heater
MOUDI	Micro-orifice uniform impactor
N_{LV}	Number concentration of less volatile particles (# cm^{-3})
NGMD	Number geometric mean diameter (µm, nm)
NGSD	Number geometric standard deviation
OC	Organic carbon
PB	Pellet boiler
POM	Particulate organic matter (µg m^{-3})
PM	Particulate matter (µg m^{-3})
PSAP	Particle soot absorption photometer

SMPS	Scanning mobility particle sizer
SDI	Small deposit area impactor
SSWC	Small scale wood combustion
TD	Thermodenuder
TOA	Thermal optical carbon analyzer
TOC	Total organic carbon
VGMD	Volume geometric mean diameter (μm, nm)
VGSD	Volume geometric standard deviation
VI	Virtual impactor
WSOC	Water soluble organic carbon
WSPOM	Water soluble particulate organic matter
VTDMA	Volatility tandem differential mobility analyzer

Contents

Acknowledgements 6
Abbreviations 8
List of Publications 13
1 Introduction 14
2 Objectives of the Study 16
3 Review on the state of the research on particle emissions from combustion processes 17
4 Theoretical background 19
4.1 Combustion appliances and cleaning techniques 19
4.1.1 Spark ignition and diesel engines of road traffic 19
4.1.2 Small-scale wood fuel heaters and boilers 20
4.1.3 Heavy fuel oil-fired boilers 21
4.1.4 Coal-fired boilers 22
4.2 Formation of particle emissions of combustion processes 24
4.2.1 Gaseous emissions and organic particles 25
4.2.2 Ash particles 26
4.2.3 Soot particles 26
4.2.4 External and internal mixture of particles 27
5 Experimental 27
5.1 Measurement sites 27
5.1.1 Ambient air influenced by traffic emissions 28
5.1.2 Small-scale wood and wood pellet combustion 28
5.1.3 Coal-fired heating and power plant 28
5.1.4 Heavy fuel oil-fired heating station 29
5.2 Dilution of sample flow 30
5.3 Measurements of particle optical properties 30
5.4 Particle number and volume size distribution measurements 31
5.5 Sampling systems 36
5.5.1 Virtual Impactor 36
5.5.2 Small deposit area impactor 36
5.5.3 PM_1 sampling system 36
5.5.4 Micro-orifice uniform deposit impactor (MOUDI) 37
5.6 Chemical analysis of filter samples 37

5.6.1 Filters and sampling substrates 37
5.6.2 Analytical methods 38
5.7 Data analysis 41
5.7.1 Determination of less volatile particle size distribution 41
5.7.2 Mie modeling 41
5.7.3 Conversion and normalization of particle emissions to the standard conditions 42
5.7.4 Correction of optical data and calculation based on optical results 43
6 Results and discussion 45
6.1 Less volatile traffic related particle emissions 45
6.2 Particle emissions of wood fuel, coal and heavy fuel oil combustion 48
6.2.1 Particle emissions and their chemical composition 48
6.2.2 Size distributions 54
6.2.3 Optical properties 59
6.2.4 Hygroscopic growth of particles emitted from large-scale combustion of HFO 62
7 Review of articles and author's contributions 63
8 Summary 66
9 Outlook of the used techniques and research field 71
References 73

List of Publications

I. Frey, A., Rose, D., Wehner, B., Müller, T., Cheng, Y., Wiedensohler, A. and Virkkula, A. (2008). Application of the Volatility-TDMA Technique to determine the number size distribution and mass concentration of less volatile particles. *Aerosol Sci. Technol.*, 42:10,817 – 828.

II. Frey, A., Tissari, J., Saarnio, K., Timonen, H., Tolonen-Kivimäki, O., Aurela, M., Saarikoski, S., Makkonen, U., Hytönen, K., Jokiniemi, J., Salonen, R.O. and Hillamo, R. (2009). Chemical composition and mass size distribution of fine particulate matter emitted by a small masonry heater. *Boreal Env. Res.*, 14, 225-271.

III. Frey, A., Saarnio, K., Lamberg, H., Mylläri, F., Karjalainen, P., Teinilä, K., Carbone, S., Tissari, J., Niemelä, V., Häyrinen, A., Rautiainen, J., Kytömäki, J., Artaxo, P., Virkkula, A., Pirjola, L., Rönkkö, T., Keskinen, J., Jokiniemi, J. and Hillamo, R. (2014). Optical and chemical characterization of aerosols emitted from coal, heavy and light fuel oil and small-scale wood combustion. *Environ. Sci. Technol.*, 48 (1), 827-836.

IV. Happonen, M., Mylläri, F., Karjalainen, P., Frey, A., Saarikoski, S., Carbone, S., Hillamo, R., Pirjola, L., Häyrinen, A., Kytömäki, J., Niemi, J., Keskinen, J. and Rönkkö, T. (2013). Size Distribution, Chemical Composition, and Hygroscopicity of Fine Particles Emitted from an Oil-Fired Heating Plant. Environ. Sci. Technol., 47 (24), 14468-14475.

1 Introduction

Ambient air consists of mixture of gases and solid or liquid particles – called aerosol. Particles in this mixture are formed either from natural or anthropogenic sources. Anthropogenic particles are mainly formed in combustion processes, such as combustion engines of vehicles, small-scale biomass combustion with various burning appliances and large-scale combustion of oil, gas or coal. Particles emitted from combustion sources are harmful to human health and affect radiative balance in the atmosphere. Aerosol particles affect air quality locally and regionally but have global influences as well (e.g. Flanner et al., 2007; Robinson et al., 2007).

Adverse health effects are a concern especially when considering local and regional particle emissions. Local emissions are mostly produced by the sources with low emission height such as traffic and small-scale combustion. These emissions can also impact regionally. Instead, large-scale combustion of fossil fuels where emission height is high mainly has regional influence. Overall, fresh combustion particles are mostly in particle size range below 1 μm of diameter (PM_1, fine particles) (e.g. Virtanen et al., 2006; Sippula et al., 2009). These emissions contain ultrafine particles (i.e. particles with diameter <100nm) that are poorly soluble and may be more likely than larger particles to translocate from the lung to the blood and other parts of the body (Pope and Dockery, 2006). An association between these fine particulate pollutions and cardiovascular diseases has been found even though the evidences are still uncertain (Pekkanen et al., 2002; Boman et al., 2003; Pope et al., 2004). Particularly sensitive to adverse effects of particles are asthmatics and elderly and children patients of cardio-respiratory diseases (e.g. Larson and Koenig, 1994; Boman et al., 2003).

The health effects of particles are influenced by local, regional and long-range transported emissions but the climate effects are global due to intercontinental transport of polluted air masses (Flanner et al., 2007). According to the Intergovernmental Panel on Climate Change (IPCC) the effective radiative forcing of anthropogenic aerosols including both cooling (scattering) and warming (absorbing) particle types is estimated to be negative (-0.45 W m^{-2}) (Stocker et al., 2013). Black carbon (BC, also referred to as soot) emitted from fossil fuel and biomass burning gives a positive feedback to the atmospheric and surface forcing by absorbing solar radiation effectively (e.g. Podgorny et al., 2000; Shindell et al., 2012). For example, Jacobson (2001) suggested the global climate forcing of BC particles emitted by the fossil fuel burning to be ca. 0.5 W m^{-2}. The IPCC has estimated the surface forcing of BC on ice and snow to be between 0.02 and 0.09 W m^{-2} (Stocker et al., 2013). On the other hand, in contrast to the previous estimations of the forcing effect

of BC, the study of Cappa et al. (2012) showed the possibility of the overestimation of warming effect of BC.

When BC particles are deposited on snow surfaces they affect the albedo of the snow cover, accelerate melting of the snow and glaciers, and thus affect the complex climate system in general (Hansen and Nazarenko, 2004; Koch and Hansen, 2005). Globally, anthropogenic contribution to the total snow forcing has been suggested to be at least 80 % (Flanner et al., 2007).

Typically particles emitted by burning processes of small-scale appliances, like vehicle engines or small-scale biomass combustion, consist of organic compounds, soot and ash components with composition depending on fuel and combustion conditions (e.g. Sandradewi et al., 2008; Schneider et al., 2008; Tissari et al., 2009; Lamberg et al., 2011; Pirjola et al., 2012). Instead, the large-scale burning of fossil fuels emits particles with minor fraction of organic compounds and soot. These emissions are rather composed of ash components with mineral and metallic compounds (e.g. Linak et al., 2000; Sippula et al., 2009; Wang et al., 2010).

Particles released from combustion processes can be defined as refractory particles based on the definition: refractory materials are chemically and physically stable in high temperatures, i.e. heat resistant. In aerosol science, refractory particles have been overall associated with black carbon BC, low-volatile organics and inorganic mineral components such metals or trace elements typical for solid fuels (Ninomiya et al., 2004; Onasch et al., 2012). In previous studies, the term refractory has been used for example in emission studies of e.g. oil or coal combustion: there, refractory part of the particles is considered to be the fraction of particles that is non- or less volatile in high temperature combustion including e.g. various metal components (e.g. Linak et al., 2000; Ninomiya et al., 2004). On the other hand, the definition of the term refractory can be method dependent: in the instruments that analyze particle composition after vaporization of particles, the refractory is operationally defined to mean species that do not evaporate in a certain temperature (Canagaratna, et al., 2004; Onasch et al., 2012). In this thesis, the term refractory refers to components of the particles that are released from various high temperature combustion processes. However, not only heat resistant components are considered but also for example organics that are evaporated in combustion processes are taken into account.

This thesis gives an insight to the physical and chemical characteristics of the particle emissions of various burning processes. The primary particle emissions were studied for residential wood and wood pellet combustion, heavy fuel oil (HFO)-fired heating station and coal-fired heating and power plant. The mixing state of less volatile (soot) traffic related particle emissions were

investigated by ambient measurements. Overall, chemical and physical (e.g. size distribution) properties of aerosols from various combustion sources are widely studied individually for example investigating a certain particle property (e.g. size distribution, chemical composition or some certain chemical components such as metals) for one or more combustion source (e.g. Virtanen et al., 2006; Reddy et al., 2005). This thesis connects chemical and physical properties of particle emissions more versatile than previously. For example, optical properties of particles emitted from combustion processes are not widely studied together with chemical and other physical properties of emitted particles. Also, versatile factors affecting particle emissions were considered: combustion source, fuel and combustion conditions. The experiments of this thesis including optical characterization enabled e.g. the estimation of the influence of particles emitted from different combustion sources on the radiative forcing of the earth radiation balance.

2 Objectives of the Study

The purpose of this thesis was to clarify the characteristics of particle emissions from various combustion sources. Chemical composition as well as physical and optical properties of the particle emissions were versatilely determined. In the investigations of traffic related particle emissions, the measurements were conducted at an ambient air measurement station. In ambient air both primary and secondary particles, i.e., particles formed from gas-to-particle conversion are present. Instead, primary emissions were studied in the cases of small-scale wood combustion, HFO-fired heating station and coal-fired heating and power plant.

The objectives of this thesis were following:

- to test the suitability of a volatility tandem differential mobility analyzer and a differential mobility particle sizer to determine less volatile particle fraction (soot) of ambient aerosol influenced by traffic. The way to establish mixing state of measured aerosol masses was presented (Paper I).
- to clarify the influence of optimization of combustion processes or cleaning techniques on properties of particle emissions (Papers II, III and IV).
- to determine chemical composition and fraction of light absorbing material of particle emissions of various combustion processes (Papers II, III and IV).
- to assess the influence of combustion technology and combustion process on optical properties of particle emissions and thus, on their radiative effect in the atmosphere (Paper III).

- to investigate the hygroscopicity of particles emitted from large-scale HFO burning because of the possibility of those particles to affect cloud formation in the atmosphere (Paper IV).

3 Review on the state of the research on particle emissions from combustion processes

Particle emissions of combustion processes have been a concern many decades because of the recognized adverse health and environmental effects of them. Even though burning and flue gas cleaning techniques are developed, it is not obvious that best techniques are used worldwide. On the other hand, development of the techniques requires research on emissions to reach the best results. Further, even though particle emissions from combustion processes are widely studied during past decades, the formation mechanisms of the particles are still uncertain. Thus, the field still requires further scientific research in many areas.

Ambient air particles influenced by traffic are reported to increase BC fraction in the local ambient air (e.g. Pakkanen et al., 2000; Rose et al., 2005; Sandradewi et al., 2008). The previous studies on motor vehicle emissions, especially equipped with diesel engines, have shown that these particles include remarkable amount of nucleation mode - and nanoparticles (diameter ~10-40 nm) right after the emission source that could be composed e.g. of metal or pyrolyzed hydrocarbon core (Virtanen et al. 2006; Meyer and Ristovski, 2007; Rönkkö et al., 2007). Studies of Rönkkö et al. (2007) and Meyer and Ristovski (2007) also showed that formation of these particles is dependent on the load of the engine (Meyer and Ristovski, 2007; Rönkkö et al., 2007). Soot particles of traffic emissions are approximately in the size range between 60 and 80 nm (Rose et al., 2005; Virtanen et al., 2006). The particle properties emitted from motor vehicles have been studied with several measurement techniques. Many of the assumption are based on size distribution, absorption and volatility measurements techniques (e.g. Philippin et al. 2004; Virtanen et al., 2006; Meyer and Ristovski, 2007; Sandradewi et al., 2008).

Small-scale wood fuel combustion includes several combustion techniques where fuel quality and operational practices vary remarkably. There are many factors influencing combustion conditions in various appliances and thus, particle emissions. Some examples are fuel seasoning, fuel pattern size and arrangement inside the chamber and possibility to affect primary and secondary combustion air supply. The emissions also depend on the phase of the combustion because biomass combustion rarely is operated continuously but can be divided into three phases: firing, combustion and burn out phase. The investigations have shown that particle emissions of small-scale wood combustion can

include remarkable amount of particulate organic matter (POM) and BC (or elemental carbon) that are basic tracers of incomplete combustion (e.g. Johansson et al., 2004; Lamberg et al. 2011). The influence of wood or other biomass combustion on the ambient air is also widely studied based on the known tracers such as ratio between BC or elemental carbon to organic carbon (OC) and monosaccharide anhydrides (e.g. Khalil and Rasmussen, 2003; Saarnio et al., 2012). If rather complete conditions with high combustion temperature are reached, such as in cases of modern pellet boilers, the chemical composition of emitted fine particles is reported to be dominated by inorganic ash species formed via evaporation-nucleation-condensation path (e.g. Davidsson et al., 2002; Sippula et al., 2009; Lamberg et al., 2011). Size distributions of small-scale wood combustion also vary depending on the appliance, fuel and combustion conditions. Previous studies have shown that particle size distributions (both number and mass) shift to larger particles and are wider as combustion conditions deteriorate when compared with the sufficient conditions (e.g. Tissari et al., 2009, Lamberg et al., 2011). Usually the number size distributions have a dominating mode in size range between 0.1 and 1 µm with geometric mean diameter in the range of 100 and 200 µm (Sippula et al., 2007; Tissari et al. 2009).

Large-scale combustion of fossil fuels, such as coal and heavy fuel oil, is better controlled than small-scale combustion. Large-scale burning techniques allow higher combustion temperature and better control of the fuel and air supply than small-scale combustion. Also oil burning in small boilers is fairly efficient because of e.g. developed burner technique and fuel supply. Thus, particle emissions of those sources do not usually contain significant amount of BC or OC but some exceptions are also reported (e.g. Cao et al., 2006; Bond and Bergstrom, 2006; Sippula et al. 2009). For example, Bond and Bergstrom (2006) showed that oil combustion could emit remarkable amount of absorbing particles. The research on particle emissions of large-scale combustion or overall on fossil fuel particle emissions is mainly concentrated on studies of ash forming elements, especially toxic ones and formation of particles from these elements (e.g. Linak et al., 2000; Ninomiya et al., 2004; Yoo et al., 2005; Sippula et al., 2009; Wang et al., 2010; Córdoba et al. 2012). Also size distributions of particle emissions of coal and oil burning have been studied (Linak et al., 2000; Ninomiya et al., 2004; Yoo et al. 2005; Sippula et al. 2009). Bond and Bergstrom (2006) also reported results of the light absorption due to particles emitted from residual oil burning. They concluded that these particles would have surprisingly high net warming effect. Particle emissions of trace elements are a bit different for coal and oil fuels but vary also depending on the ash content of coal or oil (Linak et al., 2000; Yoo et al., 2005). Some typical trace elements of particles emitted from coal combustion are reported to be Fe, Mg, Cu, As and Zn (e.g. Linak et

al., 2000; Reddy et al., 2005). The typical elements found from the oil combustion particle emissions are Al, K, Ba, Zn, Ca, Fe, V, Cu and As (e.g. Linak et al., 2000; Reddy et al., 2005; Wang et al., 2010). Particle mass or volume size distributions of fossil fuel emissions are reported to consist of two or three modes including a possible ultrafine mode (maximum at ~100 nm), a mode with maximum at ~1 µm and a coarse mode between 1 and 10 µm (Linak et al., 2000; Ninomiya et al., 2004; Sippula et al., 2009). Some clearly unburned residual particles have also been determined in particles >10µm (e.g. (Linak et al., 2000; Ninomiya et al., 2004). Ultrafine and fine particles of fossil fuel combustion are expected to be formed from vaporized and nucleated volatile heavy metals and fragmentation of inherent minerals (Linak et al., 2000; Ninomiya et al., 2004). The previous studies suggest that the coarse mode of particles emitted from fossil fuel combustion is composed primarily of unburned carbon char, inherent trace elements and fragments of inorganic (e.g. calcium-alumino-silicate) fly ash including trace elements (coal) (Linak et al., 2000; Ninomiya et al., 2004).

4 Theoretical background

4.1 Combustion appliances and cleaning techniques

4.1.1 Spark ignition and diesel engines of road traffic

Spark ignition (SI) and diesel engines are the most common sources of traffic-related particle emissions. SI vehicles are usually light-duty passenger cars whereas diesel vehicles include also heavy-duty traffic. The most commonly used fuels in the SI and diesel engines are gasoline and diesel that both are fractional distillates of petroleum oil.

The operation principles of the SI engines are based on the Otto cycle that converts pressure into a rotating motion with a four-stroke cycle (Flagan and Seinfeld, 1988, p. 227-229). The diesel engine differs from the gasoline powered Otto cycle by using highly compressed hot air to ignite the fuel instead of using a spark plug. There, air is supplied into the cylinder and compressed to high pressure leading to high temperature of the air. The sprayed fuel is injected into the high temperature compressed air. The fuel ignites and expansion of combustion gases lead to the power production to the crankshaft. (Flagan and Seinfeld, 1988, p. 269)

In the gasoline engines, air and fuel are mixed for the entire compression stroke, ensuring complete mixing of the air and fuel. Instead, diesel fuel is injected just before the power stroke. As a result, the fuel cannot burn completely unless it has a sufficient amount of oxygen. Inadequate oxygen

amount can result in incomplete combustion and black smoke in the exhaust. Diesel engines are known to produce more particulate emissions when compared with the emissions of the gasoline engines. On the other hand, diesel engines burn less fuel than gasoline engines performing the same work. Overall, motor vehicles emit hydrocarbons, carbon monoxide, NO_x, particulate matter (PM), Sulfur oxide (SO_x) volatile organic compounds (VOC) that all have negative effect on human health and environment.

Improved engine design has decreased vehicle emissions but tightened emission goals cannot be reached only with advanced engine technology. Thus, additional emission control technologies, such as secondary air injection, exhaust gas recirculation (EGR), catalytic converter and diesel particulate filter (DPF), are essential. Air injection is used to support the catalytic converter's oxidation reaction, and to reduce emissions when an engine is started from cold. The EGR is a NO_x emissions reduction technique used in gasoline and diesel engines. EGR recirculates a portion of exhaust gas back to the engine cylinders. The catalytic converter placed in the exhaust pipe converts hydrocarbons, carbon monoxide, and NO_x into less harmful gases by catalytic reactions (Flagan and Seinfeld, 1988, p. 266-269). The particulate matter (PM) emissions, including a larger amount of soot (black carbon, BC) produced by the diesel engines can be reduced using DPF technique where particles of the exhaust gas are trapped into the filter walls and burned. The combustion temperature needs to be high (~400-500ºC) to burn particles containing soot.

4.1.2 Small-scale wood fuel heaters and boilers

In developed countries, various small-scale heaters and boilers using wood fuels are used in households as primary but more often as secondary heating sources. Commonly used burning appliances include batch and continuous combustion appliances that can be used with different forms of wood fuels (e.g. wood logs, densified logs and pellets and wood chips). For example van Loo and Koppejan (2008) have described some common type small-scale combustion devices. Here, masonry heaters and pellet boiler were used as combustion source and these appliances will be described. Figure 1 shows simplified examples of operation principles of a conventional masonry heater and a top feed pellet boiler system.

Masonry heaters are wood batch burning devices that can be made of e.g. masonry products or soapstone. The heat production is based on the high mass of the appliance (~800-3000 kg) that stores and releases heat long after burning process. The released energy is typically between 40 and 100 kWh. These heaters usually consist of an upright firebox with a glass door. Combustion devices can be conventional or modern masonry heaters. Conventional techniques have a conventional grate

through which the main air is supplied. The only way to control the burning rate is by the main air supply through the ash box below the firebox grate. In a modern masonry heater, the primary and secondary airflows are controlled and directed to surround fuel batch to improve combustion efficiency and therefore, reduce emissions. In both types of the masonry heaters, the exhaust gas flows from the firebox to an upper combustion chamber, goes down through the ducts and into the chimney from the bottom or top of the heater.

Modern pellet boilers are integrations of the burner and the boiler. They are almost completely automated combustion appliances: The feeding of the pellets from the fuel tank to the burner and combustion air supply are usually automated. In addition, modern combustion appliances have heat control with O_2 sensors, movable grates and effective heat exchangers (Strehler, 2000). The boilers are operated based on the thermostat control that results in the intermittent operation of the burner. There are three typical burner types classified based on the feeding system: top-feed, under feed and side feed burners.

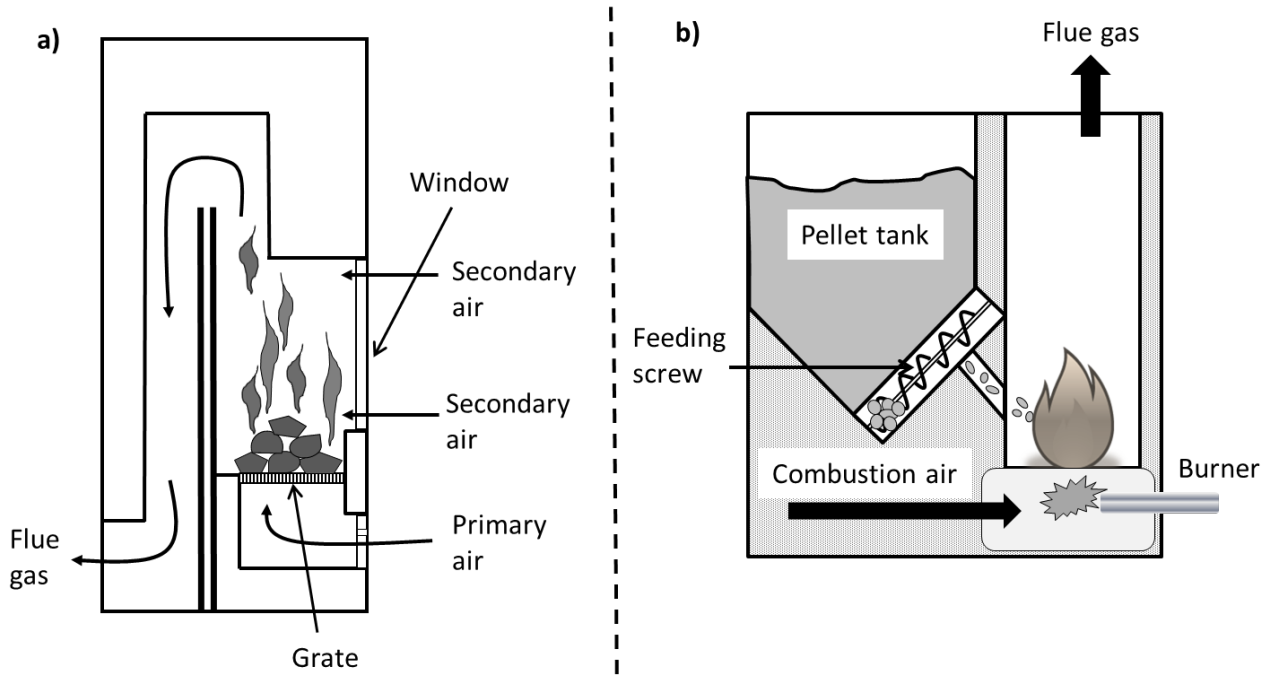

Figure 1 Schematic drawings of a) a conventional masonry heater and b) a pellet boiler system.

4.1.3 Heavy fuel oil-fired boilers

Heavy fuel oil (HFO)-fired boilers can be used for the production of district heat in large-scale combustion. Light fuel oil (LFO) is mainly used for the start-up of these plants because of clearly higher costs of LFO when compared with the costs of HFO. A common boiler configuration type is a water tube boiler. In a water tube boiler, water circulates in tubes heated externally by the

combustion flue gases. Fuel is burned inside the furnace, creating hot gas which heats water in the steam-generating tubes. (ASME, 2010). A simplified example of the boiler working principle is shown in Figure 2.

Heavy fuel oil needs to be preheated before the supply of the fuel into the furnace by burners. The preheated fuel is atomized to micrometer size droplets or vaporized by pressurizing it or by a mechanical spinning cup to allow stable combustion and minimum amount of unburned oil char. This atomized spray burns in the flame of the burner. The emissions of the HFO combustion can be influenced by combustion conditions and techniques: one of the major concerns is gas emissions of nitrogen oxides (NO). NO can be formed from nitrogen in combustion air in high temperatures (thermal NO) and from fuel-bound nitrogen (fuel-NO). Further, part of the NO reacts with oxygen and forms nitrogen dioxide (NO_2). In most cases, the fuel NO has a bigger influence than the thermal NO on NO_X (NO and NO_2) emissions. The low-NO_X combustion techniques are based on influencing known NO formation mechanisms. Thermal NO is reduced by flue gas recirculation that reduces flame temperature and oxygen concentration or by decreasing the air-fuel ratio below stoichiometric value. Stoichiometric value is the point where exactly all oxygen is consumed and all fuel burned. NOx emissions can be reduced by low air-fuel ratio, flame internal flue gas recirculation, flue gas recirculation and combustion air or fuel staging. (Finnish Environment Institute, 2001, p. 26)

More efficient burning of the sprayed fuel, especially when particle emissions are concerned, can be reached by water emulsion. The influence of emulsion can be explained by the occurrence of a “micro-explosion” of evaporating water. A “micro-explosion” creates numerous new auto-ignition centers of combustion, leading to more efficient burning. (Fu et al., 2002)

4.1.4 Coal-fired boilers

The operation principles of power generation in coal combustion plants are the same as in oil combustion: heat from the hot combustion gases in the furnace boils the water in the water tubes to produce the high-temperature, high-pressure steam. The steam is separated from boiler water and sent to the steam turbine.

Large-scale coal-fired boilers are widely equipped with pulverized fuel burners. Coal is first dried and ground in coal mills to fine powder to enable stable flame in all burners. The burners in the boiler can be located on one or two opposite walls (so-called wall firing, Figure 2) or in the furnace corners (so-called tangential firing) at multiple height levels. Pulverized combustion allows a high combustion temperature, which is important for the coal char to burn efficiently. High combustion

efficiency usually results fly ash with low unburned coal content (< 5 %). The drawback of the high combustion temperature in pulverized coal combustion is that it causes high primary NO and NO_2 emissions. These emissions can be minimized with modern low- NO_x burners. The low-NO_x burners operate at the under-stoichiometric combustion range (air/fuel ratio 0.85-0.95) and a high combustion temperature is needed to ensure ignition. (Finnish Environment Institute, 2001, p. 29) A simplified example of the operation principle of the coal fired boiler is shown in Figure 2.

Modern coal-fired power plants are nowadays often equipped also with technologies that reduce particle and sulfur emissions. Flue gases after furnace can be passed through an electrostatic precipitator that removes effectively particles from the flue gas (Miller, 2011, p. 438-442). In addition, the plant can include flue gas desulfurization (FGD) process that cleans flue gas for remained particles and sulfurdioxide. In the FGD, calciumhydroxide (or lime) is mixed into the flue gas passing the desulfurization area to decrease sulfurdioxide concentration (Miller, 2011, p. 388-390). Further, fabric filters can be installed after desulfurization part to reduce particles drifted through the previous processes and formed in the desulfurization reactions (Miller, 2011, p. 447-450).

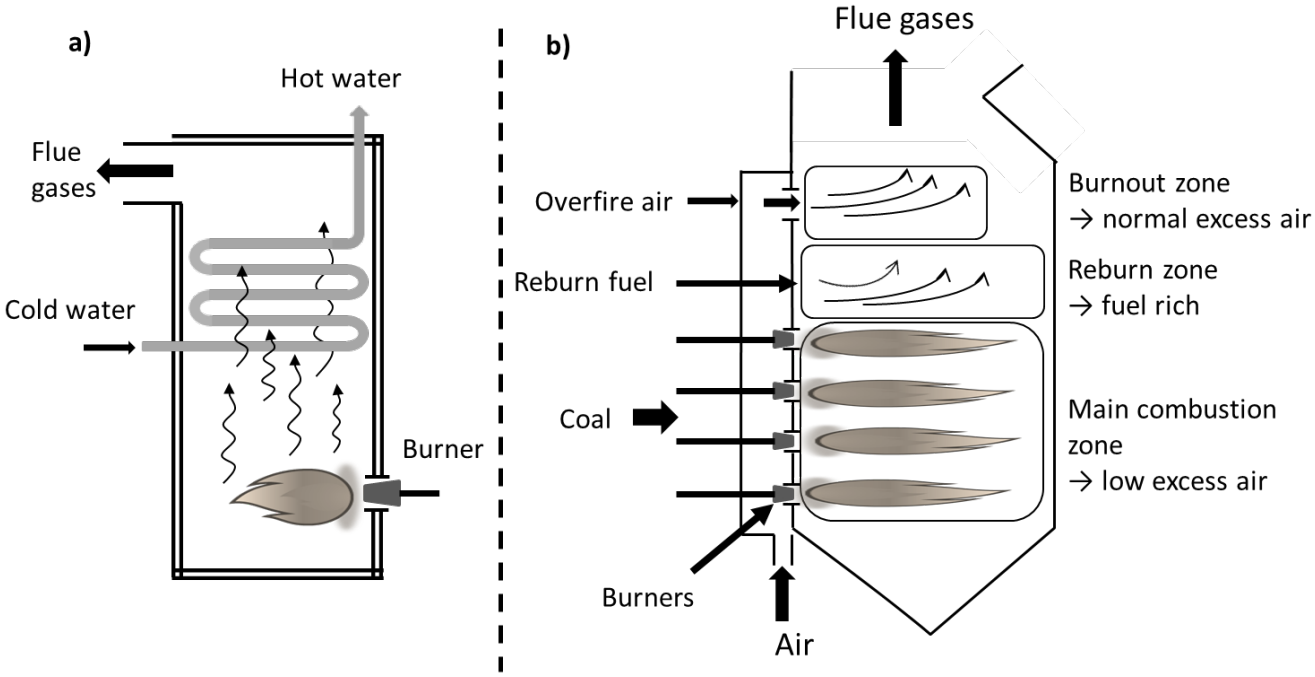

Figure 2 Simplified illustrations of a) an oil fired water tube boiler and b) a pulverized coal fired boiler equipped with front wall boilers (based on presentation of Xu et al., 2010).

4.2 Formation of particle emissions of combustion processes

In a combustion process, the reaction of a fuel with oxygen produces heat energy. To get to this point, the fuel first needs to get through drying and pyrolysis phases. Drying phase consumes heat but within pyrolysis and combustion, heat is released more than used. In the complete combustion, only CO_2 and H_2O are produced. However, hardly ever burning process is complete leading to formation of unwanted combustion products both in gaseous and liquid or solid particle form. The interest within this thesis was in the formation of particles during combustion processes. A simplified description of formation of soot, inorganic ash and organic aerosol particles in a combustion process is shown in Figure 3. Naturally, the formation paths depend on the fuel and combustion appliance but Figure 3 represents the most probable cases.

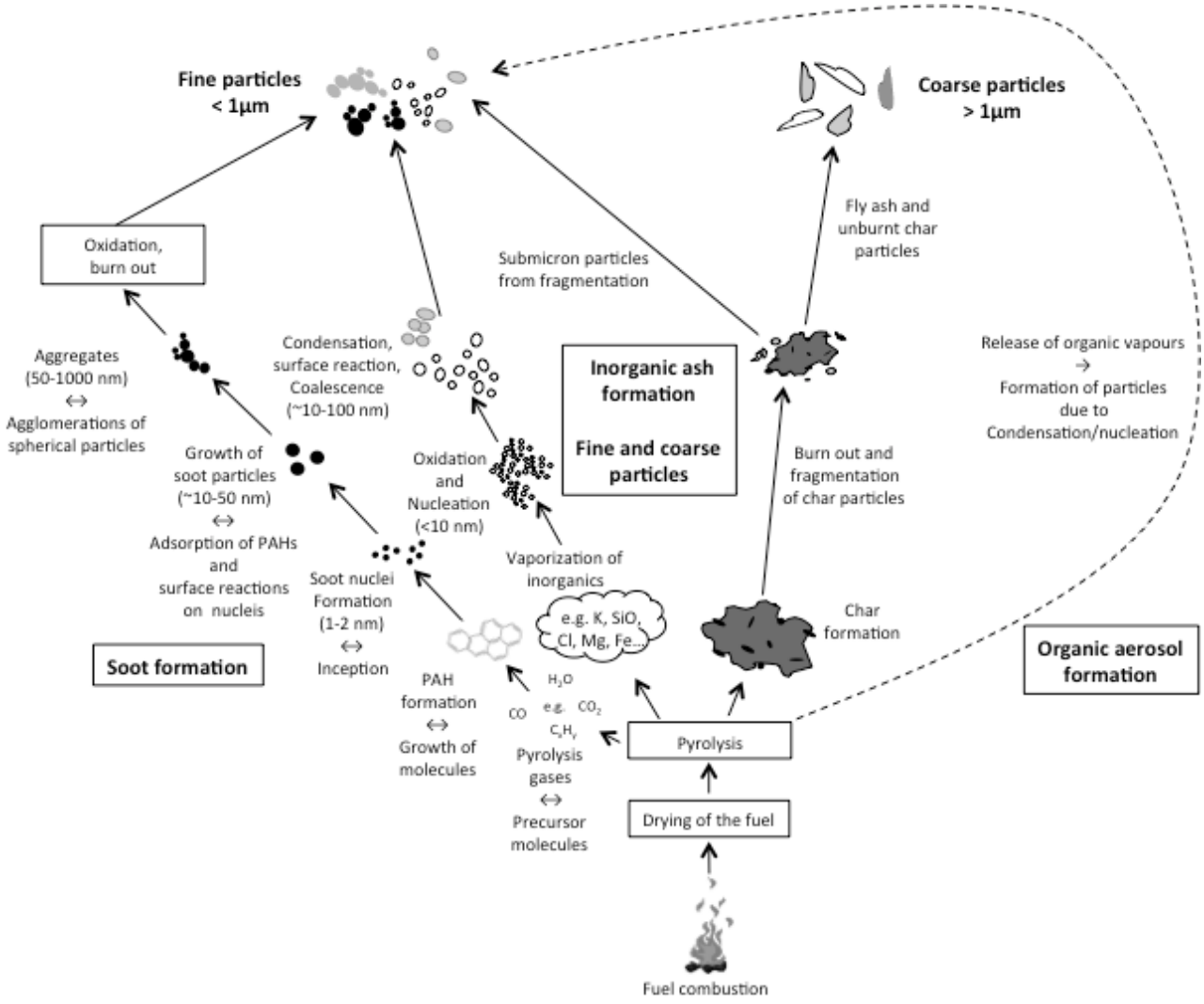

Figure 3 Description of particle formation via various production paths according to Haynes et al. (1982), Bockhorn (1994) and Linak and Wendt (1994).

4.2.1 Gaseous emissions and organic particles

Typical gaseous emissions from combustion processes are carbon dioxide (CO_2), nitrogen oxides (NO_x), sulfur oxides (SO_x), carbon monoxide (CO) and organic compounds that can occur both in gaseous and particle phase. The composition of gaseous compounds of the flue gas depends on fuel and combustion technique. CO_2 emissions of wood combustion are considered to be compensated by bounding of the gas when growing. Instead, fossil fuels are not renewable and thus, CO_2 emitted by them increase greenhouse gas concentration in the atmosphere.

In burning process, both nitric oxide (NO) and nitrogen dioxide (NO_2) are produced but majority of NO_x is emitted as NO and further converted to NO_2 in the flue gas and atmosphere. NO can be formed from the fuel and from the atmospheric nitrogen (N_2). Formation of NO due to oxidation of N_2 requires high combustion temperature and thus, e.g. in the small-scale wood combustion appliances this path is unlikely. (e.g. Flagan and Seinfeld, 1988, p. 167-200; Miller and Tillman, 2008, p. 21)

SO_x gas emissions are formed from the sulfur species of the fuel (e.g. pyrite (FeS_2) in the coal or organic sulfur forms). Sulfur is oxidized to SO_2 and further to SO_3 that is corrosive to the boilers. In addition, SO_3 may react with water to form sulfuric acid (H_2SO_4). SO_x compounds are also involved in the formation of fine ash particles. (e.g. Flagan and Seinfeld, 1988, p. 217-221; Miller and Tillman, 2008, p. 21)

CO emissions are likely in the insufficient combustion conditions. CO can be oxidized only if sufficient air is mixed with combustion gases at high temperatures. Thus, CO levels are high in low combustion temperatures and in the fuel-rich conditions. Also hydrocarbon emissions are consequence of incomplete burning. Fuel and lubricant evaporation, that are non-combustion sources of hydrocarbons, is major contributor to the hydrocarbon emissions. (Flagan and Seinfeld, 1988, p. 201-217). Polycyclic aromatic hydrocarbons (PAH) are a significant class of combustion-generated hydrocarbons because of their toxicity (e.g. Kaivosoja et al., 2013). They are formed in the fuel-rich flame areas when hydrocarbons polymerize instead of oxidizing (Flagan and Seinfeld, 1988, p. 215).

Also emissions of organic compounds (organic carbon, OC), that occur both in gas and particle phase, indicate the combustion conditions and techniques. In incomplete combustion, organics may condensate onto existing particles or form new particles by nucleation (e.g. Rönkkö et al., 2007; Shi and Harrison, 1999). These freshly emitted organics are primary organic aerosols (POA). When the flue gas cool after combustion chamber, emitted organics form secondary organic aerosols (SOA)

by oxidation of gas-phase precursors. The gas-particle partitioning of the organics depends on the volatility distribution of the organic emissions (Robinson et al., 2007).

4.2.2 Ash particles

The ash produced in combustion processes arises from noncombustible mineral inclusions in the fuel and from heteroatoms (i.e. molecules that do not include carbon or hydrogen) of the fuel molecules. Ash particles include inorganic constituents of the fuel such as silicon, aluminum, iron, calcium, magnesium, sodium and potassium. These often are expressed as oxides but can form other chemical compounds as well. Also trace metals, such as cadmium, chromium, lead, copper, nickel, vanadium and zinc, present in various fuels are found from the ash particles. The behavior of inorganic species in the combustion processes is highly dependent on the combustion temperature because of susceptibility of these species to temperature (Miller and Tillman, 2008, p. 22). There are two major mechanisms for the evolution of ash particles: residue particle formation and ash particle formation through vaporization-nucleation paths. Residue ash particles remain when carbon burns out in the combustion process. The smallest ash residue particles in the flue gases are mineral inclusions of the unburned fuel. These inclusions can also agglomerate to form larger particles. Further, these ash agglomerates may melt in high temperature and coalesce to form large droplets of molten ash on the surface of the burning char. The ash particles formed via vaporization-nucleation path are smaller than ash residue particles. Here, the ash vaporizes in high combustion temperature. Part of this volatilized ash forms very small particles by homogeneous nucleation that further grow by coagulation and condensation of additional vaporized ash. As the flue gases cool, these particles form solid particles that may coagulate with each other to produce chain agglomerate structure. (Flagan and Seinfeld, 1988, p. 358-361).

4.2.3 Soot particles

The formation process of soot is still not well understood e.g. due to the complexity of hydrocarbon chemistry in the flame. Basically, soot particles form in insufficient burning conditions with lack of combustion air, poor mixing of air and combustion gases and low combustion temperature. Soot particles are mainly composed in the fuel-rich areas of the flame from hydrocarbons (e.g. polycyclic aromatic hydrocarbons (PAHs)). The formation process begins with pyrolysis of the fuel leading to transition of flue gas components from the gas phase to a solid phase. This process occurs with an extremely complex nature of conversion of the hydrocarbon fuel molecules containing a few carbon atoms to carbonaceous particles containing a few millions of carbon atoms. The smallest particles are first formed by coagulation of PAHs. After that, the soot concentration increases as a result of adsorption of PAHs and especially as a result of particle surface reactions that increase this surface.

This process involves hydrogen detachment and carbon attachment. The primary particles coagulate into large aggregates (size range of 0.01-0.1 μm) including small spherical particles. (Mansurov, 2005; Flagan and Seinfeld, 1988, p. 373)

Soot absorbs light efficiently and therefore often the term black carbon (BC) is used as a synonym of soot although the definition of BC is unclear. Actually soot contains both organic and elemental carbon (OC and EC). They are measured using thermal methods leading to an instrumental definition of these components. BC is measured with techniques based on light transmission through a filter because of its light absorbing character (e.g., Aethalometer, the Multi-Angle Absorption Photometer (MAAP) and Particle Soot Absorption Photometer (PSAP)). (e.g. Andreae and Gelencsér, 2006; Bond and Bergstrom, 2006). This technique leads to determination of absorption coefficient that is converted to BC mass concentration based on mass absorption efficiency (MAE) that depends on the wavelength of light, size distribution and chemical composition of particles of the sample air. Usually, this factor is assumed to be constant. In this thesis, BC is also refereed as absorbing material when filter based techniques were used.

4.2.4 External and internal mixture of particles

Particles are usually externally mixed immediately after emission. In this state, an individual particle compose of one component or compound (e.g. soot, metallic compounds). During aging, externally mixed particles may coagulate with other particles or get coated with chemical compounds like sulfates, nitrates or organics by condensation and thus get internally mixed.

5 Experimental

5.1 Measurement sites

The measurement campaigns of this thesis composed of campaigns studying chemical and physical properties of particles emitted from various combustion sources. The campaign determining particle emissions of engines used in traffic differed from the other campaigns being the only one where measurements were conducted for the ambient air. The campaigns studying small-scale biomass combustion where performed in laboratory conditions for the fresh primary particle emissions. Primary emissions of large-scale oil and coal combustion were investigated at a district heating station fired by HFO and a coal fired heat and power plant. The description of the campaigns is given in Table 1.

5.1.1 Ambient air influenced by traffic emissions

The measurements were done from December 22, 2005 to January 15, 2006 on the roof of the Leibniz Institute for Tropospheric Research (IfT) in Leipzig, Germany. The site is located on the outskirts of Leipzig, between heavily trafficked roads but far enough of these so that for most of the time the air can be considered representing urban background. A PM_{10}-inlet was used upstream all the instruments to allow sampling of particles with diameters below 10 μm.

5.1.2 Small-scale wood and wood pellet combustion

Particle emissions of small-scale wood fuel burning appliances were studied in two campaigns that were performed in laboratory conditions. Two commercially available conventional masonry heaters and a top-feed fuelled pellet boiler with integrated fixed grate burner were used in the experiments. The combustion conditions mimicked real life situation with accurate control of burning conditions. The combustion appliances (masonry heaters (MH) and pellet boiler (PB), Papers II and III) were situated on a balance for control of fuel mass flow. The flue gases were conducted through the stack that was placed below a hood with a flue gas fan. The draught in the stack was adjusted with the hood and flue gas fan to mimic natural draught conditions. The fuel flow rate, stack pressure and temperature of combustion gases were measured continuously. In addition, concentrations of different combustion gases, like organic gaseous carbon compounds (OGC), NO, NO_2, CO, CO_2 and O_2, were measured and recorded.

5.1.3 Coal-fired heating and power plant

Paper III included experiments at a coal-fired heating and power plant (C-PP) that operated on average with nominal power of 300 MW. The boiler of the plant was a natural circulation steam boiler equipped with front-wall HTNR burners (high temperature NO_X reduction burners). Burners were high temperature NO_X reduction (HTNR) burners that enabled combustion of pulverized coal and HFO. This low-NO_X-technology was in use to minimize nitrogen oxide (NO_X) emissions. The flue gases were cleaned for particles and sulfurdioxide in a cleaning system containing an electrostatic precipitator (ESP) and a desulfurization plant (DSP) comprising of semi-dry flue gas desulfurization (FGD) and fabric filters. The plant was fuelled by coal or mixture of coal and pellet (pellet content 4.5 ± 1.4 % of the total fuel volume).

The particle emissions of the coal combustion were measured in the smokestack at 35 meter height. The results of the coal-fired power plant experiments were based on the emissions during steady state operation. The influence of the DSP on particle emissions was investigated bypassing the DSP.

5.1.4 Heavy fuel oil-fired heating station

Particle emissions of a HFO-fired heating station (HFO-HS) operated with two various oil-fired water tube boilers were investigated at different operation conditions (Paper III and IV). The boilers were equipped with rotary cup type burners. The nominal outputs of the boilers were 120 MW and 47 MW (Paper III and Paper IV, respectively). In the study of Paper III, the boiler was operated at 78 MW fuelled by HFO, at 78 MW fuelled by HFO with water emulsion and at 120 MW fuelled by a mixture of HFO (84 %-w) and light fuel oil (LFO, 16 %-w). In the experiments of the Paper IV, the boiler was operated at 30 MW power. There, the properties of particle emissions were determined for the following combinations of the fuel and combustion conditions: HFO combustion, HFO combustion with emulsion and combustion of mixture of HFO and LFO with emulsion. The particle sample flows in the investigations of the Paper III and IV were taken from the flue gas tunnels approximately 10 or 20 meters (Paper III and IV, respectively) after the boilers and particle instruments were situated ca. 10 meters below the flue gas tunnel and dilution system.

Table 1 Description of the campaigns of this thesis.

Paper	**I**	**II**	**III**	**IV**
Experiment type	urban background influenced by traffic	combustion laboratory	combustion laboratory, C-PP[1] (smokestack), HFO-HS[2]	HFO-HS[2]
Emission source	gasoline/diesel engine	MH[3]	MH[3], PB[4], C-PP[1], HFO-HS[2]	HFO-HS[2]
Abbreviation of campaign		SSWC1	SSWC2, C-PP, HFO-HS1	HFO-HS2
Fuel	gasoline/diesel oil	wood logs (pine)	wood logs, wood pellet, coal and coal+wood pellet, HFO and LFO	HFO and LFO
Measurement type	continuous measurements, 22nd Dec 2005 -15th Jan 2006	batch combustion; normal and smouldering	various combustion sources, steady state operation	comparison of fuels and operation conditions, steady state operation
Dilution	-	dilution tunnel, DR 180:1-330:1	dilution tunnel (DT) and DT+ejector diluter (ED), fine particle sampler (FPS), DR 20:1-2450:1	FPS, DR 60:1

[1]C-PP= coal-fired heating and power plant, [2]HFO-HS= heavy fuel oil-fired heating station, [3]MH= masonry heater, [4]PB= pellet boiler

5.2 Dilution of sample flow

In the studies of small-scale wood and wood pellet combustion (Papers II and III), the combustion air from the stack was first diluted in a dilution tunnel (DT) according to the ISO 8178-1 standard (Sippula et al., 2007). The dilution was done with dry, particle-free air. Also nitrogen oxides and hydrocarbons were filtered from the dilution air. The dilution ratio (DR, typically between 50 and 300) of the DT was adjusted controlling the flow rate and low pressure of the tunnel. The DT dilution was used for the filter sampling methods such as virtual impactor (VI) and PM_1 sampler presented in Sections 5.5.1 and 5.5.3 (Papers II and III). The optical instrumentation presented in Paper III needed additional dilution because of the determination limits of the measurement techniques. Therefore, an ejector diluter (ED, Dekati Ltd., Lyyränen et al., 2004) was installed after the DT. The DR of the ED was approximately eight.

The sample air at the coal fired power plant of Paper III was diluted with a fine particle sampler dilution system (FPS-4000, Dekati Ltd., Tampere, Finland; perforated tube and ejector) including a control unit to reach measurable particle concentrations for the instruments used in the study. The control unit calculates the dilution ratio based on monitored temperature and pressure differences within the dilution system. The FPS allows dilution ratios between 20 and 200. In the study of Paper III, the DR varied between 18 and 45.

At the HFO-fired heating station (Paper III and IV), the sample flow was diluted with a fine particle sampler (FPS-4000, Dekati Ltd.). The dilution ratio was in the range 55-62.

5.3 Measurements of particle optical properties

Instruments measuring particle optical properties were used in the studies of Papers I and III. They were used to characterize absorption and scattering of light by the particles that are important properties when climatic effects of particles are discussed. In addition, absorption measurements were used to estimate the content of black carbon (BC) in the particle emissions. The specifications of the optical instrumentation used in the studies of this thesis are shown in Table 2.

PSAP. 3-wavelength particle soot absorption photometer (3λ PSAP, Radiance Research) was used in Paper III for estimation of contribution of absorbing material to emission particles. The measurement of absorption is based on transmission of light through filter material (Bond et al., 1999; Virkkula et al., 2005). The transmission is measured by wavelengths of 467, 530 and 660 nm.

MAAP. In the Papers I and III, a multi-angle absorption photometer (MAAP; Thermo Fisher Scientific Inc., Model 5012) was used to determine absorption coefficient (σ_{AP}) and BC mass

concentration (M_{BC}) of particles. The MAAP determines absorption coefficient of the particles deposited on a filter by a simultaneous measurement of transmitted and backscattered light (Petzold and Schönlinner, 2004). The instrument uses wavelength of 637 nm determined by Müller et al. (2011). The σ_{AP} is converted to the M_{BC} with mass absorption efficiency (MAE) of 6.6 $m^2\ g^{-1}$.

The principles of absorption coefficient (σ_0) measurements are based on the Beer-Lambert law:

$$\sigma_0 = \frac{A}{V} \ln \frac{I_{t-\Delta t}}{I_t} \quad (1)$$

where A is the area of the sample spot, V is the volume of air drawn through the spot area during a given time period Δt, and $I_{t-\Delta t}$ and I_t are the filter transmittances before and after the time period. The resulting absorption measured by filter-based methods is not straightforward: measured absorption is influenced by transmission decrease affected by filter loading and scattering particles that decrease amount of transmitted light through the filter leading to underestimation of absorption coefficient. In the MAAP this problem is solved by measuring the decrease of transmission and also light scattering from the aerosol-filter system. The data evaluation algorithm includes multiple-scattering effects into the analysis of the aerosol-filter system (Petzold et al. 2002, 2005). Instead, the PSAP results need to be corrected afterwards because there is no determination of backscattered light from the filter. The scattering correction demands also determination of scattering coefficient (see Section 5.7.4). The correction algorithms are presented e.g. by Bond et al. (1999), Virkkula et al. (2005) and Virkkula (2010).

Nephelometer. Scattering coefficients (σ_{SP}) at wavelengths 450, 550 and 700 nm were measured using a TSI nephelometer (Model 3563) (Anderson et al., 1996; Anderson and Ogren, 1998).The instrument is an integrating nephelometer that provides a direct method to determine light scattering by particles based on Beer-Ambert law. The sample air is led into the sample volume where it is illuminated over angle range from 7 to 170º. The instrument determines scattering and backscattering of the light and also corrects the results for the scattering influenced by gas phase, background and scattering influenced by the walls of the instrument. Because scattering measurement angle range is limited, the results need to be truncation corrected afterwards (Anderson and Ogren, 1998) (see Section 5.7.4).

5.4 Particle number and volume size distribution measurements

Real-time measurements of particle number and volume size distributions were done in Papers I, III and IV. In Paper I, number and volume size distributions were used to fit the size distributions of less volatile particles determined by a VTDMA (see Section *VTDMA*) and for the Mie calculation to

model the scattering and absorption coefficients. The information of the instruments is presented in Table 2.

DMPS/SMPS. A differential and scanning mobility particle sizer (DMPS and SMPS) are systems for particle size distribution measurements. These instrumentations consist of a differential mobility analyzer (DMA) and a condensation particle counter (CPC). The operation of the system is based on electrical mobility of particles: polydisperse charged aerosol is lead through an electrical field between two cylinders with sheath flow. Particles with higher electrical mobility (small size) will diffuse on a cylinder because of electrical forces affecting between opposite charges between particle and cylinder. Particles with low mobility (large particles) are not affected as strong by the electrical field and they will be lead out from the DMA with excess flow. Particles with certain mobility, and thus certain size, will be allowed to penetrate DMA. The penetrating particle size can be chosen changing the voltage of the DMA. The DMA can be operated two ways: first, the DMA voltages are stepped in distinct increments yielding a discrete, channel-wise size distribution (DMPS). Alternatively, the same hardware set-up may be operated as a scanning mobility particle sizer (SMPS, Wang and Flagan, 1990) which involves a quasi-continuous ramping of the DMA voltage. After DMA, classified particles are detected and counted by a CPC. The CPC detects particles optically. Before optical counting, particles need to be enlarged to be detectable. This is done by saturating particles by water or alcohol vapor (e.g. butanol) leading to an increase of particles.

In the studies of this thesis, different size ranges were determined with various combinations of DMA and CPC models. In Paper I, the twin-DMPS presented by Birmili et al. (1999) consisted of two Hauke-type DMAs and CPCs (TSI, Models 3025 and 3010) that determined mobility particle size range of 3-800 nm. In the campaigns of Paper III, two different SMPS instrumentations were used: DMA 3071 with CPC 3775 (mobility size range 10-414 nm) and DMA 3085 with CPC 3025 (mobility size range 2-163 nm but in the study, particle sizes larger than 10 nm were considered reliable) (TSI Inc.). In Paper IV, two SMPS were used to measure mobility size range 3–400 nm. The instrumentation consisted of a DMA 3071 with CPC 3775 (TSI Inc.) and a DMA 3085 with CPC 3025 (TSI Inc.).

VTDMA. A volatile tandem differential mobility analyzer (VTDMA, Philippin et al., 2004) is an application of DMPS that enables determination of volatility of size segregated particles. It consists of two Differential Mobility Analyzers (DMA), two Condensation Particle Counters (in Paper I, CPC, TSI Model 3010), and a heating unit. The heating unit includes two parallel heating tubes that

are held at temperatures of 25 and 300ºC. In the first DMA, monodisperse particles are selected from the polydisperse aerosol. The total number concentration of the initially selected particles is measured with a CPC. Next the monodisperse aerosol passes through the heating tubes. At 25ºC the particles remain unchanged and the VTDMA measurement acts as a reference of behavior of untreated aerosol particles while at 300ºC volatile compounds such as sulfates, nitrates, and most of the organic carbon will evaporate. In the last step, the number size distribution of non-volatile particles, divided into the number of more and less volatile particles, is measured by using a second DMA/CPC combination. The residual particles that are non-volatile at 300ºC are usually clearly separated in two modes (Wehner et al. 2004), representing either externally mixed non-volatile particles that do not shrink significantly during the heating (less volatile particles), or particles that evaporate partly in the heating unit and are then smaller than before heating. These so called more volatile residual particles may consist for instance of aged, coated soot or other non-volatile particles such as polymers. In Paper I, the initial particle sizes 20, 30, 50, 80, 150, and 250 nm were chosen for the VTDMA treatment. The measured size distributions (at 25 and 300ºC) were corrected for the CPC counting efficiency and for particle losses due to thermophoresis and diffusion in the VTDMA using an empirically determined loss function that depends on the particle size and heater temperature.

HTDMA. In a hygroscopic tandem differential mobility analyzer (HTDMA, Swietlicki et al, 2008) a certain particle size is chosen from the particle size distribution with the DMA (in Paper IV, DMA 3085, TSI Inc.) after which the sample is subjected to chosen relative humidity. The second DMA (in Paper IV, short Vienna type) and the following CPC (in Paper IV, CPC 3025, TSI Inc.) then work as an SMPS and measure the particle size distribution after the humidity conditioning. Thus, the HTDMA measured the hygroscopic growth of emitted particles providing additional information about their behavior in the atmosphere. A HTDMA was used in the experiments of Paper IV. There the hygroscopicity of particles was studied for particle diameters of 20, 47 and 72 nm in ca. 90 % relative humidity.

Thermodenuder. A thermodenuder (TD) can be used to remove volatile and semivolatile compounds from the particles. In the TD, the sample is led through a heater where the volatile compounds are evaporated. After the heater, the evaporated compounds are gradually cooled and absorbed into active charcoal to allow only nonvolatile part of the particles to pass the system. In studies of Paper IV, a TD was set prior HTDMA and size distribution measurements. The sample was alternately measured with and without TD.

FMPS. A fast mobility particle sizer (FMPS, TSI Inc., Model 3091) measures particles in the mobility size range from 5.6 to 560 nm. The particles are positively charged using a corona charger. Charged particles are introduced to the measurement column where they flow downwards near the high voltage electrode column with filtered sheath airflow. The electrode is positively charged creating an electric field that repels the particles outward according to their electrical mobility. Outward of the column, there are low-noise electrometers that are struck by charged particles. The charges of particles are detected by electrometers. A particle with high electrical mobility is detected by an electrometer near the top of the column whereas particles with low electrical mobility are introduced further in the measurement column.

ELPI. The Electrical Low Pressure Impactor (ELPI, Dekati Inc., Keskinen et al., 1992) is a real-time particle size spectrometer for real-time monitoring of particle size distribution. The ELPI measures particle size distribution in the size range of 0.03-10 µm with 12 channels. With filter stage the size range can be extended down to 7 nm (Marjamäki et al., 2002). The main components of the instrument are a corona charger, low-pressure cascade impactor and multi- channel electrometer. Particles of the sample flow are first electrically charged by the corona charger. These particles are then inertially classified based on their aerodynamic diameters in the low-pressure cascade impactor. The electrical current produced by charged particles is detected from the electrically insulated impactor stages equipped with the electrometers. The current value of each channel is proportional to the number of particles collected, and thus to the particle concentration in the particular size range. The current values are converted to a (aerodynamic) size distribution using particle size dependent relations describing the properties of the charger and the impactor stages.

APS. An aerodynamic particle sizer (APS, TSI Inc., Model 3321) was used in the studies of this thesis to measure particles in size range from 0.5 to 20 µm. The operation principle of the instrument is based on the acceleration of particles by sheath airflow in a nozzle and analyzing the time-of-flight of different particle sizes. APS measures particle number size distribution in size range between 0.5 and 20 µm (aerodynamic diameter).

The DMPS, SMPS and FMPS measure the particle mobility diameter (D_n) which equals the geometric diameter (D_p) for spherical particles (e.g. DeCarlo et al., 2004) but the APS measures the aerodynamic diameter (D_a). When these quantities are handled together, the relationship between them needs to be taken into account. This relationship is presented by Equation 2 (e.g. Hinds, 1999):

$$\frac{D_a}{D_p} = \left(\frac{C_c(D_p)}{C_c(D_a)}\right)^{1/2} \left(\frac{\rho_p}{\rho_0}\right)^{1/2} \quad (2)$$

where $C_c(D_p)$ and $C_c(D_a)$ are slip correction factors of geometric and aerodynamic diameters, ρ_0 is the unit density (1 g cm^{-3}) and ρ_p is the particle density.

Table 2 Specification of the real-time instruments used in this thesis.

Instrument	Manufacturer	Quantity	Unit	Paper
3λ PSAP	Radiance Research, Seattle (WA), USA	σ_{AP}	Mm^{-1}	III
MAAP 5012	Thermo Fisher Scientific Inc., Waltham, MA, USA	σ_{AP}, M_{BC}	Mm^{-1}, $\mu g\ m^{-3}$	III, IV
Nephelometer 3563	TSI Inc., Shoreview, MN, USA	σ_{SP}	Mm^{-1}	I, III
Twin-DMPS (Hauke-type DMAs + CPCs 3025 and 3010)	CPC: TSI Inc., Shoreview, MN, USA	number/volume size distribution	# cm^{-1}/ $\mu m^3\ cm^{-3}$	I
SMPS (DMA 3071+CPC 3775, DMA 3085+ CPC 3025, DMA 3081+CPC 3025)	TSI Inc., Shoreview, MN, USA	number/volume size distribution	# cm^{-1} /$\mu m^3\ cm^{-3}$	III, IV
VTDMA (2 × DMA + CPC 3010)	CPC: TSI Inc., Shoreview, MN, USA	number/mass size distribution	# cm^{-1} /$\mu g\ m^{-3}$	I
HTDMA (DMA 3085, Hauke-type DMA + CPC 3025)	DMA 3085: TSI Inc., Shoreview, MN, USA CPC: TSI Inc., Shoreview, MN, USA	Number size distribution	# cm^{-1}	IV
FMPS	TSI Inc., Shoreview, MN, USA	number/volume size distribution	# cm^{-1} /$\mu m^3\ cm^{-3}$	II
ELPI™	Dekati Inc., Tampere, Finland	volume size distribution	$\mu m^3\ cm^{-3}$	IV
APS 3321	TSI Inc., Shoreview, MN, USA	number/volume size distribution	# cm^{-1} /$\mu m^3\ cm^{-3}$	I, III

5.5 Sampling systems

Particle samples of this thesis were collected with various sampling techniques to analyze particle mass concentration and chemical composition. Both size distribution samples and samples of e.g. PM_1 or $PM_{2.5}$ were taken. Size classification of the samplings is usually based on inertia of particles. The inertia increases with increase of particle size. The sample flow is accelerated in a nozzle that is followed by a flat plate directed horizontally with the flow. The streamlines of the sample flow pass the plate. Depending on the inertia of particles that is dependent on aerodynamic diameter, particles either follow the streamlines or impact on the plate. As the diameter of the nozzle is decreased the flow is accelerated and smaller particles are collected on the plate.

5.5.1 Virtual Impactor

In a virtual impactor (VI, Loo and Cork, 1988), impaction plate is replaced by a nozzle followed by filter holder for the sample collection. The sample flow is divided into a major and minor flow with the portions of 90 and 10 % from the total flow, respectively. The main flow is curved whereas the minor flow follows straight streamlines. Particles with higher inertia follow the minor flow and the smaller particles are directed into the major flow line. The nozzle size determines the cut-off diameter of the VI. The filter holders are placed after major and minor flows. Thus, the VI separates sample flow into two size classes. In this thesis, VI with cut-off diameter of 2.5 µm was used in Paper II. The total flow rate in the study was 16.7 l min^{-1}.

5.5.2 Small deposit area impactor

Small deposit area impactor (SDI, Maenhaut et al., 1996) is a low pressure cascade impactor where several impactor stages with different cut-off sizes are operated in series. The SDI segregates the particle sample into 12 size classes. With the flow rate of 11 l min^{-1} the aerodynamic cut-off diameters of the SDI are 0.045, 0.088, 0.142, 0.235, 0.380, 0.580, 0.800, 1.06, 1.61, 2.60, 4.07 and 8.40 µm.

5.5.3 PM_1 sampling system

In the studies of this thesis, PM_1 samples were collected using a combination of a filter cassette (Gelman Science) and a Berner low pressure impactor (BLPI, Berner and Lürzer, 1980; Saarikoski et al., 2008). The BLPI is a cascade impactor and here it determines the cut-off diameter. In order to collect the submicrometer particle size fraction of PM only (aerodynamic particle diameter <1µm, PM1), the five upper stages (7–11) of the BLPI were installed prior to the filter to remove supermicrometer particles. The cut-size of the preimpactor (D50) is determined by the lowest stage, the others are used to divide the PM loading to several stages and to ensure removal of particles

well above the lowest cut-size. Here, the cut-off size of 1µm was reached with flow rate of 25 l min^{-1}.

5.5.4 Micro-orifice uniform deposit impactor (MOUDI)

Micro-orifice uniform impactor (MOUDI) is a cascade impactor that segregates particles into nine size classes within the size range from 0.056 to 10 µm (Marple et al., 1991). A back-up filter can be used below the MOUDI to sample the particles smaller than 0.056 µm. The sample flow rate is 30 l min^{-1}. A rotating nano-MOUDI (model 125B, MSP Corporation, Shoreview, MN, USA) (Marple and Olson, 1999) is an advanced version of the MOUDI. It segregates particles into 13 size channels in the size range of 0.01-10 µm. A back-up filter below the lowest stage collects particles smaller than 0.01 µm. The rotation of the sampling stages during the sampling allows uniform samples for the chemical analysis. The flow rate of the instrument is 10 l min^{-1}.

5.6 Chemical analysis of filter samples

Chemical composition of particles emitted from various sources was determined from the samples collected within the Papers II, III and IV. The samples were collected using the samplers described in the section 5.5.

5.6.1 Filters and sampling substrates

Polytetrafluoroethylene (PTFE) filters. Polytetrafluoroethylene (PTFE) filters (Millipore, 3.0 µm, FSLW04700) with a diameter of 47 mm were used in the VI, PM_1 samplers and nano-MOUDI. PTFE filters were gravimetrically analyzed before and after sampling for determination of total mass concentration of the particles (Mettler M3-microbalance, Mettler Instrumente AG, Zurich, Switzerland). The handling and weighing of the PTFE-filters have been described in detail by Sillanpää et al. (2005) and Sillanpää et al. (2006). Within this thesis, chemical analysis of PTFE filters included major ion, monosaccharide anhydrides (MA), water soluble organic carbon (WSOC) and trace element analysis.

Quartz filters. Quartz filters (Whatman, QM-A, 47 mm diameter) were used in the study of Paper II for the analysis of elemental, organic and water soluble organic carbon (EC, OC and WSOC, respectively) of the VI samplings. In addition, quartz fiber substrates for the SDI (diameter 21 mm) were punched from quartz filter sheet (Whatman, QM-A). The quartz filters and substrates were purified by keeping them at 550 ºC approximately 5 hours. Because quartz material was used to determine the fraction of organic compounds in the particles, the organic vapors were removed from the sample flow setting three annular denuders (URG-2000, 30×242 mm, Chapel Hill, NC, USA) coated with XAD-4 material before the samplers (Gundel et al., 1995).

Polycarbonate filters. Samples for elemental, ion and monosaccharide anhydride analysis were collected on polycarbonate film and filters in the samplings done with the SDI and nano-MOUDI in the Papers II and III. In the SDI sampling, 21 mm diameter punched polycarbonate film (Nuclepore poreless polycarbonate films, thickness 10 µm) was used. These films were coated with Apiezon L-vacuum grease to reduce the particle bounce Polycarbonate filters (Millipore, 3.0 µm, GTTP04700, 0.2 µm) with diameter of 47 mm were used in the nano-MOUDI.

5.6.2 Analytical methods

IC. Ion chromatography (IC) is a process that allows the separation of ions based on the interactions between the sample ions, stationary phase (analytical column) and mobile phase (eluent). Cations and anions are typically analyzed separately because of different types of eluents (basic for anions and acidic for cations). The detection of ions can be based on the conductivity of the eluent or mass spectrometry.

In this thesis, the analyses were done with Dionex DX500 (Paper II) and Dionex ICS-2000 (Papers III and IV). The major analyzed ions were sodium (Na^+), ammonium (NH_4^+), potassium (K^+), magnesium (Mg^{2+}), calcium (Ca^{2+}), chloride (Cl^-), nitrate (NO_3^-) and sulfate (SO_4^{2-}). In the Paper II, also nitrite (NO_2^-) and oxalate were analyzed.

Prior the analyses sample substrates were extracted with methanol and deionized water (Milli-Q, Millipore Gradient A10). Analytical columns for anion analyses were AS-11 (Paper II) and AS-17 (Papers III and IV). Analytical column for cations was CS-12A. In Paper II, eluents for the anions and cations were NaOH and methanesulfonic acid, respectively. In Papers III and IV, eluents were KOH (anions) and methanesulfonic acid (cations).

ICP-MS and ICP-OES. An inductively coupled plasma mass spectrometer (ICP-MS) or combination of ICP-MS and inductively coupled plasma optical emission spectrometer (ICP-OES) can be used to determine elements from the particle samples. In the ICP-MS and ICP-OES, the sample is ionized in high temperature argon plasma and components are analyzed in the MS or OES part based on their mass-to-charge ratios.

In Paper II, a PerkinElmer ICP-MS (PerkinElmer Sciex Elan 6000, The PerkinElmer Corporation, Norwalk, USA) was used to analyze following elements: Al, As, Cd, Co, Cr, Cu, Fe, Mn, Ni, Pb, Sb, V and Zn. The extraction of the samples was made with a HNO_3-HF mixture (3:1) (Jalkanen et al., 1996). A combination of an ICP-MS and IPC-OES (ICP–MS; DRC II, Perkin-Elmer SCIEX, Concord, Ontario, Canada and ICP–OES; Vista Pro Radial, Varian Inc., Melbourne, Australia) was

used for elemental analyses of Papers III and IV. The analyzed elements were Al, Ar, Ba, Cd, Ca, Co, Cr, Cu, Fe, Mg, Mn, Ni, Pb, K, Si, Na, V, and Zn. The used analysis method was based on the standard SFS-EN 14902:2005 (Ambient air – Standard method for the measurement of Pb, Cd, As and Ni in the PM_{10} fraction of suspended particulate matter). A closed vessel microwave oven (MARS Xpress, CEM Corp., Matthews, NC, USA) was employed in the acid digestion (12 ml conc. HNO_3 and 3.0 ml 30 % H_2O_2) of the samples followed with dilution to 30 ml with deionized water. Before elemental analysis, the samples were further diluted 1:1 with deionized water. Rhodium (Rh) was added as an internal standard with the final concentration of 20 µg l^{-1}.

LC-MS. A liquid chromatograph coupled with an ion trap mass spectrometer is an analytical chemistry technique that combines the physical separation capabilities of liquid chromatography with the mass analysis capabilities of mass spectrometry (MS). The separation of sample components in the LC part is based on the supply of high pressurized liquid and sample mixture through a column filled with a sorbent. Each analyte in the sample interacts slightly differently with the adsorbent material, thus retarding the flow of the analytes. The MS part measures mass-to-charge ratio of charged particles that are ionized by the analysis process. The charged ions are separated according to their mass-to-charge ratio, detected and finally the signals are processed into mass spectras.

In Paper II, a LC-MS (LC-MS, Agilent Technologies SL) was used to analyze monosaccharide anhydrides (MAs including levoglucosan, galactosan and mannosan) that are degradation products of cellulose and hemicelluloses. PTFE-Filter samples were extracted with a 5-ml mixture of tetrahydrofuran and water (1:1) in the ultrasonic bath for 30 minutes. Polycarbonate substrates were first wetted with methanol. Thereafter, the solution was diluted to 5 ml with Milli-Q water finally including 10 % of methanol. In this study, a LC-MS method was used with deionized water (Milli-Q, Millipore Gradient A10) as an eluent at a flow rate of 0.1 ml min-1. Two LC columns (Atlantis, dC18 3 µm, 2.1 × 150 mm, Waters) were used at 7 ºC. The ionization technique was electrospray and the monitored ion was m/z 161. The uncertainty of the LC-MS method used for the MA analysis was estimated to be at least 20 %.

HPAEC-MS. A high-performance anion-exchange chromatograph coupled with electrospray ionization to a quadrupole-mass spectrometer is an analytical method for separation and analysis of chemical components from a sample. In anion exchange chromatography, negatively charged molecules are attracted to a positively charged solid support.

HPAEC-MS technique (HPAEC–MS, Dionex Corp.) was used in the study of Paper III to determine MAs from the small-scale combustion samples. The method is presented in detail by Saarnio et al. (2010). Shortly, the analysis procedure was following: the sample preparation included extraction with 5 ml of deionized water including internal standard, shaking (15 min.) and filtration. The column system consisted of CarboPac^{TM} PA10 guard and analytical columns (Dionex). The eluent was produced by a KOH eluent generator. An electrospray ionization technique was used for ionization of molecules and MS part was equipped with a quadrupole mass analyzer.

TOA. Organic and elemental carbon (OC and EC) can be determined with a thermal-optical carbon analyzer (Birch and Cary, 1996). The operation principle of the thermal-optical-analyzer is shortly following: a punch of sampled quartz filter is set into the oven of the analyzer. OC is volatilized at four subsequent temperature steps in pure helium atmosphere after which the EC is determined in a mixture of oxygen and helium (2 % oxygen) at six temperature steps. Optical correction is applied for the separation of pyrolysed OC from EC. In this thesis, a TOA (Sunset Laboratory Inc., Oregon) was used to determine OC and EC in Paper II. A 1.5 cm^2 piece was cut from the VI quartz filter for the analysis. The sampling area in the SDI is smaller than 1.0 cm^2 and therefore the whole deposit area can be analyzed. The temperature program used was similar to the NIOSH program except for the last temperature step in helium phase that was decreased from 850 to 800 °C. Inorganic carbon (carbonate carbon) can interfere with the determination of OC, since it volatilizes concurrently with the OC in the helium phase.

TOC analyzer. A total organic carbon analyzer is a method to determine water soluble organic carbon (WSOC) from the sample solutions. A TOC-V_{CPH} organic carbon analyzer (Shimadzu) with a highly sensitive catalyst was used in Paper II of this thesis. A non-purgeable organic carbon (NPOC) method was used. In the NPOC-method the sample is first put into 15 ml of deionized water to extract all water soluble organic carbon from the filter. Thereafter, the sample-solution is drawn through a plastic tube to the syringe using an 8-way valve. The acid addition (1 % 2M HCl) and helium bubbling (1.5 minutes) are done in the syringe. After that, all inorganic carbon should be converged to carbon dioxide and should be evaporated from the sample solution. After bubbling, the sample is injected into an oven, where it is catalytically oxidized to carbon dioxide at 680 °C.

5.7 Data analysis

5.7.1 Determination of less volatile particle size distribution

In Paper I, the method combining the VTDMA and the twin-DMPS and APS measurements yielded the number concentration of less volatile (N_{LV}) particles that mainly were expected to be soot particles. The VTDMA measurement resulted the number fraction of less volatile particles that was the ratio of N_{LV} measured in the oven temperature of 300ºC and initial number concentration (N_1) before heater treatment. Based on the simultaneous measurement of ambient particle number size distribution with the twin-DMPS and APS, the concentration of less volatile (LV) particles was calculated by multiplying the LV number fraction for each selected size by the corresponding number concentration measured with the Twin-DMPS and the APS. Finally, the size distribution of LV particles was achieved by applying a lognormal function through all data points available from the VTDMA measurements. The lognormal fitting is presented in equation 3:

$$N_{Di} = N_{max} exp\left(-\frac{(\ln D_{max} - \ln D_i)^2}{2(\ln \sigma)^2}\right) \quad (3)$$

where N_{Di} is number concentration of particles with diameter D_i (corresponding diameters of twin-DMPS and APS), N_{max} is maximum concentration of number size distribution of less volatile particles, D_{max} is particle diameter at the less volatile distribution maximum and σ is the width of the less volatile number size distribution.

The mass size distributions and total mass of LV particles were calculated assuming the density of particles to be 1.0 g cm^{-3} Hitzenberger et al., 1999). This density was chosen according to the density of loosely packed soot clusters (Ouimette & Flagan, 1982).

5.7.2 Mie modeling

Mie modeling was used in Paper I to compare measured and modeled optical properties of the LV particles and to consider the mixing state of measured ambient aerosol. In this comparison, modeled absorption was based on LV number size distribution and measured one was based on the absorption measured by the MAAP. The modeling was done by assuming that the aerosol was either internally (1) or externally (2) mixed. In case (1) the σ_{SP} and σ_{AP} were calculated from

$$\sigma_{SP}(\lambda) = \int Q_{SP}(\lambda, D_p, m)\left(\frac{\pi D_p^2}{4}\right) N(D_p) d\, D_p \quad (4)$$

$$\sigma_{AP}(\lambda) = \int Q_{AP}(\lambda, D_p, m)\left(\frac{\pi D_p^2}{4}\right) N(D_p) d\, D_p \quad (5)$$

where $Q_{SP}(\lambda,D_p, m)$ and $Q_{AP}(\lambda,D_p, m)$ are the scattering and absorption efficiencies of particles with diameter D_p, m is the complex refractive index $m = n_r + k_i i$, and $n(D_p)$ is the number concentration of all particles – volatile and non-volatile – with diameter Dp.

In case (2) σ_{SP} and σ_{AP} were calculated from

$$\sigma_{SP}(\lambda) = \sigma_{SP,V} + \sigma_{SPL,V} =$$
$$\int Q_{SP}\left(\lambda, D_p, m_V\right)\left(\frac{\pi D_p^2}{4}\right) N_V\left(D_p\right) d\, D_p + \int Q_{SP}\left(\lambda, D_p, m_{LV}\right)\left(\frac{\pi D_p^2}{4}\right) N_{LV}\left(D_p\right) d\, D_p \quad (6)$$

$$\sigma_{AP}(\lambda) = \int Q_{AP}\left(\lambda, D_p, m_{LV}\right)\left(\frac{\pi D_p^2}{4}\right) N_{LV}\left(D_p\right) d\, D_p \quad (7)$$

where $N_V(D_p)$ and $N_{LV}(D_p)$ are the number concentrations and m_V and m_{LV} the complex refractive indices of volatile and nonvolatile particles, respectively. $N_V(D_p)$ was calculated from $N(D_p) – N_{LV}(D_p)$. The refractive indices were varied so that the measured and modeled σ_{SP} and σ_{AP} agreed within a few percent.

The Mie modeling was also used in the Supporting Information of Paper III to simulate optical properties of the small-scale wood combustion campaign to ensure validity of measured values.

5.7.3 Conversion and normalization of particle emissions to the standard conditions

All the results in emissions of Papers II and III were converted to the NTP conditions (0°C and 101.3 kPa) and normalized from the oxygen content in the flue gas to the reference oxygen content of each fuel (13 % for wood and pellet, 3 % for HFO and LFO and 6 % for coal).

The conversion and normalization were based on formulas (8) and (9):

$$c_{NTP} = c_m \frac{T_{NTP}}{T_m} \times \frac{p_m}{p_{NTP}} \quad (8)$$

and

$$c_{O_2} = c_m \frac{20.9 - O_{2,ref}}{20.9 - O_{2,m}} \quad (9)$$

where

c_{NTP} = measured quantity converted to the NTP conditions

c_m = measured quantity

T_{NTP} = NTP temperature, 0°C

p_{NTP} = NTP pressure, 101.3 kPa

T_m = measured temperature

p_m = measured pressure

C_{O2} = measured quantity normalized from the oxygen content in the flue gas to the reference oxygen content of fuel

20.9 = oxygen content in the air

$O_{2,ref}$ = reference oxygen content of certain fuel

$O_{2,m}$ = measured oxygen content of burned fuel

Emission results excluding optical data for the studies of Paper II and III were presented as emission factors (E_F), i.e. in the relation to the mass of burned fuel or energy input to the burning processes, respectively. E_Fs of these studies were calculated based on the standard SFS 5624.

5.7.4 Correction of optical data and calculation based on optical results

The nephelometer and PSAP data (i.e. σ_{SP} and σ_{AP}) suffer from the instrumental limitations. Thus, σ_{SP} and σ_{AP} data have to be corrected based on the methods shown by Anderson and Ogren (1998) and Virkkula (2010), respectively. The truncation correction of the nephelometer data (σ_{SP}) determined by Anderson and Ogren (1998) is based on the following equation (10):

$$\sigma_{SP}(\lambda) = a + b\alpha_{SP}^{b} \tag{10}$$

where a and b are empirical factors for the wavelengths of 400, 550 and 700 nm presented by Anderson and Ogren (1998) and α_{SP} is scattering Ångström exponent that describes the wavelength dependence of the scattering by particles. α_{SP} is formulated as follows:

$$\alpha_{SP,1-2} = -\frac{\log\frac{\sigma_1}{\sigma_2}}{\log\frac{\lambda_1}{\lambda_2}} \tag{11}$$

where the numbers 1 and 2 describe wavelengths that are considered. In the studies of this thesis (Papers I and III), the σ_{SP} values measured at λ=700 nm were interesting ones because of comparison with σ_{AP} at λ=660 nm (PSAP) or at λ=637 nm (MAAP) and thus, the α_{SP} for truncation error calculation was determined between wavelengths of 550 and 700 nm. . The Ångström exponent of absorption is calculated similarly from wavelength-dependent absorption coefficients.

σ_{SP} measured at λ= 700 nm and σ_{AP} measured by the PSAP were interpolated logarithmically to the MAAP wavelength (637 nm) assuming that the ångström exponent α is constant within the wavelength interval:

$$\alpha_{1-2} = -\frac{\log\frac{\sigma_1}{\sigma_2}}{\log\frac{\lambda_1}{\lambda_2}} \leftrightarrow \sigma_2 = \sigma_1 \frac{\lambda_1}{\lambda_2}^{\alpha_{1-2}} \quad (12)$$

$$if\ \alpha_{1-x} = \alpha_{1-2} \rightarrow \sigma_x = \sigma_1 \left(\frac{\lambda_1}{\lambda_x}\right)^{\alpha_{1-2}} \quad (13)$$

In this study, the abbreviations 1 and 2 describe wavelength range measured by the nephelometer (450 – 700 nm) or PSAP (437 – 660 nm) and abbreviation x is the wavelength to which the results are needed to interpolate (637 nm). Ångström exponent for scattering (α_{SP}) can also be related to particle size: α_{SP} increases with decreasing particle sizes (e.g. Eck et al., 1999; Doherty et al., 2005; Pereira et al., 2011) and thus, α_{SP} can be compared with size distribution studies (Paper III).

The single scattering albedo (ω_0), that is the ratio of σ_{SP} to the sum of σ_{SP} and σ_{AP} (extinction coefficient, σ_{EP}), was calculated based on the corrected σ_{SP} and σ_{AP} at wavelength of 637 nm in the studies of Paper III. ω_0 is an important factor in the estimations of radiative forcing of the aerosol particles (e.g. Takemura, 2002).

The mass extinction efficiency (MEE), that is dependent on particle size composition and size distribution, can be calculated based on the ratio of extinction coefficient ($\sigma_{EP}=\sigma_{SP}+\sigma_{AP}$) to mass concentration (for example PM_1). Accurate estimates of MEE are important when computing the radiative forcing effects of aerosols and in the chemical extinction budgets used for the visibility regulatory purposes (Hand and Malm, 2007). In this thesis, the MEE values were calculated in the studies of Paper III.

Radiative forcing effect of particles can be assessed by aerosol forcing efficiency (ΔF/δ, i.e. aerosol forcing per unit optical depth, W m^{-2}) (e.g. Sheridan and Ogren, 1999; Delene and Ogren, 2002):

$$\frac{\Delta F}{\delta} = -DS_0T_{at}^2(1-A_c)\omega_0\beta\left\{(1-R_s)^2 - \left(\frac{2R_s}{\beta}\right)\left[\left(\frac{1}{\omega_0}\right)-1\right]\right\} \quad (14)$$

where D is the fractional day length, S_0 is the solar constant, T_{at} is the atmospheric transmission, A_c is the fractional cloud amount, R_s is the surface reflectance, and β is the average upscatter fraction calculated from hemispheric backscatter ratio b (backscattering-to-scattering) based on formula $\beta = 0.817+1.8495b-2.9682b^2$ (Delene and Ogren, 2002). ΔF/δ were determined for the studies of Paper

III. There, $\Delta F/\delta$ were estimated for each of the combustion cases using the average values of ω_0 and b for 637 nm. The constants used were $D = 0.5$, $S_0 = 1370 W\ m^{-2}$, $T_{at} = 0.76$, $A_c = 0.6$, and $R_s = 0.15$ as suggested by Haywood and Shine (1995).

6 Results and discussion

In the Results and discussion section, traffic related particle emissions are partly considered separately from the other combustion sources because they were measured from the ambient air. Thus, measurement conditions differed from the emission measurements of wood fuel, coal and heavy fuel oil combustion appliances.

6.1 Less volatile traffic related particle emissions

Traffic related particle emissions are formed by small combustion engines such as gasoline and diesel engines. When compared with large-scale combustion, the burning process of these engines is less efficient leading to formation of e.g. organic compounds and BC. Especially diesel engines without particle filtration emit substantial amount of BC particles indicating with insufficient burning of the fuel. In the scope of this thesis, BC emissions played an important role. In the Paper I, BC particles were considered as less volatile (LV) because of the measurement technique used.

Mass concentration of LV (M_{LV}) particles determined by the VTDMA was compared with BC mass concentration (M_{BC}) measured by the MAAP. In addition, comparison between measured and modeled scattering and absorption coefficients (σ_{SP} and σ_{AP}, respectively) was done. As Figure 4 (Paper I) shows, M_{BC} was most of the time higher than M_{LV}. Figure 4 also shows the volume weighed LV particle fraction $<\phi_{LV}>$ that weakly correlated with the fraction of M_{LV} to M_{BC}. As the M_{LV} and M_{BC} closely followed each other, the wind was coming from the urban area influenced by the traffic emissions. During these periods dominated by fresh vehicle emissions (hatched areas in Figure 5), the fraction of less volatile particles (i.e. BC) was around 0.2 when otherwise it was clearly smaller. Local traffic emissions were also seen in the measured and modeled optical properties of particles: as $<\phi_{LV}>$ increased, the modeled σ_{AP} assuming external mixture of particles agreed with the measured one when overall the modeled absorption of light due to externally mixed particles was smaller than measured σ_{AP}. For the whole period the average (± std) refractive index was 1.55 (±0.09) – 0.04 (±0.02)i when internal mixing was assumed. When $<\phi_{LV}>$ was >0.2 the average refractive index of LV particles was 1.96 – 0.8 (±0.18)i when σ_{AP} was modeled assuming external mixing.

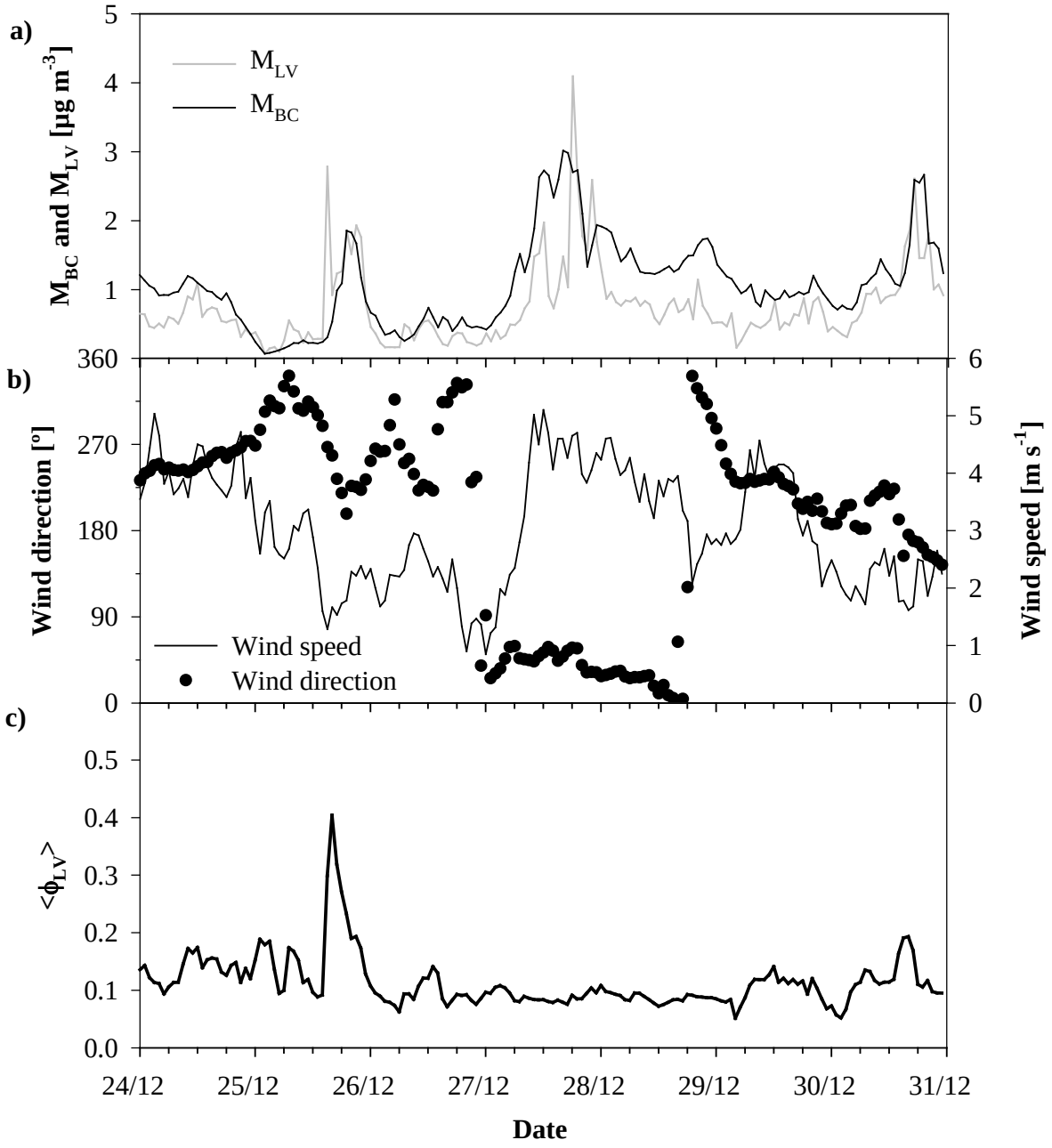

Figure 4 Hourly-averaged (a) M_{LV} and M_{BC} concentrations, (b) wind speed and direction and (c) volume-weighted less-volatile particle fraction $<\phi_{LV}>$ measured between December 24 and 31, 2005 (Paper I).

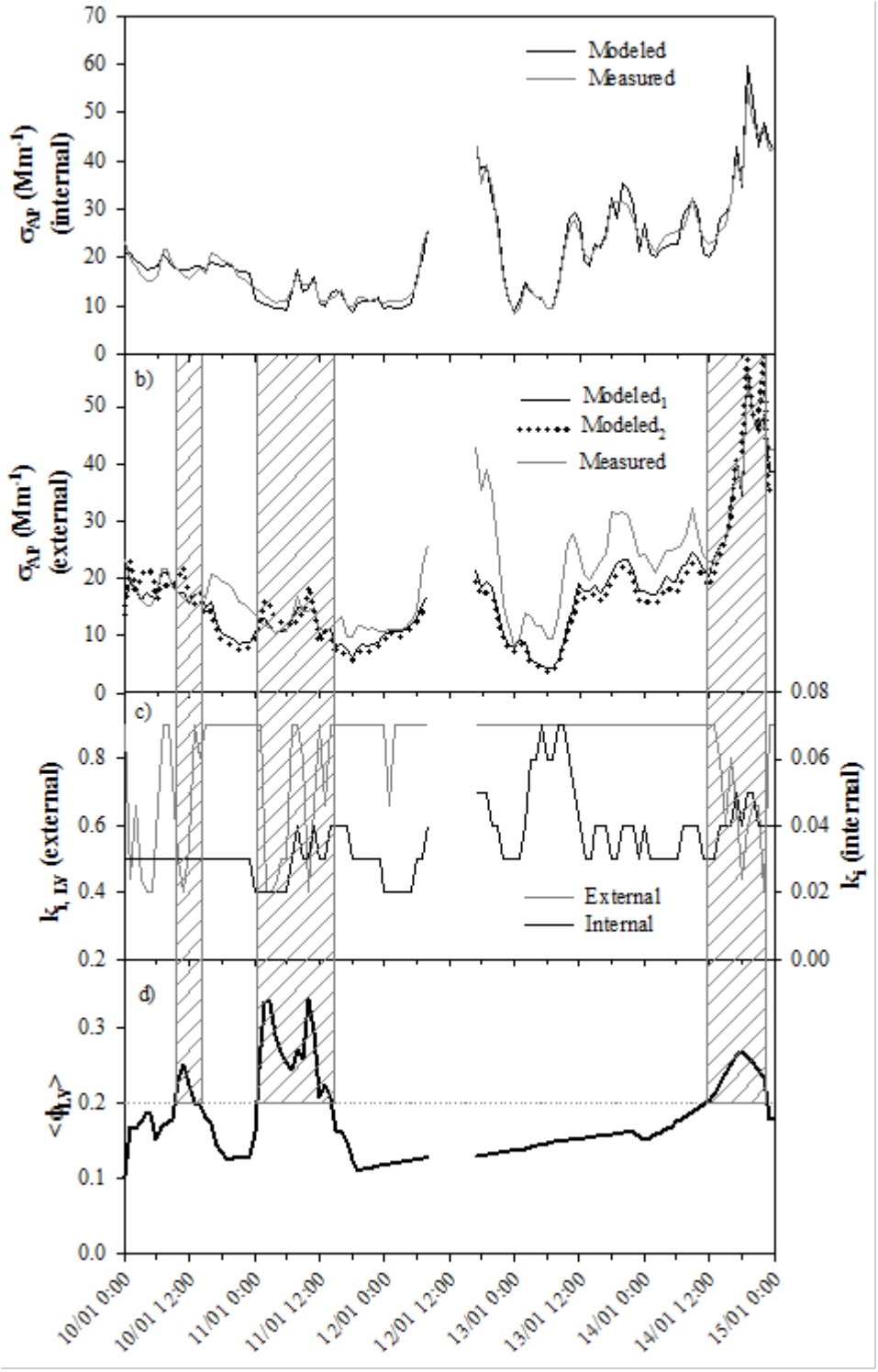

Figure 5 Hourly-averaged (a) measured and modeled σ_{AP} assuming internally mixed particles, (b) measured and modeled σ_{AP} assuming externally mixed particles -modeled σ_{AP} is given for the data based on the fitted refractive index (Modelled$_1$) and a literature value for the refractive index of soot, m = 1.96 – 0.66i (Modelled$_2$), (c) imaginary part k_i of externally and internally mixed particles and (d) less-volatile particle fraction $<\phi_{LV}>$ between January 10 and 15, 2006 (Paper I).

6.2 Particle emissions of wood fuel, coal and heavy fuel oil combustion

The wood fuel combustion (including wood logs and pellets) considered in this thesis (campaigns SSWC1 and SSWC2, Paper I and III, respectively) represented small-scale combustion that in Finland is commonly used as secondary heating system in households. Instead, coal and both heavy and light fuel oil (HFO and LFO, respectively) combustions described large-scale energy production. Coal-fired power plant produced both power and heat (campaign C-PP, Paper III) whereas oil was combusted in a heating station (campaigns HFO-HS1 and HFO-HS2 Papers III and IV).

6.2.1 Particle emissions and their chemical composition

The chemical composition of PM emitted from burning processes is dependent on both fuel and combustion process. Overall, large-scale combustion is better controlled than small-scale combustion. Large-scale combustion techniques allow higher combustion temperature and better control of the fuel and air supply than small-scale combustion.

Emission factors of the PM_1 (E_F) determined within this thesis are shown in Table 3 and corresponding mass closures in Figure 6. The abbreviations in Table 3 and Figure 6 represent following cases: SSWC1+MH+N and SSWC1+MH+S1/S2 describe small-scale wood log combustion in a masonry heater combusted with normal and smouldering conditions (Paper II). In the SSWC2+PB and SSWC2+MH, small-scale combustion was carried out in a pellet boiler fuelled with wood pellets and in a conventional masonry heater fuelled with birch wood logs, respectively (Paper III). Coal combustion was studied in the cases of C+DSP, C+P+DSP and C+P+bypassDSP that described coal combustion emissions after the ESP and DSP, emissions of mixture of coal and pellet fuels after ESP and DSP and emissions of mixture of coal and pellet fuels in the case of bypassing the DSP, respectively (Paper III). HFO+78MW, HFO+E+78MW and HFO+LFO+120MW are the emission cases at the heating station fuelled with heavy fuel oil (HFO) with the power of 78 MW, HFO with water emulsion with the power of 78 MW and mixture of HFO and light fuel oil (LFO) with the power of 120 MW, respectively (Paper III). The other experiment at the HFO-fired heating station (HFO-HS2) included the cases HFO+30MW, HFO+E+30MW and HFO+LFO+E+30MW meaning the HFO combustion tests with addition of LFO and water emulsion in a boiler run with 30 MW power.

The studies of this thesis showed that PM_1 emissions of the small-scale wood or pellet combustion were clearly higher than PM_1 emissions of large-scale burning of coal/coal-pellet mixture and HFO/HFO-LFO mixture. In addition, the variation of the emission factors of small-scale

combustion was high: E_F was lowest in the pellet boiler burning (~17 ± 2 mg MJ^{-1}) but the E_F of masonry heaters varied from ~39 to 490 mg MJ^{-1} depending from the burning appliance and combustion conditions. Smouldering combustion characterized situation where common mistakes of the operational practices, such as overloading of the firebox and insufficient air supply, were present. Thus, particle emissions in these situations were clearly highest.

Particle emissions were lowest at the coal-fired power plant when the flue gases were cleaned in the DSP (Paper III). The E_F was 0.18 ± 0.06 mg MJ^{-1} for the C-DSP case (Paper III) (Table 3). The studies at the coal-fired power plant showed that the DSP effectively removed particles from the flue gas: within the study of Paper III, particle emissions were ~90 % smaller with the DSP when compared with the case where the DSP was bypassed. When emissions were determined by bypassing the DSP, E_Fs was at the same range or a little smaller as the ones for the combustion of HFO and mixture of HFO and LFO at the heating station where no cleaning technique was used. In these cases, E_Fs varied between ~1.3 and 4.0 mg MJ^{-1} (Papers III and IV). The maximum difference between E_F of various combustion cases was between smouldering small-scale wood combustion in a masonry heater (SSWC1+MH+S2) and combustion of the mixture of coal and pellet fuel when the DSP was used (C+P+DSP). In this case, the E_F of the SSWC1+MH+S2 was approximately 3270 times higher than E_F of the C+P+DSP.

Table 3 Average emission factors (E_F) (±standard deviation) of the PM_1 of the combustion cases of the thesis determined based on the weighed filter samples.

Paper	Combustion case	E_F (mg MJ^{-1})
II	SSWC1+MH+N	150 ± 23
	SSWC1+MH+S1	478*
	SSWC1+MH+S2	494*
III	SSWC2+PB	17 ± 2
	SSWC2+MH	39 ± 2
III	C+DSP	0.18 ± 0.1
	C+P+DSP	0.15 ± 0.02
	C+P+bypassDSP	1.3*
III	HFO+78MW	3.1*
	HFO+E+78MW	3.6*
	HFO+LFO+12+MW	2.3*
IV	HFO+30MW	3.2*
	HFO+E+30MW	3.3*
	HFO+LFO+E+30MW	4.0*

*standard deviation could not be determined because of only one sample for the condition in question.

In most of the combustion cases of this thesis, the chemically analyzed mass did not fill the total PM_1 mass because of the limitations of the used analytical techniques. Overall, the mass closure was best reached in the SSWC1 campaign where analyzed mass contributed ~85-97 % of the total PM_1 mass. In the SSWC-PB, analyzed mass covered 63 ± 7 % of the PM_1. Here, organics and elements (i.e. metals) were not analyzed that could explain part of the missing mass. However, the study of Lamberg et al. (2011), that presented results of the same experiments as in the cases of SSWC2+PB and SSWC2+MH, showed that the organic carbon (OC) and metals would contribute less than 10 % of the PM1 mass in the pellet boiler combustion (efficient combustion (EFC) in the study of Lamberg et al., 2011). In the SSWC-MH, analyzed mass was larger than weighed PM_1 indicating uncertainty in analyze techniques or estimation of M_{BC}. In the HFO-HS1, HFO-HS2 and C-PP campaigns, the coverage of the total mass varied from 22 to 89 %. The missing mass in these campaigns could include some non-analyzed elements such as silicon (Si) that occurs especially in coal e.g. in the form of quartz (SiO_2), aluminosilicate or aluminosilicate salt (Tomeczek and Palugniok, 2002). In addition, oil and coal include a significant amount of trace metals that could form metallic oxides in the flue gas. Oxygen in these compounds could explain part of the missing

mass. Other possible components of particles that were not analyzed were, e.g., carbonate and hydroxide ions and water.

Carbonaceous compounds, e.g. organic and elemental/black carbon (OC and EC/BC, respectively), are the major chemical compounds that indicate with incomplete burning process. Here, BC was also refereed as absorbing material (Figure 6) because of the measurement techniques used (PSAP and MAAP, see sections 4.2.3 and 5.3). The absorbing part is usually proposed to be BC but can also include e.g. iron oxides that are highly absorbing in the UV and visible light wavelengths and occur in oil and coal combustion flue gases. Thus, the absorbing material fractions of the coal and oil combustion of the Papers III and IV could also include iron that was analyzed also by the analytical methods. The results of the absorbing material and iron were both summed to the analyzed mass as individual components. Thus, they might overlap if iron was in the form of iron oxides. Instead, in wood fuels, iron is not such significant component. Water soluble organic carbon (WSOC) was determined in the studies of Papers II and III. The WSOC was converted to water soluble particulate organic matter (WSPOM) by a factor based on the ratio between the molecular weight of organic compounds and carbon weight (e.g. Turpin and Lim, 2001). This ratio is dependent on the composition of organics and aging of the aerosol mass and was here chosen to be 1.8 for the WSPOM. WSPOM also includes monosaccharide anhydrides (MAs) that were separately analyzed from the filter samples. The emission of the MAs was subtracted from the WSPOM in the cases of Paper II to more clearly see the influence of the combustion process on different chemical compounds. Total OC was available for the studies of Paper II and studies at the heavy fuel oil-fired heating station (HFO-HS1 and HFO-HS2, Papers III and IV, respectively). In the study of Paper II, the total OC in addition to WSOC was analyzed and converted to particulate organic matter (POM) by a factor of 1.6. In Figure 6, the POM includes organics that are not water soluble (i.e. total POM-WSPOM-MAs).

Based on the results of the Papers II and III, particle emissions of the masonry heaters fuelled with wood logs included substantial amount of EC/BC (Figure 6, cases of Paper II (EC) and SSWC2+MH (BC, i.e. absorbing material)). In the cases of normal and smouldering combustion of the masonry heater (Paper II), EC fraction of particle emissions varied approximately in the range of 20 and 30 % being higher in the case of normal combustion. In the case of the SSWC2+MH, particle emissions surprisingly consisted mostly of the absorbing material (94 ± 28 % of the total emission) but the fraction of organic compounds was unsubstantial. For the SSWC2+MH and SSWC2+PB, total POM was not analyzed but only the WSPOM. As is seen from Figure 6, the mass closure of the SSWC2+MH was full and it only included approximately 3 % of WSPOM whereas

in the cases of Paper II, the total POM including WSPOM and MAs contributed 32 % of the mass closure of the normal combustion in a masonry heater. In the cases of smouldering combustion, the contribution of the total POM was almost 70 % to the total particle emission. The relationship between EC and OC also indicates with combustion conditions: EC fraction usually decreases in relation to the OC when fuel burning gets insufficient. This behavior was seen between normal and smouldering combustion in a masonry heater. The EC-to-OC ratio was on average 1.7±0.6 in the SSWC1+MH-N case, whereas the corresponding values in the SSWC1+MH-S1/S2 experiments were 0.60 and 0.52. The inefficient combustion conditions created by restricting air supply and overloading of the firebox in the SC were the reasons of the higher fraction OC in the SC.

In the large-scale combustion, i.e. coal and oil combustion, organic compounds were only measured at the heating station fuelled with HFO and LFO. Overall, carbonaceous emissions played a minor role in the large-scale combustion, as was expected. The POM fraction of the particle emissions at the HFO-fired heating station (campaigns HFO-HS1 and HFO-HS2) varied between 0.6 and 6.0 %. Absorbing material (BC) fraction was approximately 1 % in the HFO-HS1 campaign. Instead, the absorbing material fractions were higher in the HFO-HS2 campaign varying between 6 and 20 %. The highest fraction of absorbing material (20 %) was determined in the case of HFO+LFO+E+30MW. The reason stayed unclear but most probable reason could be some mistake in the optimization of the combustion process that led to inefficient combustion conditions. Overall, the boiler of the HFO-HS1 campaign was the main operational boiler where the combustion process was better optimized than the process of the boiler used in the HFO-HS2 campaign. The particle emissions of the power plant fuelled with coal and mixture of coal and wood pellets (pellets 4.5 ± 1.4 % of fuel volume) included 1.4 ± 0.4 and 3.7 ± 0.8 % of absorbing material when flue gases where cleaned with the DSP. Instead, when the DSP was bypassed absorbing material fraction was rather high (16 %) in the case where mixture of coal and pellets was burned. That high absorbing material content was actually not expected but one reason could be the addition of pellets into the fuel. Even though the pellet content was rather low, it could be possible that the combustion technique optimized for the coal combustion did not work properly for the mixture (e.g. grinding of the fuel, supply of the fuel into the boiler). However, the DSP seemed to remove most of the absorbing material. It has to be noted that absorbing material of emissions of coal and oil combustion of the Papers III and IV could also include iron oxides that also are highly absorbing (Ninomiya et al., 2004; Alfaro et al., 2004). In the HFO-HS1 campaign, the contribution of iron and absorbing material to the PM_1 was on average 3.3 ± 0.1 % and 0.8 ± 0.2 %, respectively. The iron contribution to the PM_1 was on average 0.3 ± 0.1 % for the C-PP campaign in the cases when the

DSP was bypassed. There were no significant differences between iron fractions of the C+DSP and C+P+DSP cases. In the case of C+P+bypassDSP, the iron fraction was 1.4 %. The absorbing material contributed 3.7 ± 0.4 %, 1.4 ± 0.8 % and 16 % of the PM_1 in the C+DSP, C+P+DSP and C+P+bypassDSP cases, respectively. The influence of iron oxides on light absorption was tested assuming iron to be in the form of ferric oxide (Fe_2O_3) and MAE to be 0.56 $m^2\ g^{-1}$ (Paper III). The results are shown in Table 4. The test results showed that for the HFO-HS1 campaign, absorption of light due to Fe_2O_3 was in the range measured by the MAAP whereas in the C-PP campaign this absorption contributed only some per cents of the measured absorption.

Table 4 Measured absorption coefficient (σ_{ap}), absorption coefficient of Fe_2O_3 ($\sigma_{ap,Fe2O3}$) and ratio between $\sigma_{ap,Fe2O3}$ and σ_{ap} (as percentage %) ± standard deviation for the C-PP and HFO-HS1 campaigns (Paper III).

Combustion case	σ_{ap} **(Mm^{-1})**	$\sigma_{ap,Fe2O3}$ **(Mm^{-1})**	$\sigma_{ap,Fe2O3}/\sigma_{ap}$ **(%)**
C+DSP	110±73	1.9±0.9	1.6±0.4
C+P+DSP	41±56	2.1±1.1	7.8±7.8
C+P+bypassDSP	3653±107	77*	2.1*
HFO+78MW	816±152	612*	75*
HFO+E+78MW	482±48	661*	137*
HFO+LFO+120MW	436±86	430*	99*

*stdev could not be determined because of only one sample for the condition in question.

In the PM_1 emissions, ions including alkali metals comprised the majority of the analyzed mass in most of the studied combustion cases. Also elements, such as trace metals, had a significant contribution to the analyzed mass in the HFO-HS1, HFO-HS2 and C-PP campaigns. For the SSWC2 campaign elements were not analyzed but the results of the SSWC1 showed that contribution of elements to the PM_1 was not remarkable. In the SSWC campaigns, the increase in the ion fraction correlated with better combustion technology: ion fraction was highest in the pellet boiler combustion and clearly higher in the normal combustion of the masonry heater than in the smouldering combustion. Especially in the high combustion temperature of the SSWC2+PB, inorganic ash species first evaporate and form particles by homogenous nucleation and subsequent condensation in the cooling flue gas (Sippula et al., 2009). In the HFO-HS emissions, the ions-to-

PM_1 and elements-to-PM_1 fractions were ~30 – 50 % and ~10 – 20 %, respectively. SO_4^{2-} contributed approximately 80 – 90 % to ions in the HFO-HS cases. The most significant elements were Fe, Ni, V, K and Mg. In the C-PP campaign, ions dominated the PM_1 in the cases when the emissions were determined after the DSP (~40 – 60 % of the PM_1). In the case of bypassing the DSP, the ionic contribution decreased to around 4 %. Also the element contribution decreased from 24 – 26 % to 11 % when the DSP was bypassed. The main reasons for the high ion fractions were the chemicals used in the DSP process. When the DSP was used, metallic components and absorbing material were effectively removed from the flue gas. Calcium hydroxide ($Ca(OH)_2$) and sodium chloride (NaCl) are added to the flue gas passing the DSP to decrease the emissions of sulfur dioxide gas (SO_2). The chemical reactions in the DSP resulted in decrease of SO_2 and metal emissions and enhanced mass concentrations of ions such as Ca^{2+}, Na^+, Cl^- and SO_4^{2-} when compared with the concentrations of these chemical components in the case of the DSP bypass.

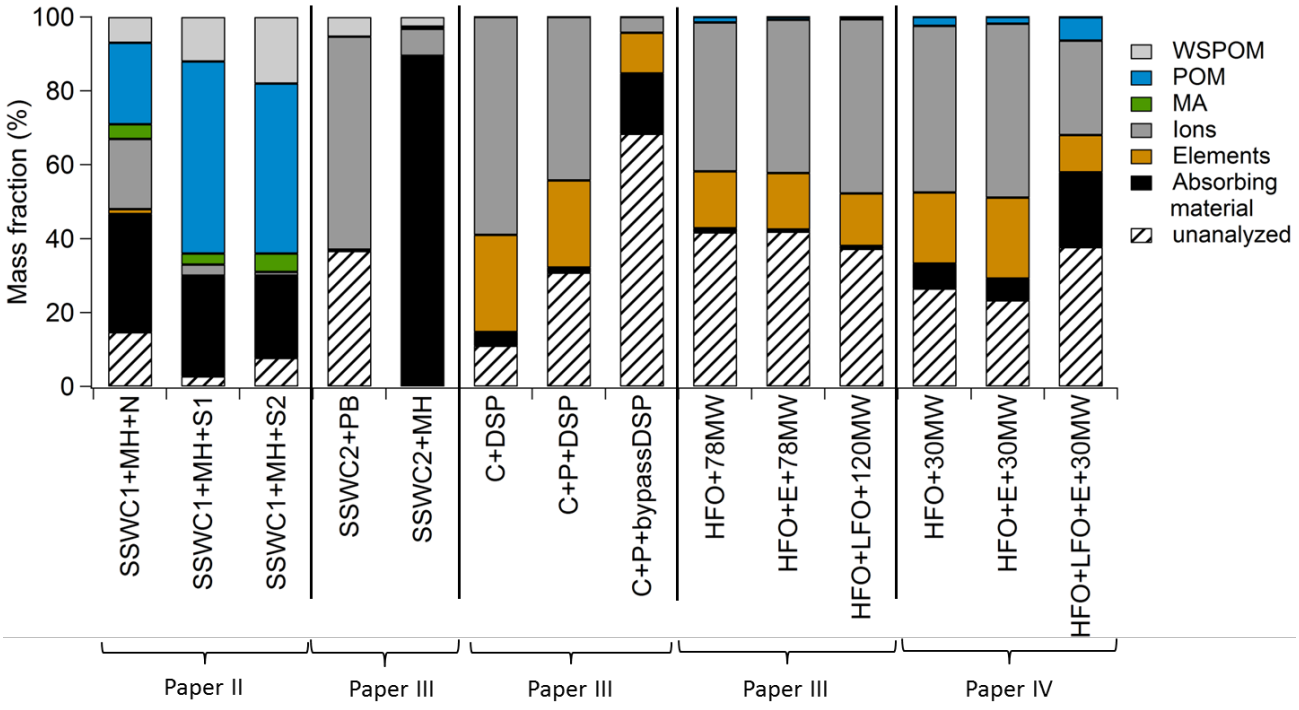

Figure 6 Chemical mass closures of the particle emissions of the small-scale wood combustion, coal and oil combustion based on the studies of Papers II-IV.

6.2.2 Size distributions

Size distributions of particle emissions of various combustion technologies were determined with the different measuring techniques in the studies of this thesis. Number and volume size distributions were based on the measurements of the real-time instruments (DMPS, SMPS, FMPS, APS). Mass and chemical size distributions were determined from the analysis of the filter samples

collected with the cascade impactors such as the SDI and MOUDI. Examples of the results of the real-time instrument measurements of Papers II and III are shown in Table 5. The table collects geometric mean diameters (GMD) and geometric standard deviations (GSD) of the number and volume size distributions of the size distributions for the aerodynamic and geometric (mobility) diameters (D_a and D_p, respectively). The density shown in the Table 5 is the one used for the conversion between D_a and D_p. The superscripts from *a* to *f* describe the instrumentation that was used to measure size distribution for which the GMDs and GSDs in question were calculated.

Size distributions of particle emissions of various combustion techniques are influenced by the burning conditions and fuel. In addition, aging of the aerosol mass changes the size distribution because of the physical and chemical reactions in the ambient air (e.g. coagulation, condensation). Thus, particle size distributions in the ambient air usually are wider than distributions of fresh aerosol masses right after the emission source. This is seen from the number GSD (NGSD) and volume GSD (VGSD) of the ambient air influenced by traffic shown in Table 5: the values were ~2.6 and 2.4, respectively whereas for the size distributions determined right after the emission sources were clearly narrower (NGSD ~1.4-1.95 and VGSD ~1.4-2.0). All the size distributions from various emission sources had an ultrafine particle mode with NGMD(D_a) between 30 and 150 nm. Also in the size distributions determined in Paper IV (not presented in Table 5) for the oil combustion, the NGMDs of various combustion cases had NGMDs in particle size of ca. 50 nm. Overall, the number concentrations of coal combustion emissions were significant up to 1 µm when compared with the size distributions of the oil combustion. Thus, in Table 5, the NGMDs of SMPS and APS are shown for C-PP campaign whereas for the HFO-HS1 campaign, there was no significant mode seen in the APS measurements. Naturally, VGMDs shifted to the larger particles. Especially in the large-scale coal combustion, modes in supermicrometer sizes were significant in the volume size distributions. Also in the oil combustion, coarse particles played an important role in volume size distribution even though it was not as clear as in the coal combustion. Ultrafine and fine particles of coal and oil combustion are most probably formed from vaporized and nucleated volatile metals. The coarse mode of oil combustion could be composed of residual particles. Coal combustion particles also form from inherent mineral matter within coal transferred into PM forming coarse particles. The emissions of small-scale wood fuel combustion including birch log and wood pellet combustion varied clearly depending on the combustion conditions and technique. For the SSWC1 campaign (Paper II), only size distributions of chemical components were determined. However, also these chemical distributions give an overview to the influence of combustion conditions on the shape of the size distributions. The mass size distributions of EC,

POM, MA and ions showed that smouldering combustion shifted the size distribution to the larger particles when compared with the size distributions of the normal conditions. Especially the ion size distribution constituted two clear modes instead of one in the inefficient burning conditions. In the SSWC2 campaign (Paper III), the size distribution of wood log combustion differed clearly from the combustion wood pellets. As is shown in Table 5, the particle number emissions of the SSWC2-MH included two modes in submicrometer range ($GMD(D_a)$= 0.03±0.01 and 0.11±0.01) whereas the number size distribution of the SSWC2-PB was unimodal ($GMD(D_a)$= 0.09±0.002). Thus, the width of the number size distribution increased with the inefficiency of combustion. Instead, VGMDs of these cases both were unimodal.

Table 5 Number and volume geometric mean diameters (NGMD and VGMD, respectively) ±standard deviations (stdev) of the various combustion cases as geometric (≈mobility) and aerodynamic diameters (D_p and D_a, respectively). Density is the one that was used for the conversion between D_a and D_p (see Section 5.4, Equation 2). In addition, the number and volume geometric standard deviations (NGSD and VGSD, respectively) of the distributions (±stdev) are shown.

Combustion case	SSWC2+MH	SSWC2+PB	C+DSP	C+P+DSP	C+P+bypassDSP
density (g cm^{-3})	1.77	2.96	2.5	2.5	2.5
NGMD1(D_a) (µm)	0.03±0.01[a]	0.09±0.002[a]	0.08±0.02[b]	0.1±0.02[b]	0.09±0.001[b]
NGMD2(D_a) (µm)	0.11±0.01[a]		1.08±0.08[c]	0.97±0.04[c]	1.06±0.03[c]
NGMD1(D_p) (µm)	0.03±0.01[a]	0.06±0.001[a]	0.04±0.01[b]	0.05±0.01[b]	0.05±0.001[b]
NGMD2(D_p) (µm)	0.09±0.01[a]		0.66±0.04[c]	0.59±0.02[c]	0.64±0.01[c]
NGSD	1.95±0.27[a]	1.48±0.01[a]	2.0±0.01[b]	1.6±0.11[b]	1.51±0.03[b]
VGMD1(D_a) (µm)	0.17±0.03[a]	0.15±0.01[a]	2.18±0.22[c]	1.90±0.27[c]	2.86±0.11[c]
VGMD2(D_a) (µm)					
VGMD1(D_p) (µm)	0.12±0.02[a]	0.08±0.01[a]	1.35±0.12[c]	1.18±0.15[c]	1.778±0.31[c]
VGMD2(D_p) (µm)					
VGSD	1.61±0.2[a]	1.52±0.16[a]	1.64±0.05[c]	1.73±0.12[c]	1.77±0.02[c]

Superscripts describe the instrumentation to which the calculation of the GMDs and GSDs is based on: [a]FMPS, [b]SMPS, [c]APS, [d]SMPS+APS, [e]twin-DMPS+APS, [f]twin-DMPS+APS+VTDMA

Table 5 Continued

Combustion case	HFO+78MW	HFO+E+78MW	HFO+LFO+120MW	ambient air	ambient air, LV
density (g cm^{-3})	2.5	2.5	2.5	1.7	1.7
NGMD1(D_a) (µm)	0.05±0.0002[b]	0.05±0.0004[b]	0.04±0.0001[b]	0.07±0.02[e]	0.13±0.03[f]
NGMD2(D_a) (µm)					
NGMD1(D_p) (µm)	0.03±0.0001[b]	0.03±0.0001[b]	0.03±0.0001[b]	0.05±0.01[e]	0.09±0.02[f]
NGMD2(D_p) (µm)					
NGSD	1.38±0.003[b]	1.39±0.003[b]	1.37±0.001[b]	2.57±0.24[e]	1.9±0.1[f]
VGMD1(D_a) (µm)	0.07±0.0003[b]	0.07±0.001[b]	0.06±0.0001[b]	0.58±0.12[e]	0.42±0.18[f]
VGMD2(D_a) (µm)	3.63±1.07[c]	1.5±0.36[c]	2.73±0.53[c]		
VGMD1(D_p) (µm)	0.04±0.0002[b]	0.04±0.0003[b]	0.04±0.0001[b]	0.44±0.09[e]	0.33±0.14[f]
VGMD2(D_p) (µm)	2.27±0.65[c]	0.92±0.2[c]	1.7±0.31[c]		
VGSD	1.35±0.002[b]	1.36±0.001[b]	1.36±0.002[b]	2.39±0.31[e]	1.97±0.21[f]

Superscripts describe the instrumentation to which the calculation of the GMDs and GSDs is based on: [a]FMPS, [b]SMPS, [c]APS, [d]SMPS+APS, [e]twin-DMPS+APS, [f]twin-DMPS+APS+VTDMA

6.2.3 Optical properties

Optical properties of PM_1 particles emitted from various combustion sources (σ_{SP}, σ_{AP} and ω_0), the dependency of optics on chemical composition and on size distribution of these particles (MEE and α_{SP}) were studied within Paper III. In addition, the influence of the energy production technology on the radiative forcing efficiency over dark surface was estimated ($\Delta F/\delta$). For the SSWC2 campaign, optical properties were also simulated by the Mie model. The results are shown in Table 6.

Table 6 Mass extinction efficiency (MEE), scattering Ångström exponent (α_{SP}), single scattering albedo (ω_0), radiative forcing efficiency ($\Delta F/\delta$) and radiative forcing efficiency $\Delta F/\delta$ per produced energy (± stdev) of studied combustion cases.

Combustion case	**MEE (m^2 g^{-1})**	**α_{SP}**	**ω_0**	**$\Delta F/\delta$ (W m^{-2})**	**$\Delta F/\delta E$ (W m^{-2} MJ^{-1})**
SSWC2-PB, measured	0.1 ± 0.02	3.8 ± 0.4	0.67 ± 0.13	-10 ± 10	-1E-1 ± 1E-1
SSWC2-PB, simulated1	0.12	3.7	0.55		
SSWC2-PB, simulated2	0.17	3.7	0.69		
SSWC2-MH, measured	7.1 ± 7.9	2.2 ± 0.2	0.16 ± 0.08	34 ± 7	0.2E-1 ± 4.9E-2
SSWC2-MH, simulated	9.8	2.3	0.2		
C+DSP	2.4 ± 0.9	1.3 ± 0.1	0.89 ± 0.05	-23 ± 4	-2E-5 ± 4E-6
C+P+DSP	1.5 ± 0.5	1.8 ± 0.2	0.93 ± 0.06	-29 ± 5	-3E-5 ± 5E-6
C+P+bypassDSP	3.3 ± 1.1	0.9 ± 0.03	0.65 ± 0.09	-6 ± 8	-5E-6 ± 7E-6
HFO+78MW	0.2 ± 0.02	1.1 ± 0.1	0.57 ± 0.03	0.3 ± 3	1E-6 ± 1E-5
HFO+E+78MW	0.2 ± 0.01	2.1 ± 0.1	0.76 ± 0.02	-19 ± 1	-7E-5 ± 6E-6
HFO+LFO+ 120MW	0.1 ± 0.01	1.4 ± 0.1	0.52 ± 0.05	4 ± 4	1E-5 ± 1E-5

The MEE values were calculated in order to connect the optical properties with the PM_1 emissions. For the measured and simulated SSWC2-PB and HFO-HS campaign, the MEEs were rather low (ca. 0.1-0.2 $m^2\ g^{-1}$). The size distributions of these cases were rather similar with the NGMD(D_p) far below 100 nm (see Table 5). The size distribution dependence of mass scattering efficiencies (MSE) reviewed by Hand and Malm (2007) also agreed with the low MEE values of this thesis showing decreasing trend of the MSE with decreasing particle sizes. Instead, The MEE of the SSWC2-MH was high according to measured and simulated results (7.1 ± 7.9 and 9.8 $m^2\ g^{-1}$, respectively). The high MEEs agreed with mass absorption efficiencies (MAE) published previously e.g. by Petzold and Schönlinner (2004). The result is consistent with the high fraction of absorbing material in the PM_1 emissions presented in Section 6.2.1 (Figure 6). The MEE values of the C-PP campaign were in the range of 1.5-3.3 that corresponds with the published MSE values for inorganic species of fine particles (2.9 ± 0.3 $m^2\ g^{-1}$) (Malm and Hand, 2007). As the chemistry and the number size distribution results showed, argumentation of the MEE values were reasonable for C-PP campaign.

Scattering Ångström exponent α_{SP} was discussed to relate scattering with the particle diameter. Overall, α_{SP} was the highest for the SSWC2 campaign (3.8 ± 0.4 and 2.2 ± 0.2 for the SSWC2-PB and SSWC2-MH, respectively). α_{SP} usually increases with increasing fraction of fine particles. This is consistent with the results shown in Table 5: the number size distribution of the SSWC2-MH was bimodal and wider than the distribution of the SSWC2-PB case. Thus, the lower α_{SP} value for the SSWC2-MH than for the SSWC2-PB was reasonable. The lowest value of α_{SP} (0.9 ± 0.03) was found for the C+P+bypassDSP case. The result could partly indicate with increasing influence of particles near 1 µm instead of ultrafine particles. This fact stands for low α_{SP} values. α_{SP} values in the HFO-HS1 campaign were in the range of ca. 1.1 – 2.1. Even though the number concentration and particle mode maximum were nearly constant in the four combustion cases, the α_{SP} varied clearly. In general, the α_{SP} seemed to be dependent also in combustion technology and fuel. The lowest values of the C-PP campaign were in agreement with the values presented for dust aerosol both including significant amount of mineral matter (Eck et al., 1999). The results of the HFO-HS1 campaign fitted best with the values of scattering Ångström exponent around 1.5 – 1.8 reported for polluted urban aerosol (Doherty et al., 2005; Lyamani et al., 2008; Pereira et al., 2011).

The average (± stdev) single scattering albedo ω_0 of the SSWC2+MH, HFO+78MW and C+DSP cases are shown in Figure 7 (black squares) and Table 6. ω_0 of the additional combustion cases are shown as black stars. In the ambient air ω_0 differs depending on the source and age of particles. In

the urban air, the values between 0.5 and 0.9 have been determined (e.g. Lyamani et al., 2008; Carrico et al., 2003). In non-polluted regions, ω_0 is usually higher than 0.9 that represents particles consisting almost only of scattering material. ω_0 of pure soot is approximately 0.3 (Mikhailov et al., 2006). As Figure 7 shows, obvious differences in ω_0 were seen between the combustion cases. ω_0 of the HFO-HS1 campaign varied between 0.52 ± 0.05 and 0.76 ± 0.02 and was in the same range with ω_0 of the SSWC2+PB case (0.67 ± 0.13). These values indicated a rather high absorbing influence of particles even though fraction of absorbing material was rather low. This discrepancy between low fraction of absorbing material and high single scattering albedo could be explained by optical properties of size distributions of these cases: The simulation process presented in Supporting Information of Paper III showed that for the SSWC1-PB, absorption efficiencies of particles approximately <60 nm (mobility diameter) were higher than scattering efficiencies. Remarkable part of particles was below this range in the SSWC2+PB case but also in the cases of the HFO-HS campaign. Thus, same behavior could be expected. The low ω_0 of the SSWC-MH (0.16 ± 0.10) was consistent with high BC fraction shown in Figure 6. The C-PP campaign seemed to emit mostly scattering particles when the DSP was used. The high fraction of ions (Figure 6) with a high sulfate fraction endorsed high ω_0 values. The contribution of absorbing material increased with the bypass of the DSP corresponding to a significant decrease of ω_0 to 0.65 ± 0.09 (Figure 7, Table 6).

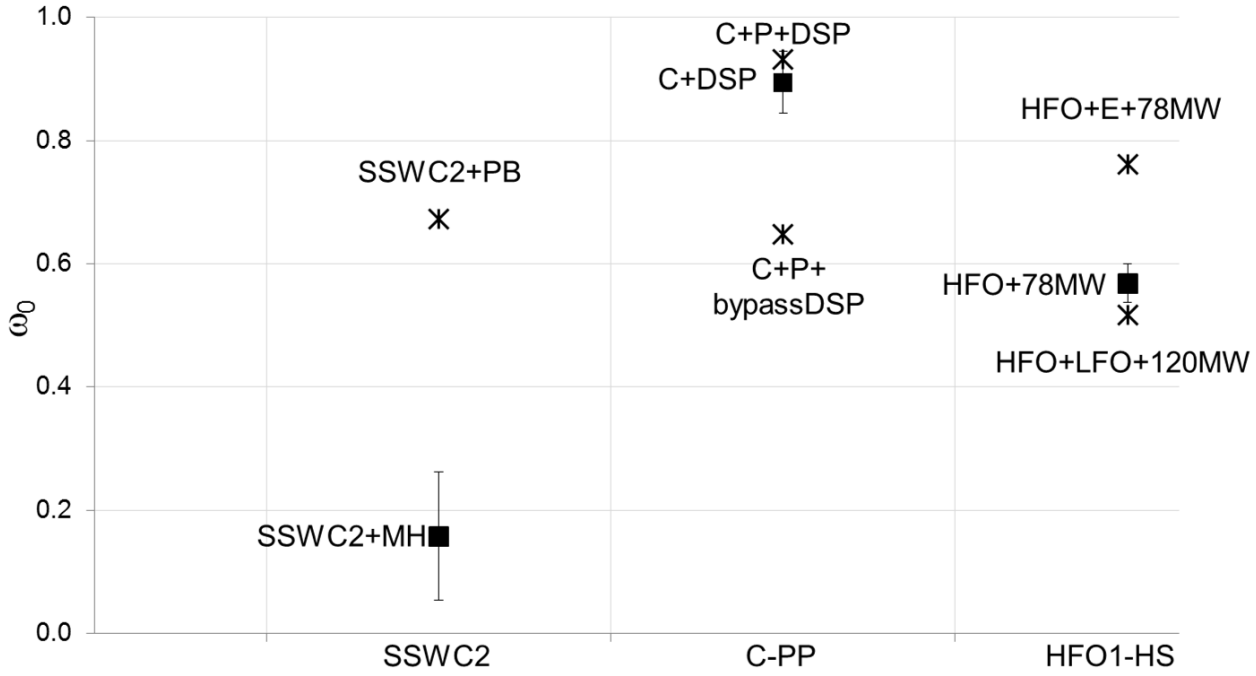

Figure 7 Single scattering albedo (ω_0) of the PM1 emissions of the combustion technologies presented in Paper III (Figure 3, Paper III).

In the ΔF/δ results (Table 6), the negative and positive sign indicate cooling and warming effect of the aerosol in question. The used surface reflectance R_s=0.15 represents dark surface such as grass. Setting R_s to value describing snow-covered ground (>0.6) would lead higher values of ΔF/δ. ΔF/δ values were negative (i.e. cooling effect) for all the other cases but SSWC2+MH, HFO+78MW and HFO+LFO+120MW (Table 6). As fresh aerosols, the SSWC2+MH would have clearly strongest warming effect (ΔF/δ =34 ± 7 W m^{-2} or (ΔF/δ)/produced energy=0.2×10^{-1} ± 4.9×$^{-2}$ W m^{-2} MJ^{-1}). The study of Virkkula et al. (2011) reported ΔF/δ values between -20 and -27 W m^{-2} for ambient background aerosol. These results were in the same range as radiative forcing efficiencies of the C1+DSP, C1+P+DSP and HFO+E+78MW cases. Overall, if primary particle emissions of this study would transport to the areas with high ground reflectance (e.g. snow-covered Arctic) as such they would have warming effect.

6.2.4 Hygroscopic growth of particles emitted from large-scale combustion of HFO

The hygroscopic growth of particles having mobility diameters of 20, 47, and 72 nm were studied using an HTDMA in Paper IV. The measurements were performed close to 90 % relative humidity both through and bypassing the thermodenuder. The results were based on averages on 2 to 7 and 4 to 7 separate HTDMA measurements with humidified and dry air, respectively.

In the case of HFO combustion (HFO+30MW), the growth factors (ratio between humidified and dry particle size, GF) were overall higher than the GFs of the HFO+E+30MW and HFO+LFO+E+30MW cases. When the water emulsion was added to the combustion of HFO, the GFs were somewhat lower than in the case of HFO+30MW. In the case of emulsion, the GFs decreased with increasing the particle size.

The effect of thermodenuder was seen in the case of the HFO+30MW and especially for the particle diameter 72 nm: the GF decreased to ~1.25 from ~1.35. This reduction may mean that there were more volatile hygroscopic compounds in this particle size that evaporated in thermodenuder than in smaller sizes.

When the HFO+LFO emulsion was used, the growth factors of the measured particle sizes changed considerably with the particle size and the GFs were mostly smaller than the corresponding GFs for the other cases of the study. The thermodenuder treatment did not noticeable affect the GF values of the HFO+LFO+E+30MW. The largest (72 nm) particles, with and without the thermodenuder treatment, actually shrank in the HTDMA treatment. The behavior indicates that 72 nm particles were agglomerates with low hygroscopicity. It has been reported by Pagels et al. (2009) that the

condensation of sulfuric acid or water on agglomerated soot initially results in shrinkage of mobility diameter due to the restructuring of the soot core.

Growth factors of smallest determined particles (20nm) were highest and in the same range studied previously by Henning et al. (2012). They claimed that soot particles coated by sulfuric acid with changing OC content were more hygroscopic with higher OC content because of the reaction of sulfuric acid with some organics. This could lead to change in hygroscopicity. Here, the OC content in relation to BC was lowest when LFO was mixed with HFO with emulsion. In this case, the GFs were lower than in the other combustion cases. This result supports the above mentioned assumptions. However, the reduction in GFs in the HFO+LFO+E+30MW case in comparison with the HFO+30MW and HFO+LFO+30MW cases can also be affected by other differences in chemical composition.

The results of Paper IV showed that the fine particles emitted from HFO combustion are quite hygroscopic even as fresh particles. However, by adding water to the combustion process and, further, by mixing HFO into LFO, the hygroscopic growth factors of emission particles decreased. Overall, it is probable that particles from HFO combustion will contribute to cloud formation, reduce visibility and, furthermore, have a detrimental effect on the overall air quality especially in large cities.

7 Review of articles and author's contributions

Paper I presents a method that enables determination of number and mass concentration of externally mixed soot particles (here called less volatile (LV) particles) based on the combination of VTDMA and DMPS. The mass concentration of LV particles (M_{LV}) was compared with the mass concentration of BC particles measured with the MAAP (M_{BC}). The DMPS and VTDMA data were also used for calculation of σ_{SP} and σ_{AP} with a Mie model. The model was run changing the refractive index and assuming external and internal mixing of absorbing and scattering aerosol. The modelled values were compared with measured σ_{AP}. The comparisons between M_{LV} and M_{BC} as well as measured and modelled σ_{AP} with the combination of wind direction information verified suitability of the VTDMA-DMPS system to measure LV particles. The instrumentation and data analysis of this study also made it possible to determine the local traffic-related particle emissions.

I contributed to this study taking care of the ready-build measurements with the co-authors, analyzed the data and wrote the article with the help of the co-authors.

Paper II contains a study of influence of combustion conditions on particle emissions of small-scale wood combustion. The chemical composition and size distribution of particles emitted from a conventional masonry heater were studied in normal and smouldering combustion conditions. The normal combustion was characterized by the best operational practice of this heater, whereas the smouldering combustion corresponded to the slow heating combustion that results from the common user mistakes in operational practice (overloading of the firebox, restriction of air supply to prolong heating). The results were based on the versatile chemical analysis of the filter samples collected using different sampling techniques. The chemical compositions and mass size distributions of the normal and smouldering combustion were compared and the estimations of the reasons for the differences were presented.

I participated in the design and preparation of the measurement setup and carried out the measurement campaign with the co-authors. I made the elemental and organic carbon analysis whereas other chemical analyses were carried out by the co-authors. I analyzed the data of the study and wrote the article.

In Paper III, the properties and differences of particle emissions produced by the various energy production technologies were studied. The studies included three combustion campaigns: small-scale wood combustion including investigations of a pellet boiler and conventional masonry heater combustion (fuelled with wood pellets and birch wood logs, respectively), combustion of coal and mixture of coal and pellets at a coal-fired power plant and combustion of heavy and light fuel oil at a heavy fuel oil-fired heating station. The chemical compositions of the particle emissions were determined based on filter sample analyses and real-time measurements of e.g. absorbing material and organic carbon. In addition, number and volume size distributions as well as optical properties of emitted particles were measured. Based on the optical results, the quantities that are important in the estimations of influence of particles on global warming were calculated (e.g single scattering albedo, aerosol forcing efficiency).

In each of the campaign of this paper, I was responsible of the design and preparation of the measurement setup as well as the measurement campaign with my co-authors. The chemical analyses were carried out by the co-authors. I was responsible of the data analyses excluding the Mie modeling and preprocessing of part of the chemical results that were made by the co-authors. I wrote the article.

Paper IV concerned size distributions, chemical and hygroscopic properties of particles emitted from large-scale oil combustion at a heavy fuel oil-fired heating station. Especially chemical properties of the particle emissions were linked with the hygroscopic growth of the particles. Hygroscopic character of particles is important when the influence of particles on cloud formation is considered. The combustion was carried out in an oil-fired water tube boiler run with 30 MW power. The investigation compared particle properties in three different cases: combustion of heavy fuel oil, combustion of heavy fuel oil with addition of water emulsion into the combustion process and combustion of mixture of heavy and light fuel oil with water emulsion. The influence of different fuel conditions on hygroscopicity (HTDMA) and number and volume size distributions of emitted particles were measured. Chemical compositions were studied based on filter sample analyses and real-time measurements of absorbing material (black carbon, BC) and organic carbon (OC). Especially changes in sulfate content and ratio between BC and OC were of interest because previous studies have shown these components to be important factors for hygroscopic properties of particles. In addition, influence of thermodenuder treatment on particle size distributions and hygroscopicity was investigated. This experiment gave information of the volatility of the particles.

I participated in the design, preparation and measurements of the campaign. The instrumentation concerning chemical properties of the particles was more of my duty whereas HTDMA and size distribution measurements were carried out by the authors from the Tampere University of Technology. The chemical analyses were carried out by the co-authors. I analyzed the chemical data of the study. The analysis of size distribution and HTDMA data was made by the co-authors from the Tampere University of Technology. The article was mainly written by the authors from the Tampere University of Technology. I participated in the writing process giving advices and ideas concerning the particle composition part of the manuscript and writing mainly technical descriptions of the chemical instrumentations.

8 Summary

Combustion processes emit remarkable amount of particles into the atmosphere. These particles are released into the atmosphere e.g. from the spark ignition (SI) and diesel engines of road-traffic and from the combustion processes of small and large-scale energy production. Burning technologies and conditions influence strongly on physical and chemical properties of particle emissions that are harmful to human health and affect the climate. This thesis focused on the investigation of the characteristics of particle emissions of various combustion sources. The primary particle emissions influenced by the energy production were versatilely investigated and the results were collected together within this thesis. The atmospheric radiative forcing effects of the particle emissions of the combustion processes were also assessed. In addition, suitable measurement and data handling techniques to verify the soot fraction and the mixing state of particles in the ambient air influenced by traffic was studied.

The traffic related particle emissions were connected to the study where a suitable technique to study soot fraction and mixing state of ambient air particles was tested. A combination of a volatility differential mobility analyzer (VTDMA) and twin differential mobility particle sizer (DMPS) was used to determine the mass concentration of less volatile (LV) particles (M_{LV}) that was assumed to be externally mixed soot. The results were compared with optically measured black carbon (BC) mass concentrations (M_{BC}). In addition, measured and modeled optical properties (scattering and absorption coefficients, σ_{SP} and σ_{AP}, respectively) with the information of wind direction were used to strengthen the estimations of suitability of the VTDMA-DMPS-technique to measure the externally mixed soot fraction of ambient aerosol.

The results of the study showed that the M_{LV} agreed with the M_{BC} during the periods when the air masses where coming from the highways indicating fresh traffic emissions. During these periods, the volume weighed LV particle fraction increased remarkably. For the periods with fresh traffic related particles, also the modeled σ_{AP} assuming external mixture of particles agreed with the measured one. Overall, the modeled absorption of light due to externally mixed particles was smaller than measured σ_{AP} that most probably indicated absorption of light due to internally mixed long range-transported aerosol mass. The measurement and analysis techniques proved to be suitable for determination of LV particle fraction in the ambient air that in most of the cases can be expected to be soot. The study also gave information about mixing state and refractive indices of the ambient aerosol particles.

The characteristics of the primary particle emissions were studied for small-scale wood and wood pellet combustion (SSWC), coal combustion and mixture of coal and pellet combustion at a coal-fired heating and power plant (C-PP) and heavy and light fuel oil combustion (HFO and LFO, respectively) at a HFO-fired heating station (HFO-HS). The SSWC campaigns included studies that concerned the influence of combustion conditions on particle emissions of a conventional masonry heater (i.e. comparison between normal and smouldering combustion) and the comparison of particle properties between the emissions of a conventional masonry heater and a pellet boiler. The particle emissions of the masonry heater and pellet boiler combustion were compared with the emissions of the HFO-HS1 and C-PP. The studies of primary emissions of the small and large-scale combustion included versatile instrumentations determining various chemical and physical properties of the particles. The chemical composition of the particles and their size distributions were mainly determined based on the analysis of the filter samples collected with various sampler and impactor techniques. Particle number and volume size distributions, optical properties were determined for the SSWC2, HFO-HS1 and C-PP campaigns. Further, hygroscopic properties of particles emitted from a HFO-fired heating station processed with various fuel combinations were investigated and connected with chemical characteristics.

The PM_1 emission factors (E_F) of the small-scale combustion of wood fuels were clearly higher than E_Fs for the large-scale burning of coal/coal-pellet mixture and HFO/HFO-LFO mixture. In the SSWC cases, E_F were clearly lowest in the pellet boiler burning but the E_F of masonry heaters varied in the wide range depending from the burning appliance and combustion conditions. Smouldering combustion characterizing inefficient burning conditions influenced e.g. by the overloading of the firebox and insufficient air supply caused the highest particle emissions. Instead, the E_Fs of the large-scale combustion at the HFO-fired heating station or coal-fired power plant were ~4 to 110 times smaller than the emissions in the cleanest case of the SSWC (pellet boiler). Particle emissions were lowest at the coal fired power plant when the flue gases were cleaned in the desulfurization plant (DSP). The DSP removed more than 90 % of the particle emissions from the flue gases. When emissions were determined without the DSP, E_Fs of particles were at the same range as the ones measured at the HFO-fired heating station where no flue gas cleaning techniques were used.

The difference between the efficiency of the combustion processes of the large and small-scale combustion was also seen in the chemical composition: organic compounds (POM) and black carbon (BC, here refereed as absorbing material) that are tracers of the incomplete combustion were the main chemical components in the SSWC cases excluding the pellet boiler that represents rather

efficient small-scale combustion appliance. Instead, the large-scale combustion of the coal, mixture of coal and pellet, HFO and mixture of HFO and LFO emitted mostly particles including ionic compounds with alkali metals and elements such as trace metals. It has to be noted that for the C-PP campaign, organic compounds were not analyzed but it was expected based on the previous knowledge that the emissions of organic compounds are insignificant. In the particle emissions of the C-PP and HFO-HS campaigns, the absorbing material determined could also indicate to iron oxides that are highly absorbing in the UV and visible light wavelengths and occur in oil and coal combustion flue gases. In the C-PP combustion cases, the DSP clearly influenced the chemical composition of the particles: the chemicals added into the DSP process resulted in a decrease of SO_2, metal and absorbing material emissions and enhanced emissions of some ionic compounds when compared with the emissions in the case of the DSP bypass.

The influence of combustion process and fuel was also seen in the particle size distributions. Overall, the number concentrations of coal combustion emissions were significant up to 1 µm when compared with the size distributions of the oil combustion. The number size distributions of the HFO-HS and pellet boiler combustion were unimodal and rather sharp whereas the number size distributions of the masonry heater and coal combustion particle emissions were wider and had many modes. Especially in the large-scale coal combustion, modes in supermicrometer sizes were significant in the volume size distributions. Ultrafine and fine particles of combustion processes are most probably formed from vaporized and nucleated volatile metals. The coarse mode of oil combustion could be composed of residual particles. Coal combustion particles also form from inherent mineral matter within coal transferred into PM forming coarse particles. The SSWC studies showed that the smouldering combustion shifted the size distributions to the larger particles when compared with the size distributions in the normal conditions.

The hygroscopic properties of particles studied in the HFO-HS2 campaign with the HTDMA were closely related to the particle size and chemical composition. The HTDMA results showed that the fine particles emitted from HFO combustion were rather hygroscopic even as fresh particles. However, by adding water to the combustion process and, further, by mixing HFO into LFO, the hygroscopic growth factors of emission particles decreased. Also sulfate content decreased with addition of water emulsion. Sulfate content indicates with sulfur in flue gas that could form sulfuric acid. Sulfuric acid has been seen important factor in particle growth. In addition, it has been shown that the decrease of organic compound (OC) content in relation to black carbon (BC) would decrease the hygroscopic growth of soot particles coated by sulfuric acid. This assumption was also supported by the observations of this thesis: in the case of emulsion added to the combustion of

mixture of heavy and light fuel oil, the OC to BC ratio was smaller than in case of the combustion of only HFO. Furthermore, growth factors of the emitted particles were strongly dependent on the size of the particles. Overall, these results indicate that particles from HFO combustion can have significant effect on cloud formation, visibility and air quality.

The information about the optical properties of the particles emitted from the various combustion processes gave the possibility to investigate the relationships between the particle optics, PM_1 emissions and size distributions as well as the possible radiative effects of these particles. The determined parameters were mass extinction efficiency (MEE) scattering Ångström exponent α_{SP}, single scattering albedo ω_0 and radiative forcing efficiency $\Delta F/\delta$. The MEE values indicated both to the chemical composition and size distribution: MEE values were lowest for the pellet boiler and HFO-HS cases where particle number size distributions were unimodal and concentrated to the sizes below 100 nm (geometric diameter). The result was in agreement with mass scattering efficiencies (MSE) presented previously for the ultrafine particles. For the masonry heater combustion including significant amount of absorbing material in the flue gas, the MEE was high and corresponded to the values of mass absorption efficiencies reported for the absorbing material. Moreover, The MEE values of the coal combustion agreed with the published MSE values for inorganic species of fine particles.

Also the results of the α_{SP} that relates scattering with the particle diameter were mostly reasonable. α_{SP} usually increases with increasing fraction of fine particles that was in partly accordance with the size distributions: α_{SP} was lowest for the coal combustion whereas for the pellet boiler, masonry heater and HFO-HS cases the α_{SP} was higher. In general, the α_{SP} seemed to be dependent also in combustion technology and fuel.

The ω_0 (ratio between scattering and extinction) varied obviously between combustion cases. ω_0 was clearly lowest for the wood combustion in a masonry heater. There, absorbing material dominated the chemical composition. Also ω_0 of the pellet boiler emissions was surprisingly low even though the fraction of absorbing material was low. This is probably because of high absorbing efficiency of the ultrafine particles. ω_0 of the HFO-HS emissions were in the same range with the pellet boiler emissions. Instead, coal combustion with the DSP treatment seemed to emit mostly scattering particles based on the high ω_0. This result was in accordance with the chemical composition of the flue gas particles. ω_0 is connected to the $\Delta F/\delta$ that represented the radiative effect of particles in the atmosphere over a surface with a certain reflectance. Here, the surface was

assumed to be dark, such as grass. $\Delta F/\delta$ values were negative (i.e. cooling effect) for all of the cases except for the wood combustion in a masonry heater and part of cases of oil combustion. As fresh aerosols, the masonry heater combustion would have clearly strongest warming effect. Instead, the radiative forcing efficiencies of the coal combustion with the DSP and HFO combustion with emulsion were in the same range as presented for the ambient background aerosol and were clearly cooling. Overall, if primary particle emissions of the studied cases would transport to the areas with high ground reflectance (e.g. snow-covered Arctic) as such they would have warming effect.

9 Outlook of the used techniques and research field

The measurement techniques used in this thesis presented mostly techniques that are widely used in aerosol science. Partly, the results were however processed in new ways. The determination of chemical properties of particles was mostly based on the filter sampling excluding the determination of BC and organics. Modern filter analyze techniques were used leading to results with high accuracy and yield. Nowadays there are also real-time techniques available to measure chemical composition of particles, such as time-of-flight aerosol mass spectrometer (ToF-AMS), but these instruments still have some restrictions that still support filter sampling at least in parallel with real-time techniques. For example, particle size range of the ToF-AMS is restricted to the range of 0.04 and ~0.7 µm.

This thesis provided detailed information about particles emitted from the small- and large-scale combustion processes taking into account various fuels and combustion conditions. One study was more concentrated on testing of the suitability of measurement method to determine LV particle fraction with the VTDMA-DMPS technique. Also in this case, the influence of combustion process on particle emissions was seen in the cases of externally mixed particles. The study on the VTDMA-DMPS technique also presented a way to connect information given by this technique with optical properties of particles determined by the measurements and Mie-modeling. The Mie-modeling gave a possibility to approve the estimation of mixing state and refractive indices of the air masses. This kind of approach is not widely used and thus, offers a new way to combine various measuring and modeling techniques.

The studies on the various combustion processes included comprehensive instrumentation that provided possibility to determine versatile particle properties leading to useful information of the influence of combustion process and conditions on the refractive particle emissions. Chemical properties and size distributions of particles emitted from various combustion processes have been studied previously and the results of this thesis supported those findings. Instead, connections of the optical properties of emitted particles to the chemical and size distribution information is not usually presented. Optical information allows the estimation of radiative forcing effect of the particles emitted from burning processes and simultaneous determination of chemistry and other physical properties of particles make it possible to assess which exact factors are the ones affecting the radiative forcing of the earth. The thesis also studied the hygroscopic properties of particles emitted from oil combustion but there was no comparison with the optical properties of particles. The information about scattering and absorption is important when e.g. the cloud properties are

considered and could be interesting field to study together with hygroscopic measurements in the future.

As the combustion processes are complex and the techniques develop all the time, the research in the field of emissions will be needed also in the future. To compare the results in the past and in the future, it is important to use comparable measurement techniques. The new measurement techniques can be tested in parallel. Real-time techniques are important if variations during combustion processes are investigated. The research in the field of the particle emission from the combustion can be shared into various pieces depending on the viewpoint. Here are some examples: comparison of suitable measurement techniques, comparison of particle emissions between different combustion processes and influences of combustion conditions in a certain combustion process on particle emissions. Also basic research on particle formation mechanisms during combustion processes is still needed.

Overall, this thesis gave inclusive insight to the influence of combustion appliance, condition and fuel on emissions of refractory particles. The information given by the thesis can be used as scientific base for the future studies. In addition, the information is valuable in the evaluations of the best available combustion technique. Particle formation mechanisms and the factors influencing them are studied widely but are still rather uncertain. Thus, this field needs further investigation that benefits from the previous research.

References

Alfaro, S., Lafon, S., Rajot, J., Formenti, P., Gaudichet, A. and Maillé, M. (2004). Iron oxides and light absorption by pure desert dust: An experimental study. *J. Geophys. Res*., 109 (D08208), doi:10.1029/2003JD004374.

Anderson, T., Covert, T, Marshall, S., Laucks, M., Charlson, R., Waggoner, A., Ogren, J., Caldow, R., Holm, R., Quant, F., Sem, G., Wiedensohler, A., Ahlquist, N. and Bates, T. (1996). Performance characteristics of a high-sensitivity, three-wavelength, total scatter/backscatter nephelometer. *J. Atmos. Ocean. Technol.*, 13, 967–986.

Anderson, T. and Ogren, J. (1998). Determining aerosol radiative properties using the TSI 3563 integrating nephelometer. *Aerosol Sci. Technol*., 29, 57–69, doi:10.1080/02786829808965551.

Andreae and Gelencsér (2006). Black carbon or brown carbon? The nature of light-absorbing carbonaceous aerosols. *Atmos. Chem. Phys*., 6, 3131–3148.

ASME (2011). An international code, 2010 ASME boiler & pressure vessel code. *VII Recommended guidelines for the care of power boilers.* The American Society of Mechanical Engineers, Three Park Avenue, New York, Library of congress catalog card number: 56-3934

Berner, A. and Lürzer, C. (1980). Mass size distributions of traffic aerosols at Vienna. *J. Phys. Chem.*. 84, 2079–2083, doi:10.1021/j100453a016.

Birch M. E. and Cary R. A. (1996). Elemental carbon-based method for monitoring occupational exposures to particulate diesel exhaust. *Aerosol Sci. Technol*., 25, 221–241.

Birmili, W., Stratmann, F., and Wiedensohler, A. (1999). Design of a DMA-based size spectrometer for a large particle size range and stable operation. *J. Aerosol Sci*., 30, 549–553.

Bockhorn, H. (1994). *Soot Formation in Combustion, Mechanisms and Models.* Springer Series in Chemical Physics, Springer-Verlag, Berlin, Vol. 59.

Boman B.C., Forsberg A.B. and Järvholm B.G. (2003). Adverse health effect from ambient air pollution in relation to residential wood combustion in modern society. *Scand, J. Work Environ. Health*. 29(4), 251–260.

Bond, T., Anderson, T. and Campbell, D. (1999). Calibration and intercomparison of filter-based measurements of visible light absorption by aerosols. *Aerosol Sci. Technol*., 30, 582–600, doi:10.1080/027868299304435 .

Bond and Bergstrom (2006). Light Absorption by Carbonaceous Particles: An Investigative Review. *Aerosol Sci. Technol*., 40, 27–67.

Canagaratna, M., Jayne, J., Ghertner, D., Herndon, S., Shi, Q., Jimenez, J., Silva, P., Williams, P., Lanni, T., Drewnick, F., Demerjian, K., Kolb, C. and Worsnop, D. (2004). Chase studies of particulate emissions from in-use New York City vehicles, *Aerosol Sci. Technol.*, 38, 555–573, doi: 10.1080/02786820490465504.

Cao, G., Zhang, X. and Zheng, F. (2006). Inventory of black carbon and organic carbon emissions from China. *Atmos. Environ*., 40, 6516–6527.

Cappa,C., Onasch, T., Massoli, P., Worsnop, D., Bates, T., Cross, E., Davidovits, P., Hakala, J., Hayden, K., Jobson, B., Kolesar, K., Lack, D., Lerner, B., Li, S.-M., Mellon, D., Nuaaman, I., Olfert, J., Petäjä, T., Quinn, P., Song, C., Subramanian, R., Williams, E. and Zaveri, R. (2012). Radiative absorption enhancements due to the mixing state of atmospheric black carbon. *Science*, 337, 1078–1081, *doi:*10.1126/science.1223447.

Carrico, C., Bergin, M., Xu, J., Baumann, K. and Maring, H. (2003). Urban aerosol radiative properties: Measurements during the 1999 Atlanta Supersite Experiment. *J. Geophys. Res*., 108 (D7), 8422, doi:10.1029/2001JD001222.

Córdoba, P., Ochoa-González, R., Font, O., Izquierdo, M., Querol, X., Leiva, C., López-Antón, M.A., Díaz-Somoano, M., Martinez-Tarazona, M.R., Fernandez, C., Tomás, A. (2012). Partitioning of trace inorganic elements in a coal-fired power plant equipped with a wet flue gas desulphurisation system. *Fuel*, 92, 145–157.

Davidsson, K., Stojkova, B. and Pettersson, J. (2002). Alkali emission from birchwood particles during rapid pyrolysis. *Energy & Fuels*, 16, 1033–1039.

DeCarlo, P., Slowik, J., Worsnop, D., Davidovits, P. and Jimenez, J. (2004). Particle Morphology and Density Characterization by Combined Mobility and Aerodynamic Diameter, Measurements. Part 1: Theory. *Aerosol Sci.* Technol., 38, 1185–1205, doi: 10.1080/027868290903907.

Delene, D. J. and Ogren, J. A. (2002). Variability of aerosol optical properties at four North American surface monitoring sites. *J. Atmos. Sci*., 59, 1135–1150.

Doherty, S., Quinn, P., Jefferson, A., Carrico, C., Anderson, T. and Hegg, D (2005). A comparison and summary of aerosol optical properties as observed in situ from aircraft, ship, and land during ACE-Asia. *J. Geophys. Res*., 110 (D04201), doi:10.1029/2004JD004964.

Eck, T., Holben, B., Reid, J., Dubovik, O., Smimov, A., O'Neill, N., Slutsker, I. and Kinne, S. (1999). Wavelength dependence of the optical depth of biomass burning; urban; and desert dust aerosols. *J. Geophys. Res*., 104 (D24), 31333–31349, doi:10.1029/1999JD900923.

Finnish Environment Institute (2001). *Finnish expert report on best available techniques in large-scale combustion plants*. Edita Oyj, Helsinki, Finland.

Flagan, R. C. and Seinfeld, J. H. (1988). *Fundamentals of air pollution engineering*. Prentice-Hall, Inc., Englewood Cliffs, New Jersey.

Flanner, M. G., Zender, C. S., Randerson, J. T. and Rasch, P. J. (2007). Present-day climate forcing and response from black carbon in snow. *J. Geophys. Res.*, 112(D11202), doi:10.1029/2006JD008003.

Fu, W., Hou, L., Wang, L. and Ma, F. (2002). A unified model for the micro-explosion of emulsified droplets of oil and water. Fuel Process. Technol., 79, 107−119 , DOI: DOI: 10.1016/S0378-3820(02)00106-6.

Gundel, L. A., Lee, V. C., Mahanama, K. R. R., Stevens, R. K. and Daisey, J. M. (1995). Direct determination of the phase distributions of semi-volatile polycyclic aromatic hydrocarbons using annular denuders. *Atmos. Environ*., 29, 1719–1733.

Hand, J. L. and Malm, W. C. (2007). Review of aerosol mass scattering efficiencies from ground-based measurements since 1990. *J. Geophys. Res*., 112 (D16203), doi:10.1029/2007JD008484.

Hansen, J. and L. Nazarenko (2004). Soot climate forcing via snow and ice albedos. *Proc. Natl. Acad. Sci. U. S. A.*, 101, 423– 428.

Haynes, B., Neville, M., Quann, R. and Sarofim, A. (1982). Factors Governing the Surface Enrichment of Fly Ash in Volatile Trace Species. *J. Colloid Interface Sci*., 87, 266–278.

Haywood, J. M. and Shine, K. P. (1995). The effect of anthropogenic sulfate and soot aerosol on the clear sky planetary radiation budget. *Geophys. Res. Lett*., 22(4), 603–606, doi:10.1029/95GL00075.

Henning, S., Ziese, M., Kiselev, A., Saathoff, H., Mohler, O., Mentel, T. F., Buchholz, A., Spindler, C., Michaud, V., Monier, M., Sellegri, K. and Stratmann, F. (2012). Hygroscopic growth and droplet activation of soot particles: uncoated, succinic or sulfuric acid coated. *Atmos. Chem. Phys*., 12, 4525–4537.

Hinds, W.C. (1999). *Aerosol technology: properties, behavior, and measurement of airborne particles*. 2nd ed., John Wiley and Sons, New York.

Hitzenberger, R., Jennings, S. G., Larson, S. M., Dillner, A., Cachier, H., Galambos, Z., Rouc, A., and Spain, T. G. (1999). Intercomparison of measurement methods for black carbon aerosols, *Atmos. Environ*. 33, 2823–2833.

Jacobson, M.Z. (2001). Strong radiative heating due to the mixing state of black carbon in atmospheric aerosols. *Nature*, 409, 695–697, doi:10.1038/35055518.

Jalkanen L. M. and Häsänen E.K. (1996). Simple method for the dissolution of atmospheric aerosol samples for analysis by inductively coupled plasma mass spectrometry. *J. Anal. At. Spectrom.*, 11, 365–369.

Johansson, L.S., Leckner, B., Gustavsson, L., Cooper, D., Tullin, C. and Potter, A. (2004). Emission characteristics of modern and old-type residential boilers fired with wood logs and wood pellets. *Atmos Environ*., 38, 4183–4195.

Kaivosoja, T., Jalava, P.I., Lamberg, H., Virén, A., Tapanainen, M., Torvela, T., Tapper, U., Sippula, O., Tissari, J., Hillamo, R., Hirvonen, M.-R., and Jokiniemi, J. (2013). Comparison of emissions and toxicological properties of fine particles from wood and oil boilers in small (20-25 kW) and medium (5-10 MW) scale. *Atmos. Environ.*, 77, 193–201.

Keskinen, J., Pietarinen, K. and Lehtimäki, M. (1992) Electrical Low Pressure Impactor. *J. Aerosol Sci*., 23, 353–360.

Khalil, M. and Rasmussen, R. (2003). Tracers of wood smoke. *Atmos. Environ.*, 37, 1211–1222.

Koch, D. and Hansen, J. (2005). Distant origins of Arctic black carbon: A Goddard Institute for Space Studies ModelE experiment. *J. Geophys. Res.*, 110 (D04204), doi:10.1029/2004JD005296.

Lamberg, H., Nuutinen, K., Tissari, J., Ruusunen, J., Yli-Pirilä, P., Sippula, O., Tapanainen, M., Jalava, P., Makkonen, U., Teinilä, K., Saarnio, K., Hillamo, R., Hirvonen, M.-R. and Jokiniemi, J. (2011). Physicochemical characterization of fine particles from small-scale wood combustion. *Atm. Environ.*, 45, 7635–7643, doi:10.1016/j.atmosenv.2011.02.072.

Larson T. V. and Koenig J. Q. (1994). Wood smoke: emissions and noncancer respiratory effects. *Annu. Rev. Public Health*, 15, 133–156.

Linak, W.P. and Wendt, J.O.L. (1994). Trace Metal Transformation Mechanisms during Coal Combustion. *Fuel Process. Technol*., 39, 173–198.

Linak, W., Miller, C.A. and Wendt, J. (2000). Comparison of particle size distributions and elemental partitioning from the combustion of pulverized coal and residual fuel oil. *Journal of the Air & Waste Management Association*, 50:8, 1532–1544, doi:10.1080/10473289.2000.10464171.

Loo B. Y. and Cork C. P. (1988). Development of high efficiency virtual impactors. *Aerosol Sci. Technol*., 9, 167–176.

Lyamani, H., Olmo, F. and Alados-Arboledas, L. (2008). Light scattering and absorption properties of aerosol particles in the urban environment of Granada, Spain. *Atmos. Environ*., 42, 2630–2642, doi:10.1016/j.atmosenv.2007.10.070.

Lyyränen, J., Jokiniemi, J., Kauppinen, E.I., Backman, U., Vesala, H. (2004). Comparison of different dilution methods for measuring diesel particle emissions. *Aerosol Sci. and Technol.*, 38, 12–23.

Maenhaut W., Hillamo R., Mäkelä T., Jaffrezo J.-L.,Bergin J.-L. and Davidson M. H. (1996). A new cascade impactor for aerosol sampling with subsequent PIXE analysis. *Nuclear Instruments and Methods*, B 109/110, 482–487.

Malm, W. C. and Hand, J. L. (2007). An examination of the physical and optical properties of aerosols collected in the IMPROVE program. *Atmos. Environ*., 41, 3407– 3427, doi:10.1016/j.atmosenv.2006.12.012.

Mansurov, Z. A. (2005). Soot formation in combustion processes (Review). *Combustion, Explosion, and Shock Waves*, 41, 727–744.

Marjamäki, M., Ntziachristos, L., Virtanen, A., Ristimäki, J., Keskinen, J., Moisio, M., Palonen, M., Lappi, M. (2002). Electrical Filter Stage for the ELPI. Society of Automotive Engineers (SAE). Technical Paper 2002-01-0055.

Marple, V.A., Rubow, K.L., Behm, S.M. (1991). A Microorifice Uniform Deposit Impactor (MOUDI): Description, calibration and use. *Aerosol Sci. Technol*., 14, 434–446.

Marple, V. A., and Olson, B. A. (1999). A Micro-Orifice Impactor with Cut Sizes Down to 10 Nanometers for Diesel Exhaust Sampling, Final Report Generic Center for Respirable Dust, Pennsylvania State University, University Park, PA.

Meyer, N. and Ristovski, Z. (2007). Ternary nucleation as a mechanism for the production of diesel nanoparticles: experimental analysis of the volatile and hygroscopic properties of diesel exhaust using the volatilization and humidification tandem differential mobility analyzer. *Environ. Sci. Technol*., 41, 7309–7314.

Mikhailov, E., Vlasenko, S., Podgorny, I., Ramanathan, V. and Corrigan, C. (2006). Optical properties of soot-water drop agglomerates: An experimental study. *J. Geophys. Res*., 111, 1–16, doi:10.1029/2005JD006389.

Miller, B.G. and Tillman, D.A. (Eds.) (2008). *Combustion Engineering Issues for Solid Fuel Systems*. Academic Press.

Miller B.G. (2011). *Clean Coal Engineering Technology*. Butterworth-Heinemann.

Müller, T., Henzing, J. S., de Leeuw, G., Wiedensohler, A., Alastuey, A., Angelov, H., Bizjak, M., Collaud Coen, M., Engström, J. E., Gruening, C., Hillamo, R., Hoffer, A., Imre, K., Ivanow, P., Jennings, G., Sun, J. Y., Kalivitis, N., Karlsson, H., Komppula, M., Laj, P., Li, S.-M., Lunder, C., Marinoni, A., Martins dos Santos, S., Moerman, M., Nowak, A., Ogren, J. A., Petzold, A., Pichon, J. M., Rodriquez, S., Sharma, S., Sheridan, P. J., Teinilä, K., Tuch, T., Viana, M., Virkkula, A., Weingartner, E., Wilhelm, R. and Wang, Y. Q. (2011). Characterization and intercomparison of aerosol absorption photometers: result of two intercomparison workshops. Atmos. Meas. Tech., 4, 245-268, doi:10.5194/amt-4-245–2011.

Ninomiya, Y., Zhang, L., Sato, A. and Dong, Z. (2004). Influence of coal particle size on particulate matter emission and its chemical species produced during coal combustion. *Fuel Processing Tech*., 85, 1065–1088, doi:10.1016/j.fuproc.2003.10.012.

Onasch, T. B., Trimborn, A., Fortner, E. C., Jayne, J. T., Kok, G. L., Williams, L. R., Davidovits, P. and Worsnop, D. R. (2012). Soot particle aerosol mass spectrometer: development, validation, and initial application, *Aerosol Sci. Technol.*, 46, 804–817, doi: 10.1080/02786826.2012.663948.Ouimette, J. R., and Flagan, R.C. (1982). The extinction coefficient of multicomponent aerosols. *Atmos. Environ*., 16, 2405–2419.

Pagels, J., Khalizov, A. F., McMurry, P. H. and Zhang, R. Y. (2009). Processing of soot by controlled sulfuric acid and water condensation – mass and mobility relationship. *Aerosol Sci. Technol*., 43, 629–640.

Pakkanen, T., Kerminen, V.-M., Ojanen, C., Hillamo, R., Aarnio, P. and Koskentalo, T. (2000). Atmospheric black carbon in Helsinki. *Atmos. Environ.*, 34, 1497–1506.

Pekkanen J., Peters A., Hoek G., Tiittanen P., Brunekreef B., Hartog J., Heinrich J., Ibald-Mulli A., Kreyling W. G., Lanki T., Timonen K. L. and Vanninen E. (2002). Particulate air pollution and risk of ST-Segment depression during repeated submaximal exercise test among subject with coronary heart disease: the exposure and risk assessment for fine and ultrafine particles in ambient air (ULTRA) study. *Circulation*, 106, 933–938, doi:10.1161/01.CIR.0000027561.41736.3C.

Pereira, S., Wagner, F. and Silva, A. (2011). Seven years of measurements of aerosol scattering properties, near the surface, in the southwestern Iberia Peninsula. *Atmos. Chem. Phys*., 11, 17–29, doi:10.5194/acp-11-17-2011.

Petzold A., Kramer H. and Schönlinner M. (2002). Continuous measurement of atmospheric black carbon using a multi-angle absorpton photometer. *Environ. Sci. Pollut. Res*., 4, 78–82.

Petzold, A., and Schönlinner,M. (2004). Multi-Angle Absorption Photometry – A new method for the measurement of aerosol light absorption and atmospheric black carbon. *J. Aerosol Sci*., 35, 421–441.

Petzold, A., Schloesser, H., Sheridan, P. J., Arnott, W. P., Ogren, J. A. and Virkkula, A. (2005). Evaluation of multi-angle absorption photometry for measuring aerosol light absorption. *Aerosol Sci. Technol*., 39, 40–51.

Philippin, S., Wiedensohler, A. and Stratmann, F. (2004). Measurements of non-volatile fractions of pollution aerosols with an eight-tube volatility tandem differential mobility analyzer (VTDMA-8). *J. Aerosol Sci*., 35, 185–203.

Pirjola, L., Lähde, T., Niemi, J., Kousa, A., Rönkkö, T., Karjalainen, P., Keskinen, J., Frey, A. and Hillamo, R. (2012). Spatial and temporal characterization of traffic emissions in urban microenvironments with a mobile laboratory. *Atmos. Environ.*, 63, 156–167.

Podgorny, I. A., Conant, W. C., Ramanathan, V. and Satheesh, S. K. (2000). Aerosol modulation of atmospheric and surface solar heating rates over the tropical Indian Ocean. *Tellus B*, 52, 947–958, doi: 10.1034/j.1600-0889.2000.d01-4.x.

Pope C. A. III, Burnett R. T., Thurston G. D., Thun M. J., Calle E. E., Krewski D. and Godleski J. J. (2004). Cardiovascular mortality and long-term exposure to particulate air pollution: Epidemiological evidence of general pathophysiological pathways of disease. *Circulation*, 109, 71–77, doi:10.1161/01.CIR.0000108927.80044.7F.

Pope, A. and Dockery, D. (2006). Health effects of fine particulate air pollution: lines that connect. *J. Air & Waste Manage. Assoc.*, 56, 709-742.

Reddy, M., Basha, S., Joshi, H. and Jh, B. (2005). Evaluation of the emission characteristics of trace metals from coal and fuel oil fired power plants and their fate during combustion. *J. Hazardous Materials*, B123, 242–249.

Robinson, A., Donahue, N., Shrivastava, M., Weitkamp, E., Sage, A., Grieshop, A., Lane, T., Pierce, J. and Pandis, S. (2007). Rethinking organic aerosols: Semivolatile emissions and photochemical aging. *Science*, 315, 1259–1262, doi:10.1126/science.1133061.

Rose, D., Wehner, B., Ketzel, M., Engler, C., Voigtländer, J., Tuch, T. and Wiedensohler, A. (2005). Atmospheric number size distributions of soot particles and estimation of emission factors. *Atmos. Chem. Phys*., 6, 1021–1031.

Rönkkö, T., Virtanen, A., Kannosto, J., Keskinen, J., Lappi, M., and Pirjola, L. (2007). Nucleation mode particles with a nonvolatile core in the exhaust of a heavy duty diesel vehicle. *Environ. Sci. Technol.*, 41, 6384–6389.

Saarikoski, S., Timonen, H., Saarnio, K., Aurela, M., Järvi, L., Keronen, P., Kerminen, V.-M. and Hillamo, R. (2008). Sources of organic carbon in fine particulate matter in northern European urban air. *Atmos. Chem. Phys.*. 8, 6281–6295, doi:10.5194/acp-8-6281-2008.

Saarnio, K., Teinilä, K., Aurela, M., Timonen, H. and Hillamo, R (2010). High-performance anion-exchange chromatography–mass spectrometry method for determination of levoglucosan, mannosan, and galactosan in atmospheric fine particulate matter. *Anal. Bioanal. Chem.*, 398, 2253–2264, doi:10.1007/s00216-010-4151-4.

Saarnio, K. Niemi, J., Saarikoski, S., Aurela, M., Timonen, H., Teinilä, K., Myllynen, M., Frey, A., Lamberg, H., Jokiniemi, J. and Hillamo, R. (2012). Using monosaccharide anhydrides to estimate the impact of wood combustion on fine particles in the Helsinki metropolitan area. *Boreal Env. Res*., 17, 163–183.

Sandradewi, J., Prévot, A., Szidat, S., Perron, N., Alfarra, M., Lanz, V., Weingartner, E. and Baltensperger, U. (2008). Using aerosol light absorption measurements for the quantitative determination of wood burning and traffic emission contributions to particulate matter. *Environ. Sci. Technol.*, 42, 3316–3323.

Schneider, J., Kirchner, U., Borrmann, S., Vogt, R. and Scheer, V. (2008). In situ measurements of particle number concentration, chemically resolved size distributions and black carbon content of traffic-related emissions on German motorways, rural roads and in city traffic. *Atmos. Environ.*, 42, 4257–4268.

SFS-EN 14902 (2005). Ambient air quality. Standard method for the measurement of Pb, Cd, As and Ni in the PM10 fraction of suspended particulate matter. Finnish Standards Association SFS, Helsinki, Finland.

SFS 5624 (1990). Air Quality. Stationary Source Emissions. Determination of the Flue Gas Conditions. Finnish Standards Association SFS, Helsinki, Finland.

Sheridan, P. J. and Ogren, J. A. (1999). Observations of the vertical and regional variability of aerosol optical properties over central and eastern North America. *J. Geophys. Res*., 104, 16793–16805.

Shi, J.P., and Harrison, R.M. (1999). Investigation of ultrafine particle formation during diesel exhaust dilution. *Environ. Sci. Technol.*, 33, 3730–3736.

Shindell, D., Kuylenstierna, J., Vignati, E., van Dingenen, R., Amann, M., Klimont, Z., Anenberg, S., Muller, N., Janssens-Maenhout, G., Raes, F., Schwartz, J., Faluvegi, G., Pozzoli, L., Kupiainen, K., Höglund-Isaksson, L., Emberson, L., Streets, D., Ramanathan, V., Hicks, K., Oanh, N.T.K., Milly, G., Williams, M., Demkine, V., Fowler, D. (2012). Simultaneously mitigating near-term climate change and improving human health and food security. *Science*, 335, 183–189, doi:10.1126/science.1210026.

Sillanpää M., Frey A., Hillamo R., Pennanen A. and Salonen R. O. (2005). Organic, elemental and inorganic carbon in particulate matter of six urban environments in Europe. *Atmos. Chem. Phys.*, 5, 2869–2879.

Sillanpää M., Hillamo R., Saarikoski S., Frey A., Pennanen A., Makkonen U., Spolnik Z., Van Grieken R., Braniš M., Brunekreef B., Chalbot M.-C., Kuhlbusch T., Sunyer J., Kerminen V.-M., Kulmala M. and Salonen R. O. (2006). Chemical composition and mass closure of particulate matter at six urban sites in Europe. *Atmos. Environ.*, 40, S212–S223.

Sippula O., Hytönen K., Tissari J., Raunemaa T. and Jokiniemi J. (2007). The effect of wood fuel on the emissions from a top-feed pellet stove. *Energy and Fuels*, 21, 1151–1160.

Sippula, O., Hokkinen, J., Puustinen, H., Yli-Pirila, P. and Jokiniemi, J. (2009). Comparison of particle emissions from small heavy fuel oil and wood-fired boilers. *Atmos. Environ.*, 43, 4855–4864, doi:10.1016/j.atmosenv.2009.07.022.

Stocker, T.F., D. Qin, G.-K. Plattner, M. Tignor, S.K. Allen, J. Boschung, A. Nauels, Y. Xia, V. Bex and P.M. Midgley (eds.) (2013). IPCC, 2013: Climate Change 2013: The Physical Science Basis. Contribution of Working Group I to the Fifth Assessment Report of the Intergovernmental Panel on Climate Change.Cambridge University Press, Cambridge, United Kingdom and New York, NY, USA, 1535 pp.

Strehler, A. (2000). Technologies of wood combustion. *Ecol. Eng.*, 16, S25–S40.

Swietlicki, E., Hansson, H.-C., Hämeri, K., Svenningsson, B., Massling, A., Mc Figgans, G., Mc Murry, P.H., Petäjä, T., Tunved, P., Gysel, M., Topping, D., Weingartner, E., Baltensperger, U., Rissler, J., Wiedensohler, A. and Kulmala, M. (2008). Hygroscopic properties of submicrometer atmospheric aerosol particles measured with H-TDMA instruments in various environments – A review. Tellus, 60B, 432−469.

Takemura, T., Nakajima, T., Dubovik, O., Holben, B. and Kinne, S. (2002). Single-scattering albedo and radiative forcing of various aerosol species with a global three-dimensional model. *Journal of Climate*, 15, 333–352, doi:10.1175/1520-0442(2002)015<0333:SSAARF>2.0.CO,2.

Tissari, J., Hytönen, K., Sippula, O. and Jokiniemi, J. (2009). The effects of operating conditions on emissions from masonry heaters and sauna stoves. *Biomass and Bioenergy*, 33, 513–520, doi:10.1016/j.biombioe.2008.08.009.

Tomeczek, J. and Palugniok, H. (2002). Kinetics of mineral matter transformation during coal combustion, *Fuel* , 81, 1251– 1258, doi:10.1016/S0016-2361(02)00027-3.

Turpin, B. and Lim, H.-J. (2001). Species contribution to PM2.5 mass concentrations: revisiting common assumptions for estimating organic mass. *Aerosol Sci. Technol.*, 35, 602–610, doi:10.1080/02786820119445.

van Loo, S. and Koppejan, J. (eds.) (2008). *Handbook of biomass combustion and co-firing*. Twenty University Press, Enschede.

Virkkula, A. , Ahlquist, N. , Covert, D. , Arnott, W. , Sheridan, P. ,Quinn, P. and Coffman, D. (2005). Modification, Calibration and a Field Test of an Instrument for Measuring Light Absorption by Particles, *Aerosol Sci. Technol.*, 39: 1, 68–83, doi:10.1080/027868290901963.

Virkkula, A. (2010). Correction of the calibration of the 3-wavelength Particle Soot Absorption Photometer (3λ PSAP). *Aerosol Sci. Technol.*, 44, 706–712, doi:10.1080/02786826.2010.482110.

Virkkula, A., Backman, J., Aalto, P.P., Hulkkonen, M., Riuttanen, L., Nieminen, T., dal Maso, M., Sogacheva, L., de Leeuw, G. and Kulmala, M. (2011). Seasonal cycle, size dependencies, and source analyses of aerosol optical properties at the SMEAR II measurement station in Hyytiälä, Finland. *Atmos. Chem. Phys*., 11, 4445–4468, doi:10.5194/acp-11-4445-2011.

Virtanen, A., Rönkkö, T., Kannosto, J., Ristimäki, J., Mäkelä, J., Keskinen, J., Pakkanen, T., Hillamo, R., Pirjola, L. and Hämeri, K. (2006). Winter and summer time size distributions and densities of traffic-related aerosol particles at a busy highway in Helsinki. *Atmos. Chem. Phys.*, 6, 2411–2421.

Wang, S.C. and Flagan, R.C. (1990). Scanning electrical mobility spectrometer. *J. Aerosol Sci*., 13, 230–240.

Wang, Y., Chao, H., Wang, L., Chang-Chien, G. and Tsou, T. (2010). Characteristics of heavy metals emitted from a heavy oil-fueled power plant in northern Taiwan. *Aerosol and Air Quality Res*., 10, 111–118, doi:10.4209/aaqr.2009.09.0056.

Wehner, B., Philippin, S., Wiedensohler, A., Scheer, V. and Vogt, R. (2004). Variability of non-volatile fractions of atmospheric aerosol particles with traffic influence. *Atmos. Environ*., 38, 6081–6090.

Xu, G., Zhou, W., Swanson, L., Moyeda, D. and Nguyen, Q. (2010). Evaluation of applying low calorific fuel as reburn fuel in an opposed wall fired boiler. *J. Thermal Sci. Eng. Appl.*, 1 (3), doi: 10.1115/1.4000985.

Yoo, J.-I., Seo, Y.-C. and Shinagawa, T. (2005). Particle-size distributions and heavy metal partitioning in emission gas from different coal-fired power plants. *Environ. Engineering Sci*., 22, 272–279.

Finnish Meteorological Institute Contributions

1. Joffre, Sylvain M., 1988. Parameterization and assessment of processes affecting the long-range transport of airborne pollutants over the sea. 49 p.

2. Solantie, Reijo, 1990. The climate of Finland in relation to its hydrology, ecology and culture. 130 p.

3. Joffre, Sylvain M. and Lindfors, Virpi, 1990. Observations of airborne pollutants over the Baltic Sea and assessment of their transport, chemistry and deposition. 41 p.

4. Lindfors, Virpi, Joffre, Sylvain M. and Damski, Juhani, 1991. Determination of the wet and dry deposition of sulphur and nitrogen compounds over the Baltic Sea using actual meteorological data. 111 p.

5. Pulkkinen, Tuija, 1992. Magnetic field modelling during dynamic magne- tospheric processes. 150 p.

6. Lönnberg, Peter, 1992. Optimization of statistical interpolation. 157 p.

7. Viljanen, Ari, 1992. Geomagnetic induction in a one- or two-dimensional earth due to horizontal ionospheric currents. 136 p.

8. Taalas, Petteri, 1992. On the behaviour of tropospheric and stratospheric ozone in Northern Europe and in Antarctica 1987-90. 88 p.

9. Hongisto, Marke, 1992. A simulation model for the transport, transformation and deposition of oxidized nitrogen compounds in Finland — 1985 and 1988 simulation results. 114 p.

10. Taalas, Petteri, 1993. Factors affecting the behaviour of tropospheric and stratospheric ozone in the European Arctic and Antarctica. 138 s.

11. Mälkki, Anssi, 1993. Studies on linear and non-linear ion waves in the auroral acceleration region. 109 p.

12. Heino, Raino, 1994. Climate in Finland during the period of meteorological observations. 209 p.

13. Janhunen, Pekka, 1994. Numerical simulations of E-region irregularities and ionosphere-magnetosphere coupling. 122 p.

14. Hillamo, Risto E., 1994. Development of inertial impactor size spectroscopy for atmospheric aerosols. 148 p.

15. Pakkanen, Tuomo A., 1995. Size distribution measurements and chemical analysis of aerosol components. 157 p.

16. Kerminen, Veli-Matti, 1995. On the sulfuric acid-water particles via homogeneous nucleation in the lower troposphere. 101 p.

17. Kallio, Esa, 1996. Mars-solar wind interaction: Ion observations and their interpretation. 111 p.

18. Summanen, Tuula, 1996. Interplanetary Lyman alpha measurements as a tool to study solar wind properties. 114 p.

19. Rummukainen, Markku, 1996. Modeling stratospheric chemistry in a global three-dimensional chemical transport model, SCTM-1. Model development. 206 p.

20. Kauristie, Kirsti, 1997. Arc and oval scale studies of auroral precipitation and electrojets during magnetospheric substorms. 134 p.

21. Hongisto, Marke, 1998. Hilatar, A regional scale grid model for the transport of sulphur and nitrogen compounds. 152 p.

22. Lange, Antti A.I., 1999. Statistical calibration of observing systems. 134 p.

23. Pulkkinen, Pentti, 1998. Solar differential rotation and its generators: computational and statistical studies. 108 p.

24. Toivanen, Petri, 1998. Large-scale electromagnetic fields and particle drifts in time-dependent Earth's magnetosphere. 145 p.

25. Venäläinen, Ari, 1998. Aspects of the surface energy balance in the boreal zone. 111 p.

26. Virkkula, Aki, 1999. Field and laboratory studies on the physical and chemical properties of natural and anthropogenic tropospheric aerosol. 178 p.

27. Siili, Tero, 1999. Two-dimensional modelling of thermal terrain-induced mesoscale circulations in Mars' atmosphere. 160 p.

28. Paatero, Jussi, 2000. Deposition of Chernobyl-derived transuranium nuclides and short-lived radon-222 progeny in Finland. 128 p.

29. Jalkanen, Liisa, 2000. Atmospheric inorganic trace contaminants in Finland, especially in the Gulf of Finland area. 106 p.

30. Mäkinen, J. Teemu, T. 2001. SWAN Lyman alpha imager cometary hydrogen coma observations. 134 p.

31. Rinne, Janne, 2001. Application and development of surface layer flux techniques for measurements of volatile organic compound emissions from vegetation. 136 p.

32. Syrjäsuo, Mikko T., 2001. Auroral monitoring system: from all-sky camera system to automated image analysis. 155 p.

33. Karppinen, Ari, 2001. Meteorological pre-processing and atmospheric dispersion modelling of urban air quality and applications in the Helsinki metropolitan area. 94 p.

34. Hakola, Hannele, 2001. Biogenic volatile organic compound (VOC) emissions from boreal deciduous trees and their atmospheric chemistry. 125 p.

35. Merenti-Välimäki, Hanna-Leena, 2002. Study of automated present weather codes.153 p.

36. Tanskanen, Eija I., 2002. Terrestrial substorms as a part of global energy flow. 138 p.

37. Nousiainen, Timo, 2002. Light scattering by nonspherical atmospheric particles. 180 p.

38. Härkönen, Jari, 2002. Regulatory dispersion modelling of traffic-originated pollution. 103 p.

39. Oikarinen, Liisa, 2002. Modeling and data inversion of atmospheric limb scattering measurements. 111 p.

40. Hongisto, Marke, 2003. Modelling of the transport of nitrogen and sulphur contaminants to the Baltic Sea Region. 188 p.

41. Palmroth, Minna, 2003. Solar wind – magnetosphere interaction as determined by observations and a global MHD simulation. 147 p.

42. Pulkkinen, Antti, 2003. Geomagnetic induction during highly disturbed space weather conditions: Studies of ground effects 164 p.

43. Tuomenvirta, Heikki, 2004. Reliable estimation of climatic variations in Finland. 158 p.

44. Ruoho-Airola, Tuija, 2004. Temporal and regional patterns of atmospheric components affecting acidification in Finland. 115 p.

45. Partamies, Noora, 2004. Meso-scale auroral physics from groundbased observations. 122 p.

46. Teinilä, Kimmo, 2004. Size resolved chemistry of particulate ionic compounds at high latitudes. 138 p.

47. Tamminen, Johanna, 2004. Adaptive Markov chain Monte Carlo algorithms with geophysical applications. 156 p.

48. Huttunen, Emilia, 2005. Interplanetary shocks, magnetic clouds, and magnetospheric storms. 142 p.

49. Sofieva, Viktoria, 2005. Inverse problems in stellar occultation. 110 p.

50. Harri, Ari-Matti, 2005. In situ observations of the atmospheres of terrestrial planetary bodies. 246 p.

51. Aurela, Mika, 2005. Carbon dioxide exchange in subarctic ecosystems measured by a micrometeorological technique. 132 p.

52. Damski, Juhani, 2005. A Chemistry-transport model simulation of the stratospheric ozone for 1980 to 2019. 147 p.

53. Tisler, Priit, 2006. Aspects of weather simulation by numerical process. 110 p.

54. Arola, Antti, 2006. On the factors affecting short- and long-term UV variability. 82 p.

55. Verronen, Pekka T., 2006. Ionosphere-atmosphere interaction during solar proton events. 146 p.

56. Hellén, Heidi, 2006. Sources and concentrations of volatile organic compounds in urban air. 134 p.

57. Pohjola, Mia, 2006. Evaluation and modelling of the spatial and temporal variability of particulate matter in urban areas. 143 p.

58. Sillanpää, Markus, 2006. Chemical and source characterisation of size-segregated urban air particulate matter. 184 p.

59. Niemelä, Sami, 2006. On the behaviour of some physical parameterization methods in high resolution numerical weather prediction models. 136 p.

60. Karpechko, Alexey, 2007. Dynamical processes in the stratosphere and upper troposphere and their influence on the distribution of trace gases in the polar atmosphere. 116 p.

61. Eresmaa, Reima, 2007. Exploiting ground-based measurements of Global Positioning System for numerical weather prediction. 95 p.

62. Seppälä, Annika, 2007. Observations of production and transport of NOx formed by energetic particle precipitation in the polar night atmosphere. 100 p.

63. Rontu, Laura, 2007. Studies on orographic effects in a numerical weather prediction model. 151 p.

64. Vajda, Andrea, 2007. Spatial variations of climate and the impact of disturbances on local climate and forest recovery in northern Finland. 139 p.

65. Laitinen, Tiera, 2007. Rekonnektio Maan magnetosfäärissä – Reconnection in Earth's magnetosphere. 226 s.

66. Vanhamäki, Heikki, 2007. Theoretical modeling of ionospheric electrodynamics including induction effects. 170 p.

67. Lindfors. Anders, 2007. Reconstruction of past UV radiation. 123 p.

68. Sillanpää, Ilkka, 2008. Hybrid modelling of Titan's interaction with the magnetosphere of Saturn. 200 p.

69. Laine, Marko, 2008. Adaptive MCMC methods with applications in environmental and geophysical models. 146 p.

70. Tanskanen, Aapo, 2008. Modeling of surface UV radiation using satellite data. 109 p.

71. Leskinen, Ari, 2008. Experimental studies on aerosol physical properties and transformation in environmental chambers. 116 p.

72. Tarvainen, Virpi, 2008. Development of biogenetic VOC emission inventories for the boreal forest. 137 p.

73. Lohila, Annalea, 2008. Carbon dioxide exchange on cultivated and afforested boreal peatlands. 110 p.

74. Saarikoski, Sanna, 2008. Chemical mass closure and source-specific composition of atmospheric particles. 182 p.

75. Pirazzini, Roberta, 2008. Factors controlling the surface energy budget over snow and ice. 141 p.

76. Salonen, Kirsti, 2008. Towards the use of radar winds in numerical weather prediction. 87 p.

77. Luojus, Kari, 2009. Remote sensing of snow-cover for the boreal forest zone using microwave radar. 178 p.

78. Juusola, Liisa, 2009. Observations of the solar wind-magnetosphere-ionosphere coupling. 167 p.

79. Waldén, Jari, 2009. Meteorology of gaseous air pollutants. 177 p.

80. Mäkelä, Jakke, 2009. Electromagnetic signatures of lightning near the HF frequency band. 152 p.

81. Thum, Tea, 2009. Modelling boreal forest CO_2 exchange and seasonality. 140 p.

82. Lallo, Marko, 2010. Hydrogen soil deposition and atmospheric variations in the boreal zone. 91 p.

83. Sandroos, Arto, 2010. Shock acceleration in the solar corona. 116 p.

84. Lappalainen, Hanna, 2010. Role of temperature in the biological activity of a boreal forest. 107 p.

85. Mielonen, Tero, 2010. Evaluation and application of passive and active optical remote sensing methods for the measurement of atmospheric aerosol properties. 125 p.

86. Lakkala, Kaisa, 2010. High quality polar UV measurements : scientific analyses and transfer of the irradiance scale. 156 p.

87. Järvinen, Riku, 2011. On ion escape from Venus. 150 p.

88. Saltikoff, Elena, 2011. On the use of weather radar for mesoscale applications in northern conditions. 120 p.

89. Timonen, Hilkka, 2011. Chemical characterization of urban background aerosol using online

and filter methods. 176 p.

90. Hyvärinen, Otto, 2011. Categorical meteorological products : evaluation and analysis.138 p.

91. Mäkelä, Antti, 2011. Thunderstorm climatology and lightning location applications in northern Europe. 158 p.

92. Hietala, Heli, 2012. Multi-spacecraft studies on space plasma shocks. 132 p.

93. Leinonen, Jussi, 2013. Thunderstorm climatology and lightning location applications in northern Europe.

94. Gregow, Hilppa, 2013. Impact of strong winds, heavy snow loads and soil frost conditions on the risks to forests in Northern Europe. 178 p.

95. Henriksson, Svante, 2013. Modeling key processes causing climate change and variability. 98 p.

96. Valkonen, Teresa, 2013. Surface influence on the marine and coastal Antarctic atmosphere. 114 p

97. Saarnio, Karri, 2013. Chemical characterisation of fine particles from biomass burning. 180 p.

98. Honkonen, Ilja, 2013. Development, validation and application of numerical space environment models. 148 p.

99. Siljamo, Pilvi, 2013. Numerical modelling of birch pollen emissions and dispersion on regional and continental scales. 156 p.

100. Anekallu, Chandrasekhar, 2013. Energy conversion across the Earth's magnetopause observations. 166 p.

101. Riihelä, Aku, 2013. The surface albedo of the arctic from space optical imagers: retrieval and validation. 164 p.

102. Lindgvist, Hannakaisa, 2013. Atmospheric ice and dust : from morphological modeling to light scattering. 154 p.

103. Tuomi, Laura, 2014. (valmisteilla / in preparation)

104. Portin, Harri, 2014. Observations of aerosols, clouds and their interactions at Puijo measurement station. 133 p.

105. Carbone, Samara, 2014. Chemical characterization and source apportionment of submicron aerosol particles with aerosol mass spectrometers. 135 p.

106. Ollinaho, Pirkka, 2014. Parametric uncertainty in numerical weather prediction models.

107. Frey, Anna, 2014. Study on soot and other refractory components from various combustion

processes. 170 p.